

Summary of Satellite Remote Sensing Concepts

Lectures in Brienza
24 Sep 2011

Paul Menzel
UW/CIMSS/AOS

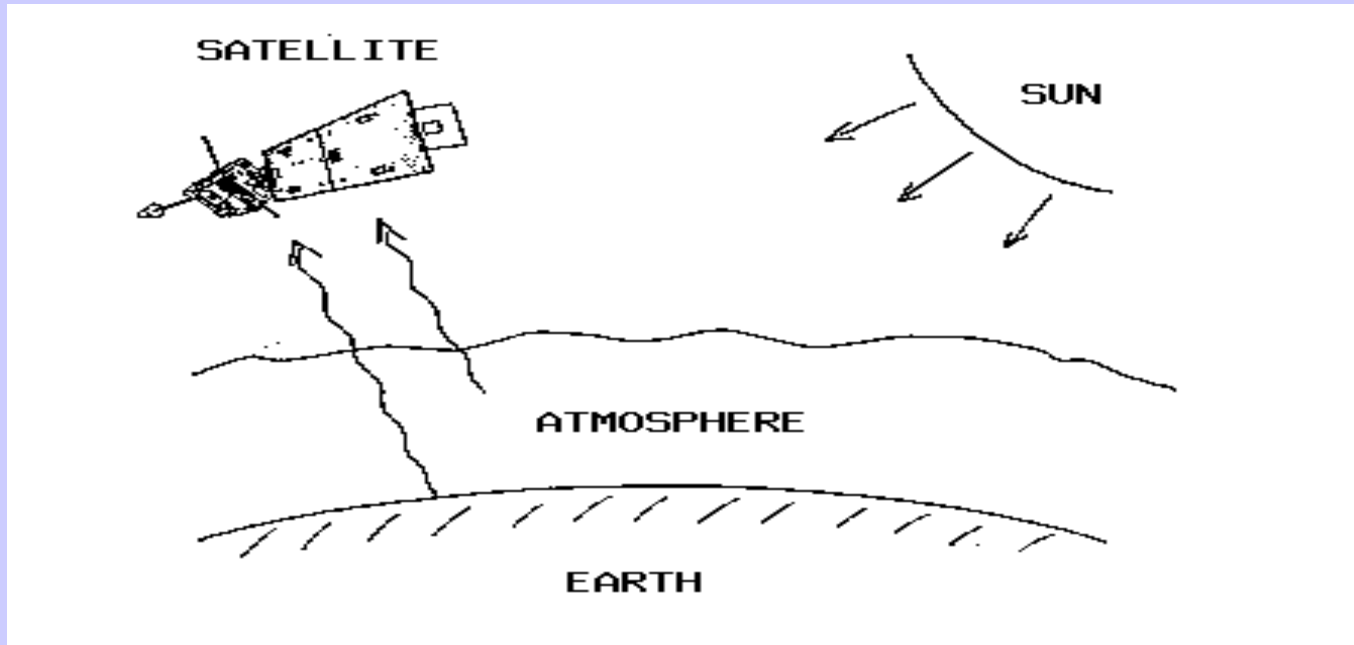
Brienza 2011



Brienza 2011



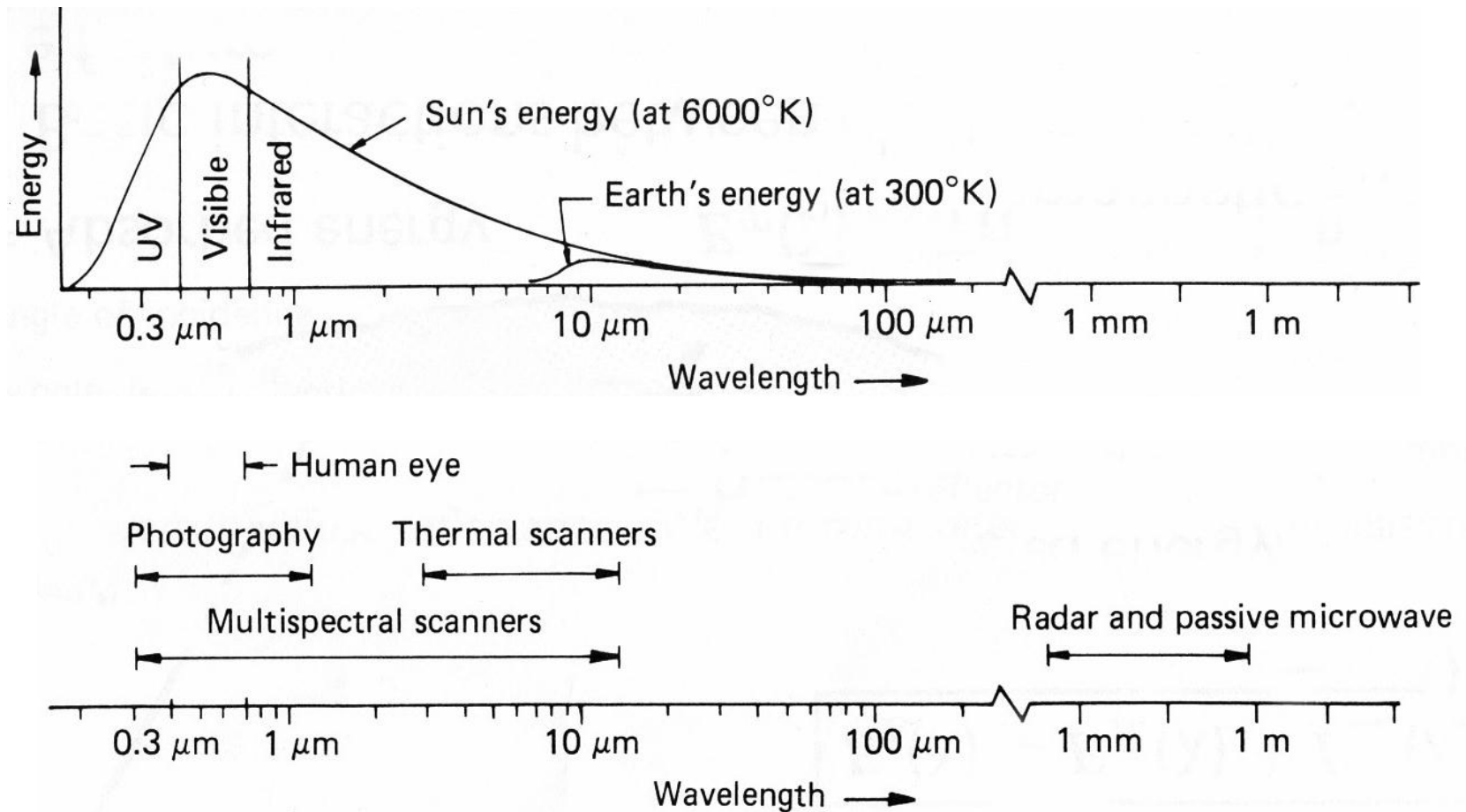
Satellite remote sensing of the Earth-atmosphere



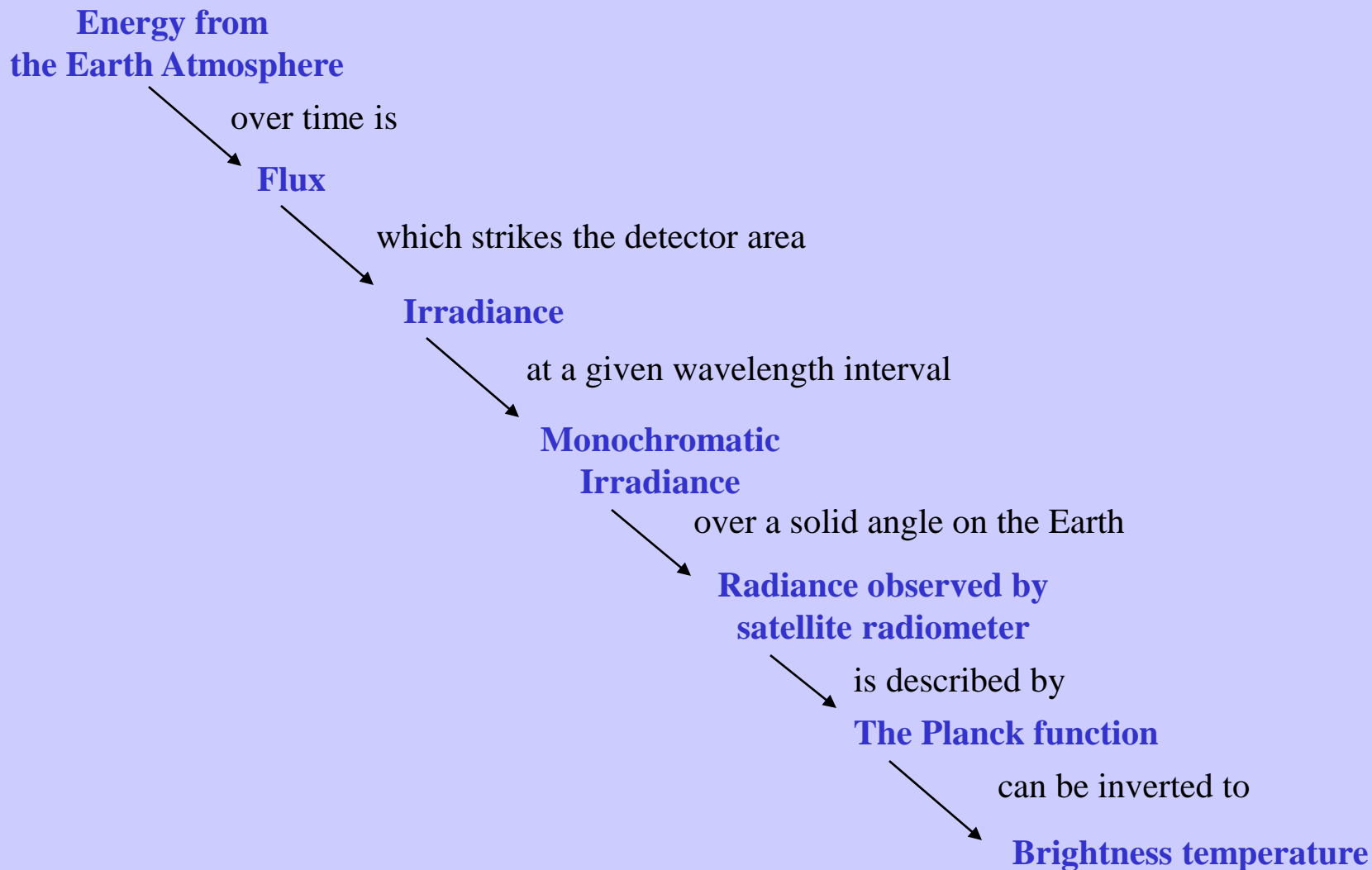
Observations depend on

- telescope characteristics (resolving power, diffraction)
- detector characteristics (signal to noise)
- communications bandwidth (bit depth)
- spectral intervals (window, absorption band)
- time of day (daylight visible)
- atmospheric state (T, Q, clouds)
- earth surface (Ts, vegetation cover)

Spectral Characteristics of Energy Sources and Sensing Systems



Terminology of radiant energy



Definitions of Radiation

QUANTITY	SYMBOL	UNITS
Energy	dQ	Joules
Flux	dQ/dt	Joules/sec = Watts
Irradiance	$dQ/dt/dA$	Watts/meter ²
Monochromatic Irradiance	$dQ/dt/dA/d\lambda$ or $dQ/dt/dA/d\nu$	W/m ² /micron W/m ² /cm ⁻¹
Radiance	$dQ/dt/dA/d\lambda/d\Omega$ or $dQ/dt/dA/d\nu/d\Omega$	W/m ² /micron/ster W/m ² /cm ⁻¹ /ster

Using wavenumbers

$$B(\nu, T) = \frac{c_2 \nu / T}{c_1 \nu^3 / [e^{-1}]} \quad -1]$$

(mW/m²/ster/cm⁻¹)

$$\nu(\text{max in cm}^{-1}) = 1.95T$$

$$B(\nu_{\text{max}}, T) \sim T^{**3}.$$

$$E = \pi \int_0^{\infty} B(\nu, T) d\nu = \sigma T^4,$$

$$T = c_2 \nu / \left[\ln\left(\frac{c_1 \nu^3}{B_\nu} + 1\right) \right]$$

Using wavelengths

$$B(\lambda, T) = \frac{c_2 / \lambda T}{c_1 / \{ \lambda^5 [e^{-1}] \}} \quad -1] \}$$

(mW/m²/ster/μm)

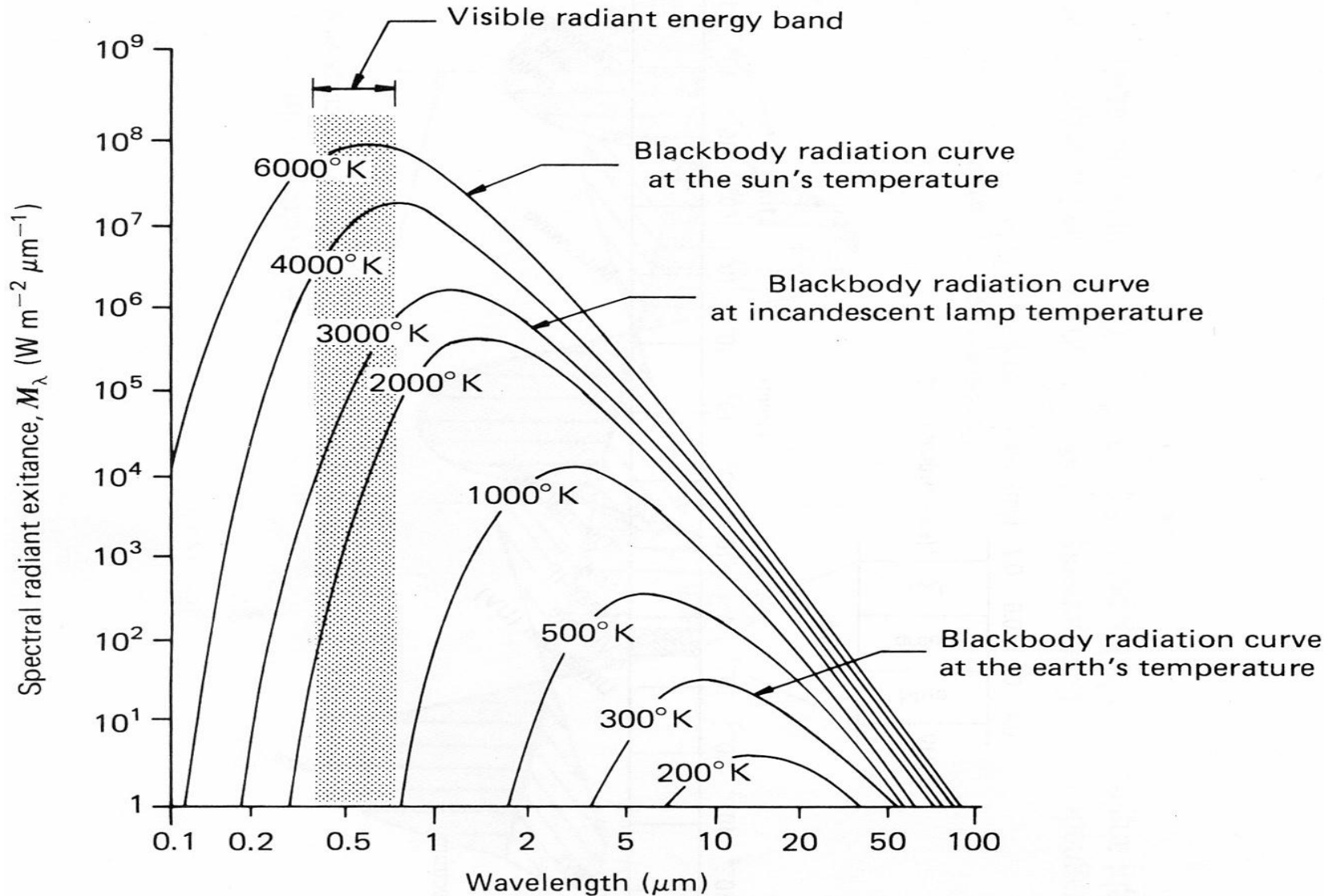
$$\lambda(\text{max in cm})T = 0.2897$$

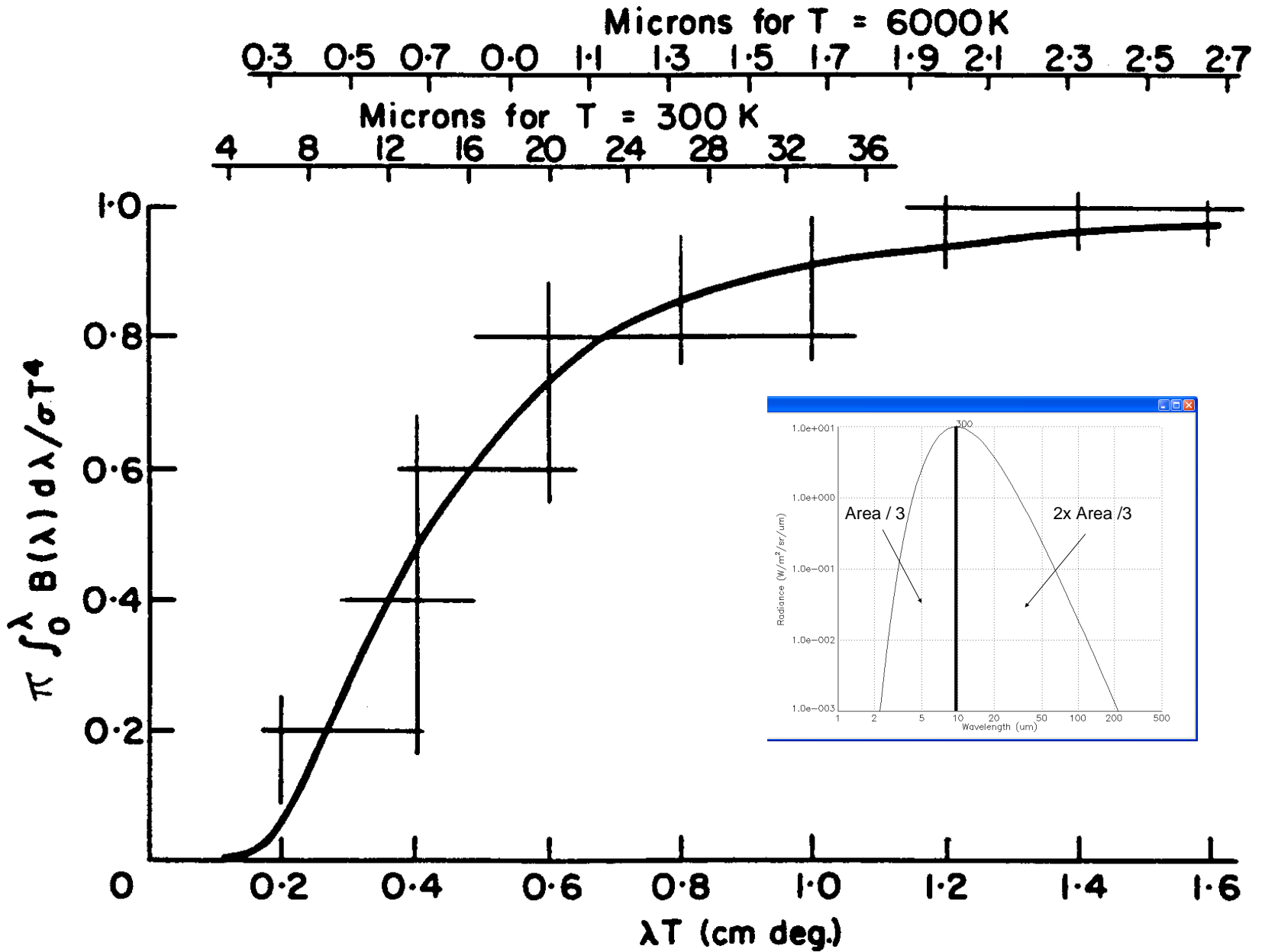
$$B(\lambda_{\text{max}}, T) \sim T^{**5}.$$

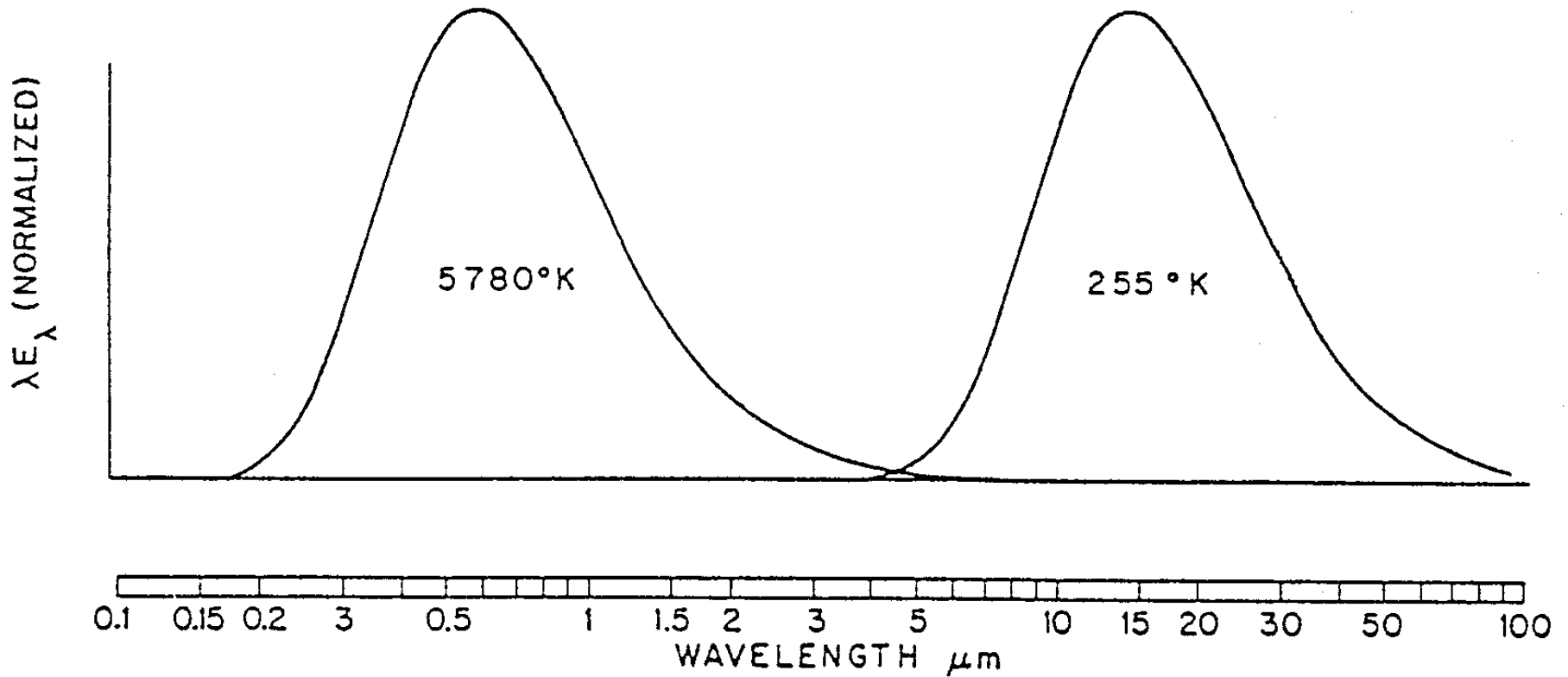
$$E = \pi \int_0^{\infty} B(\lambda, T) d\lambda = \sigma T^4,$$

$$T = c_2 / \left[\lambda \ln\left(\frac{c_1}{\lambda^5 B_\lambda} + 1\right) \right]$$

Spectral Distribution of Energy Radiated from Blackbodies at Various Temperatures



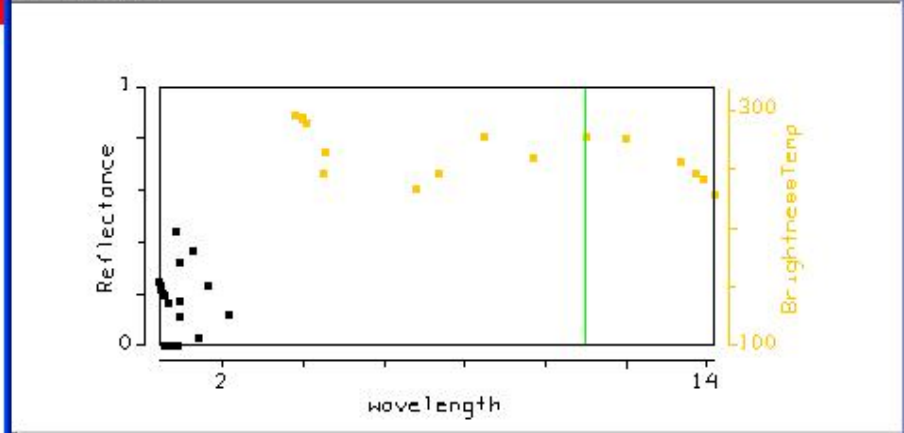
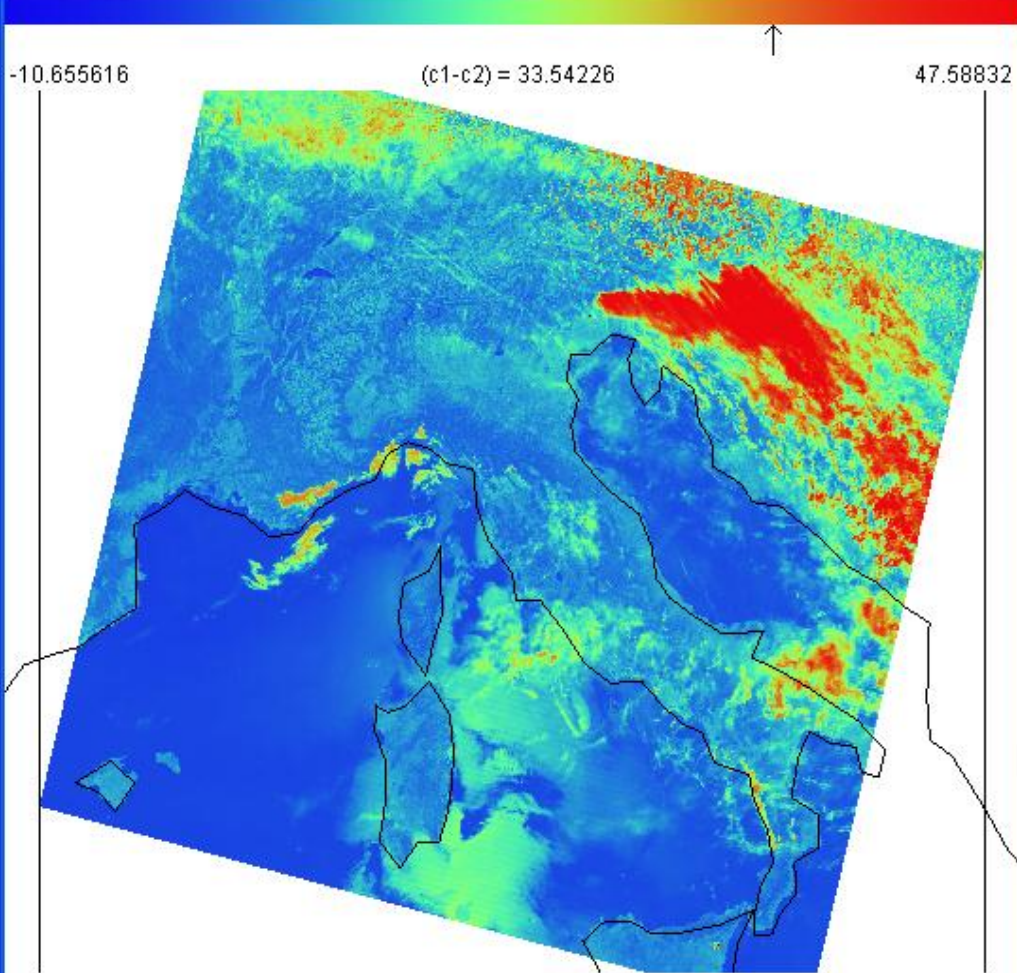




Normalized black body spectra representative of the sun (left) and earth (right), plotted on a logarithmic wavelength scale. The ordinate is multiplied by wavelength so that the area under the curves is proportional to irradiance.

Tools Settings

Tools Settings



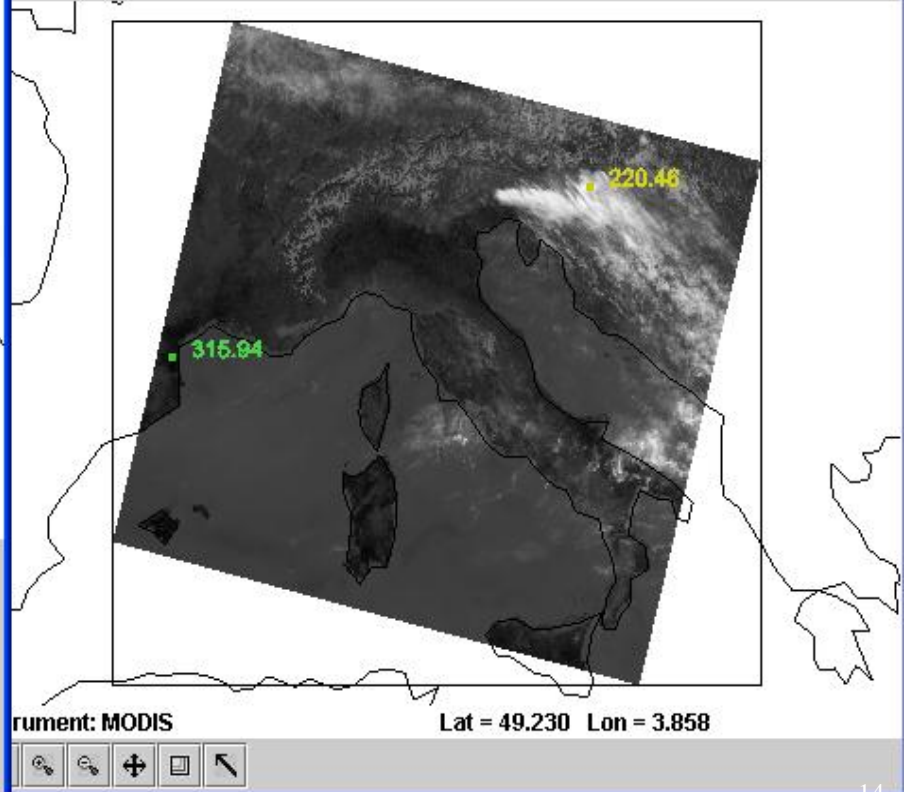
Band: 31 wavelength 11.00 μm

c1:20, c2:31

BT4 - BT11

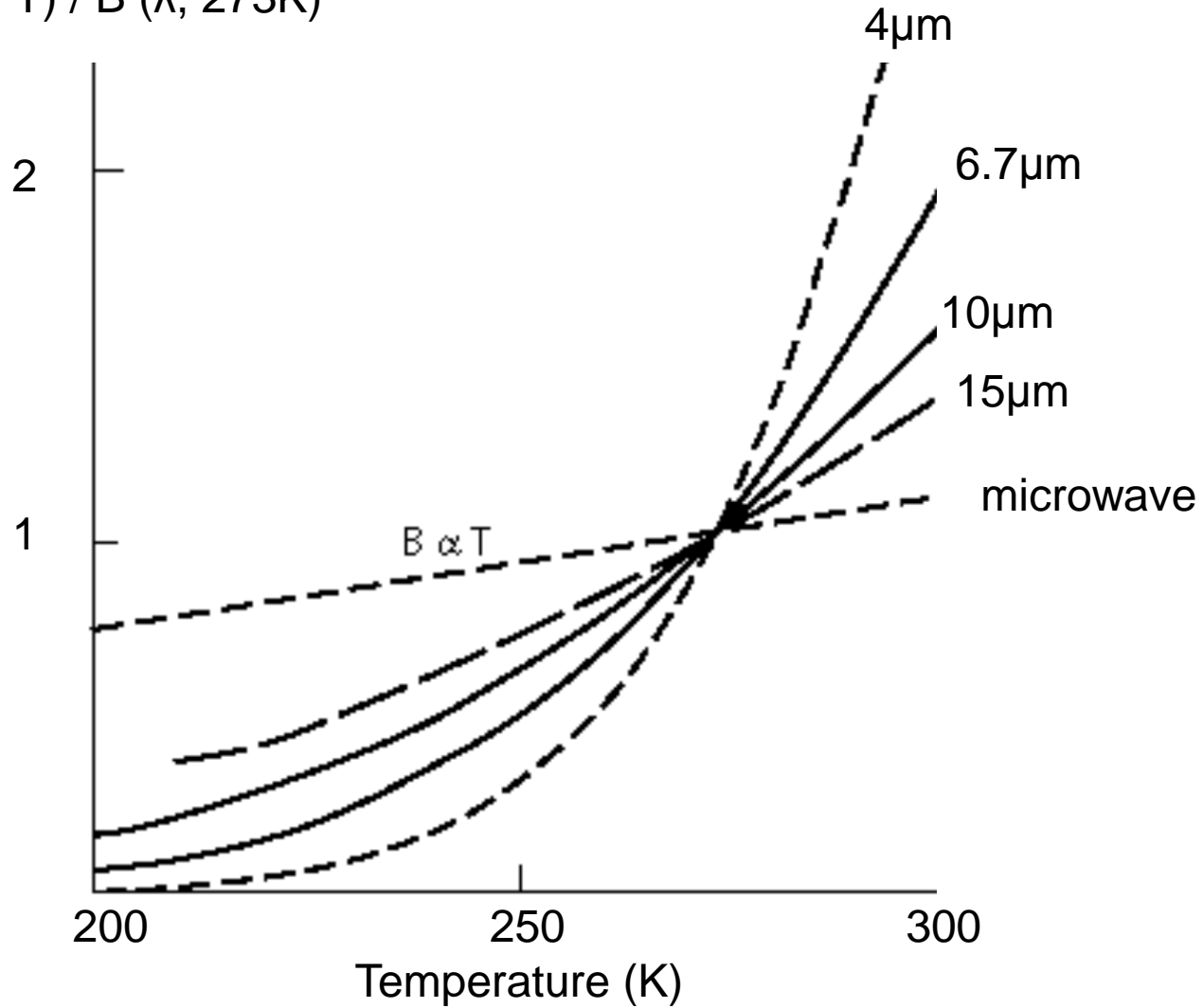
XAxis YAxis

Box Curve

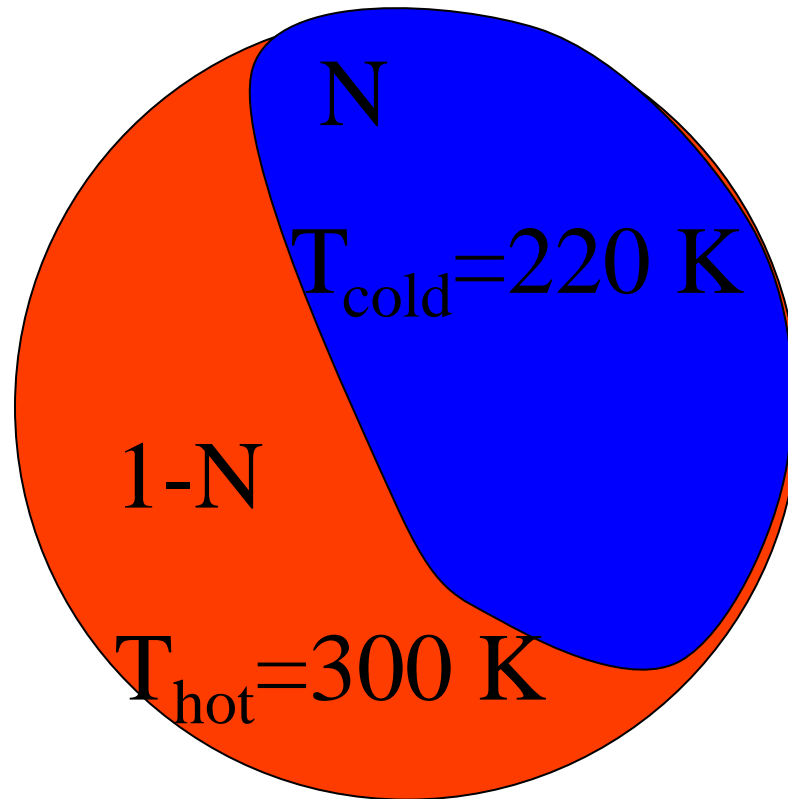


Temperature Sensitivity of $B(\lambda, T)$ for typical earth temperatures

$B(\lambda, T) / B(\lambda, 273K)$



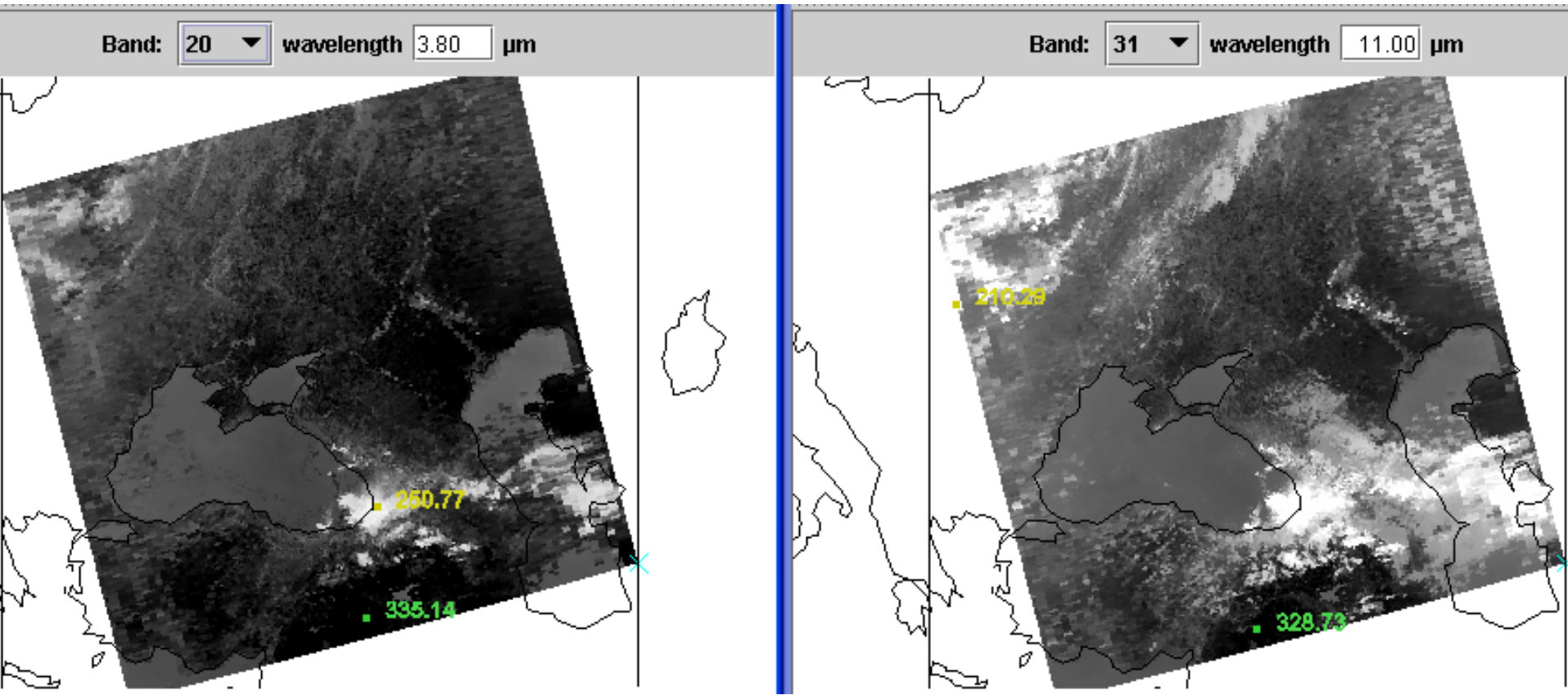
Non-Homogeneous FOV



$$B = N * B(T_{\text{cold}}) + (1-N) * B(T_{\text{hot}})$$

$$BT = N * T_{\text{cold}} + (1-N) * T_{\text{hot}}$$

The equation above is crossed out with a large red circle and a diagonal slash, indicating it is incorrect.



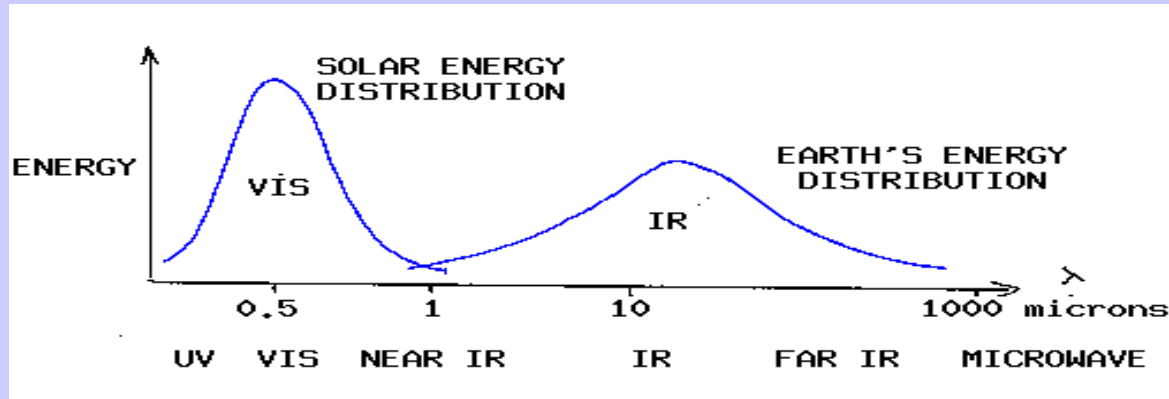
Cloud edges and broken clouds appear different in 11 and 4 um images.

$$T(11)^{**4} = (1-N) * T_{clr}^{**4} + N * T_{cld}^{**4} \sim (1-N) * 300^{**4} + N * 200^{**4}$$

$$T(4)^{**12} = (1-N) * T_{clr}^{**12} + N * T_{cld}^{**12} \sim (1-N) * 300^{**12} + N * 200^{**12}$$

Cold part of pixel has more influence for B(11) than B(4)

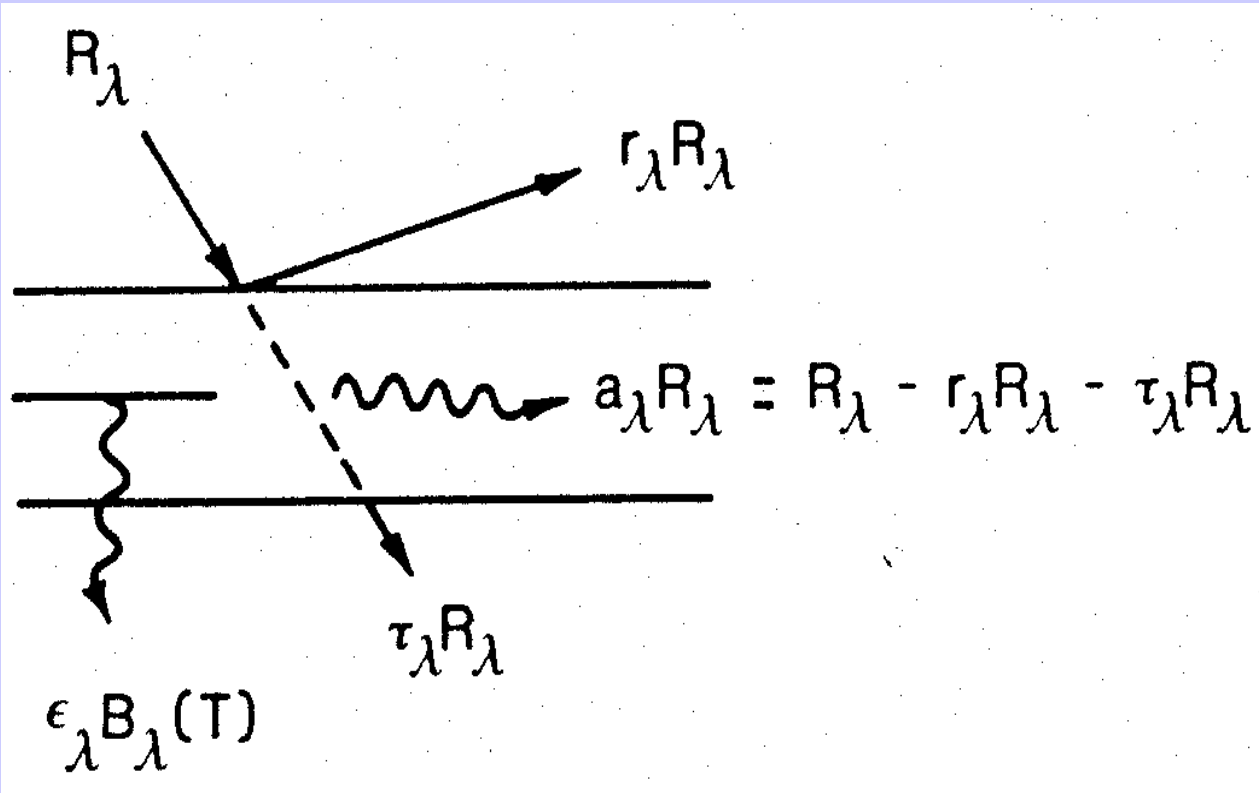
Solar (visible) and Earth emitted (infrared) energy



Incoming solar radiation (mostly visible) drives the earth-atmosphere (which emits infrared).

Over the annual cycle, the incoming solar energy that makes it to the earth surface (about 50 %) is balanced by the outgoing thermal infrared energy emitted through the atmosphere.

The atmosphere transmits, absorbs (by H₂O, O₂, O₃, dust) reflects (by clouds), and scatters (by aerosols) incoming visible; the earth surface absorbs and reflects the transmitted visible. Atmospheric H₂O, CO₂, and O₃ selectively transmit or absorb the outgoing infrared radiation. The outgoing microwave is primarily affected by H₂O and O₂.



‘ENERGY
CONSERVATION’

Selective Absorption

Atmosphere transmits visible and traps infrared

Incoming
solar

Outgoing IR

$$\downarrow E \quad \uparrow (1-a_1) Y_{\text{sfc}} \quad \uparrow Y_a$$

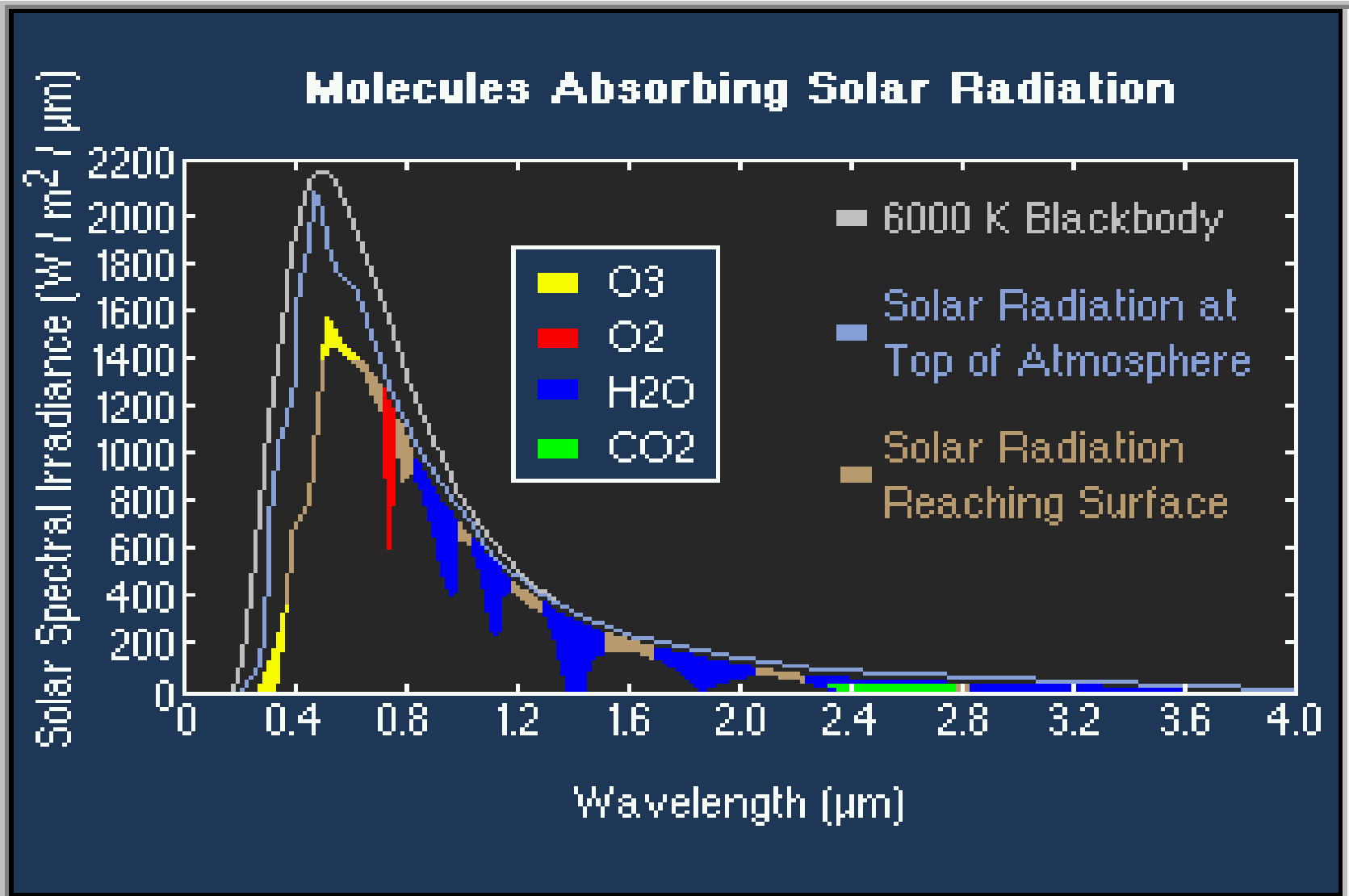
top of the atmosphere

$$\downarrow (1-a_s) E \quad \uparrow Y_{\text{sfc}} \quad \downarrow Y_a$$

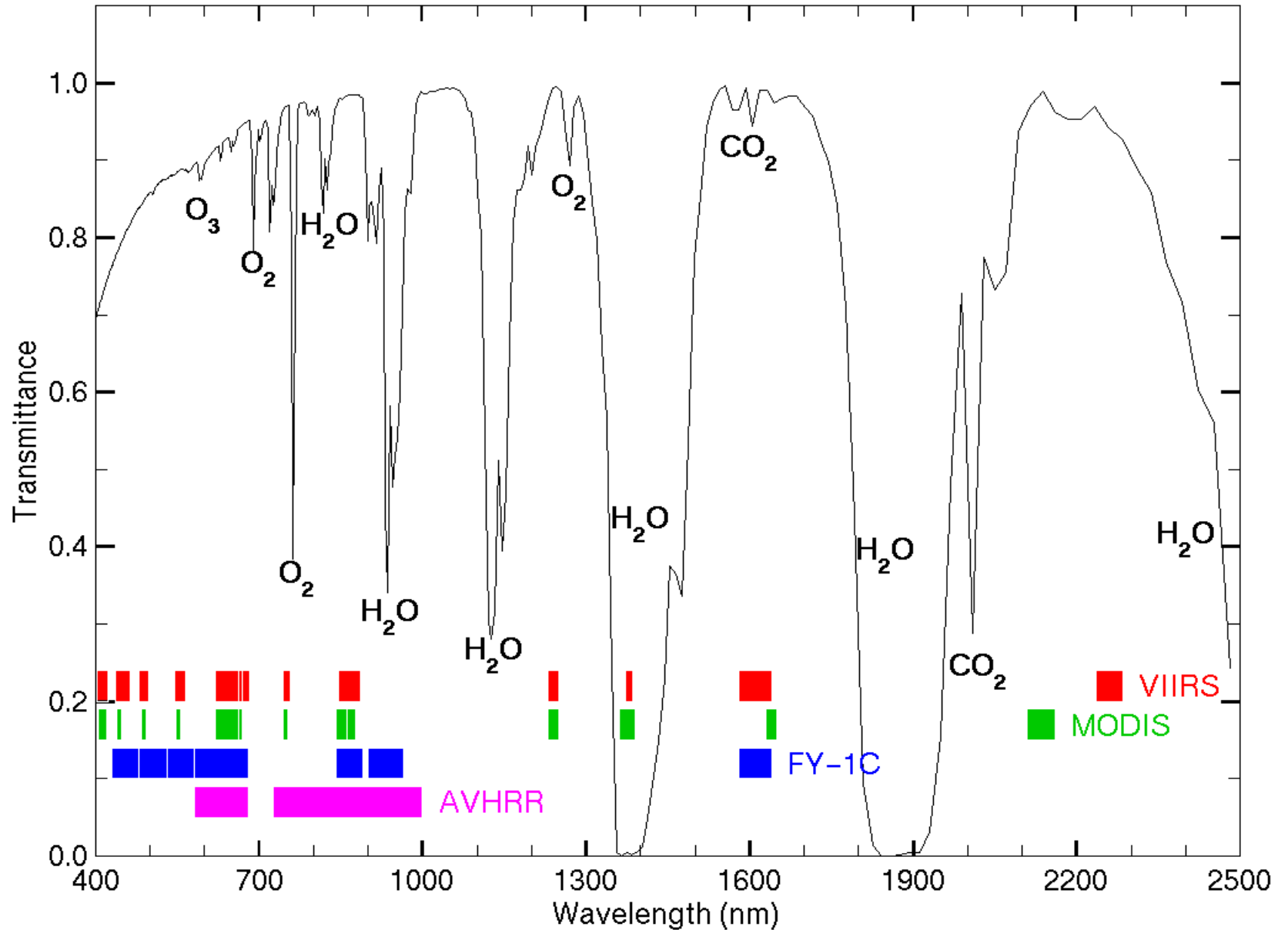
earth surface.

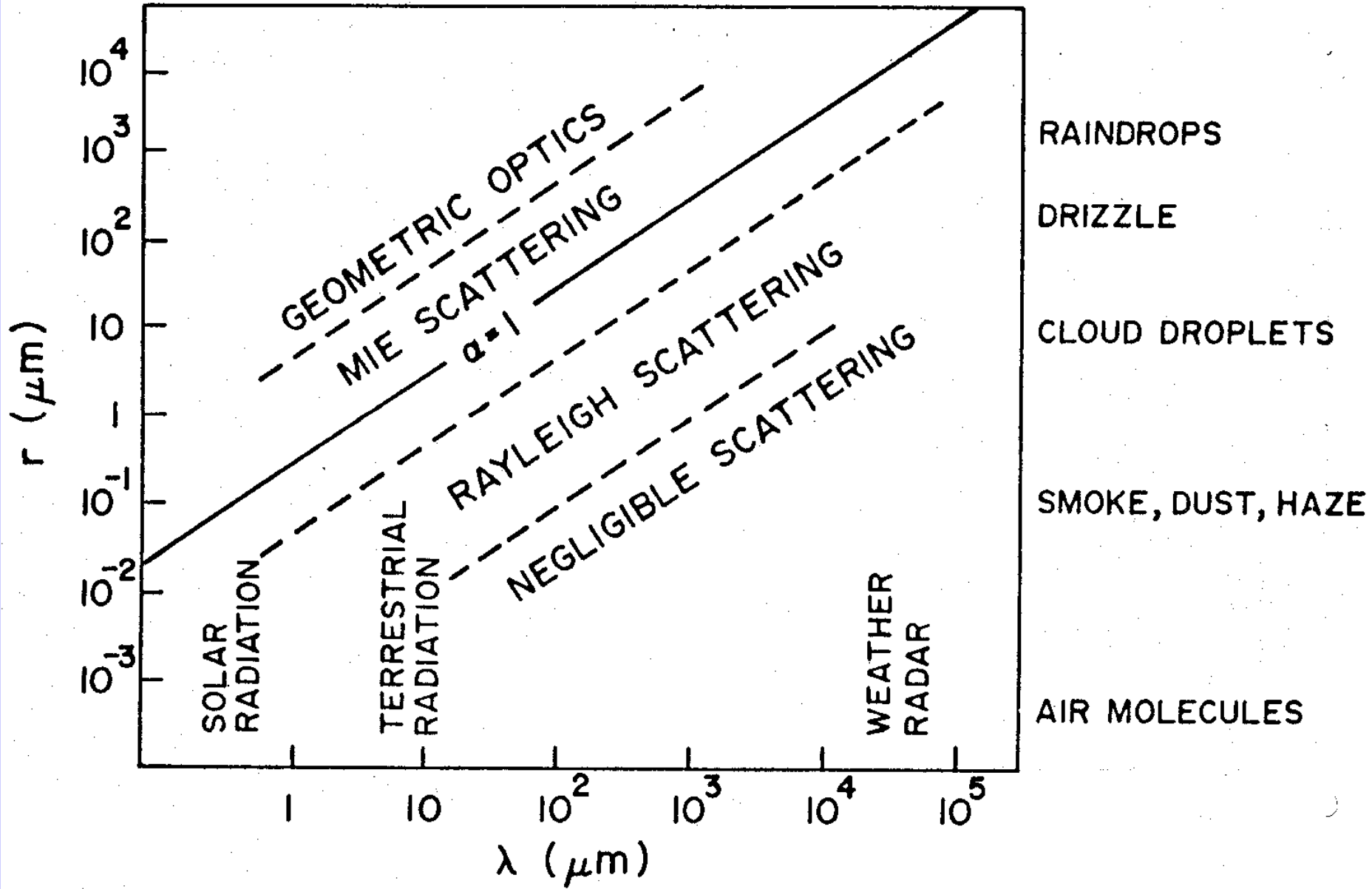
$$Y_{\text{sfc}} = \frac{(2-a_s)}{(2-a_L)} E = \sigma T_{\text{sfc}}^4 \quad \text{thus if } a_s < a_L \text{ then } Y_{\text{sfc}} > E$$

Solar Spectrum



VIIRS, MODIS, FY-1C, AVHRR



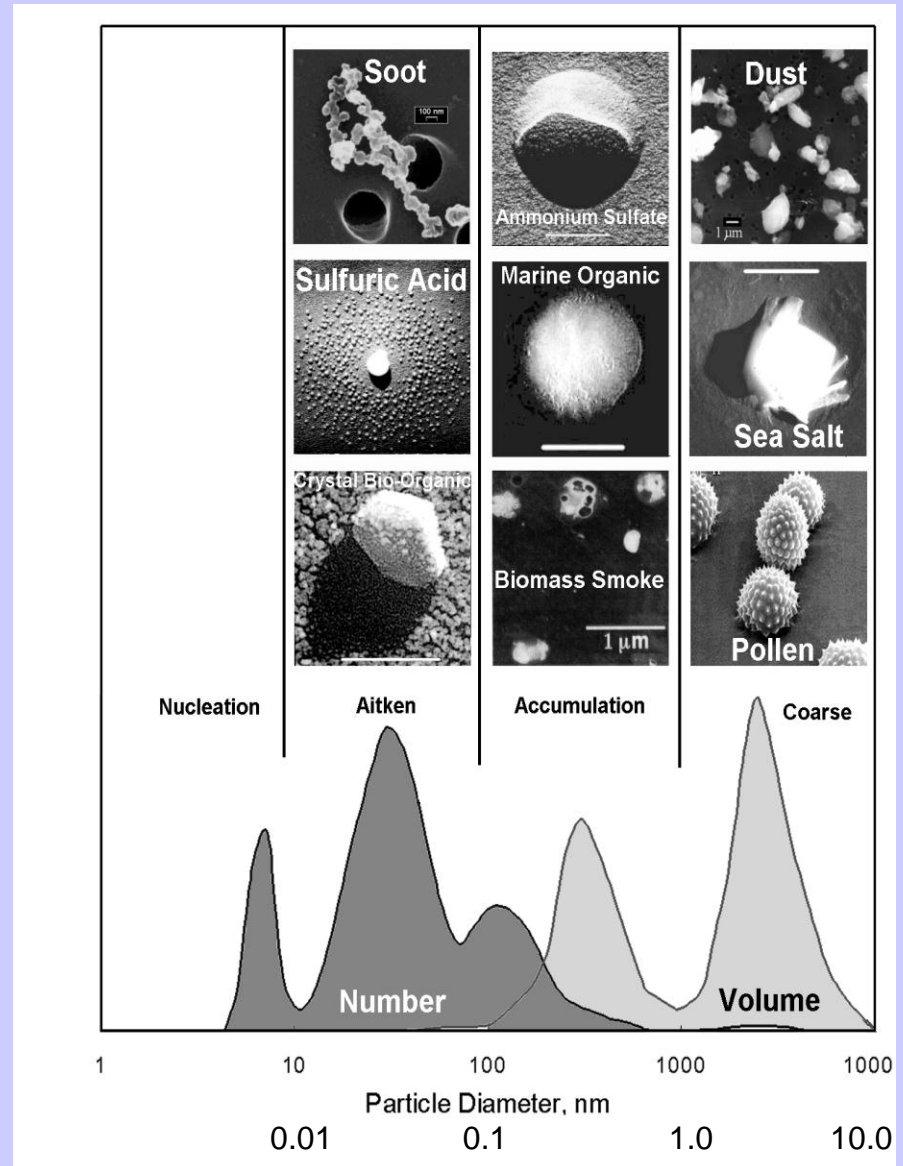


Aerosol Size Distribution

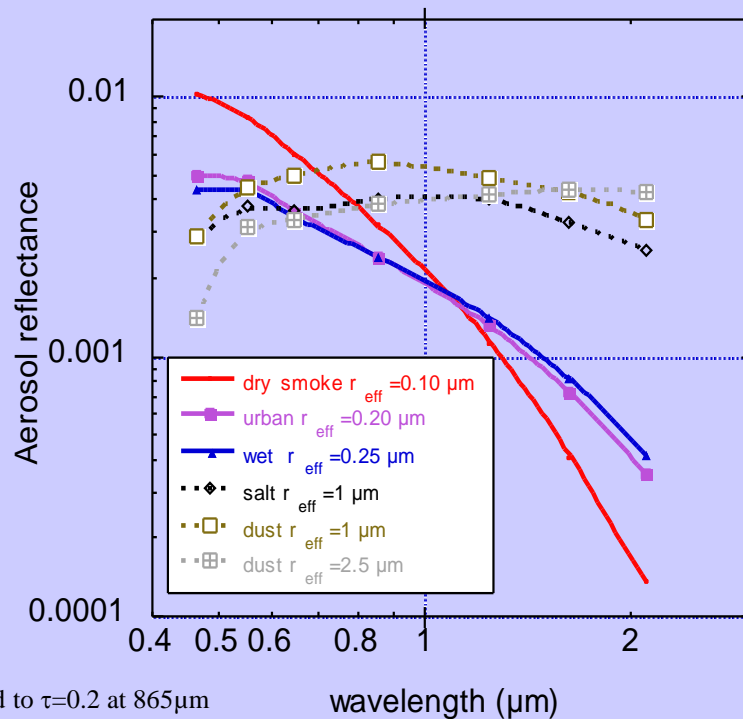
There are **3** modes :

- « **nucleation** »: radius is between 0.002 and $0.05 \mu\text{m}$. They result from combustion processes, photo-chemical reactions, etc.
- « **accumulation** »: radius is between $0.05 \mu\text{m}$ and $0.5 \mu\text{m}$. Coagulation processes.
- « **coarse** »: larger than $1 \mu\text{m}$. From mechanical processes like aeolian erosion.

« **fine** » particles (nucleation and accumulation) result from anthropogenic activities, coarse particles come from natural processes.



Aerosols over Ocean



- Radiance data in 6 bands (550-2130nm).

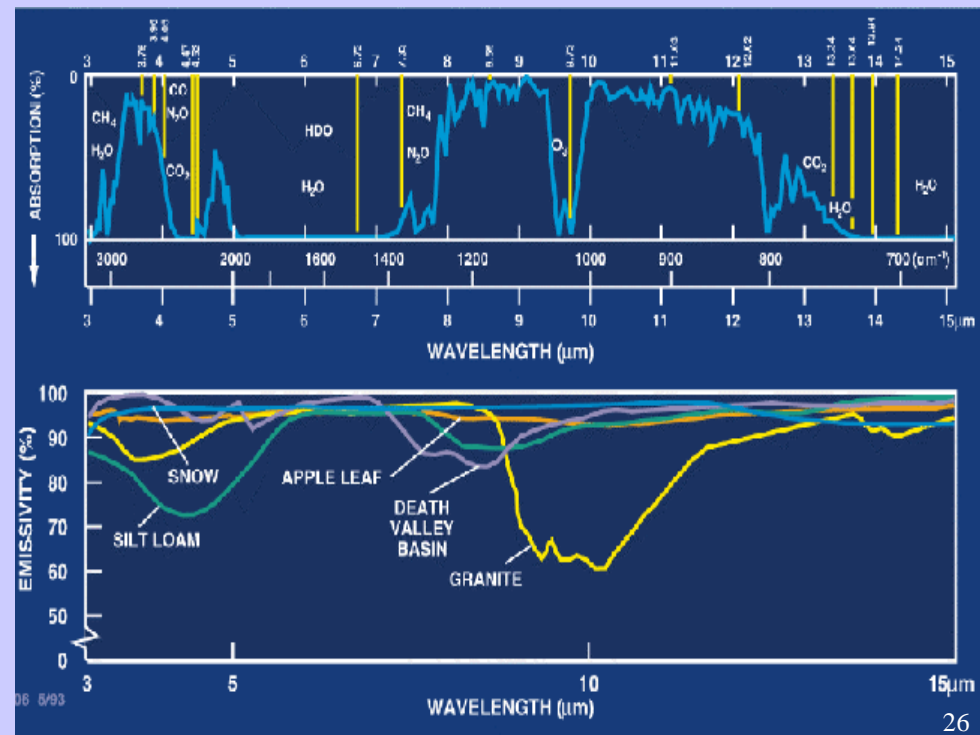
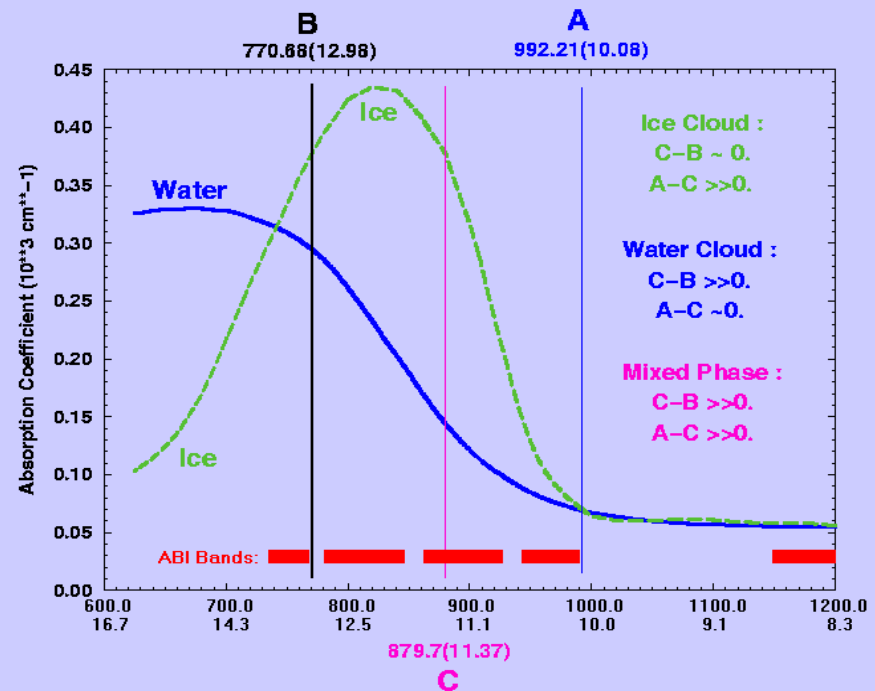
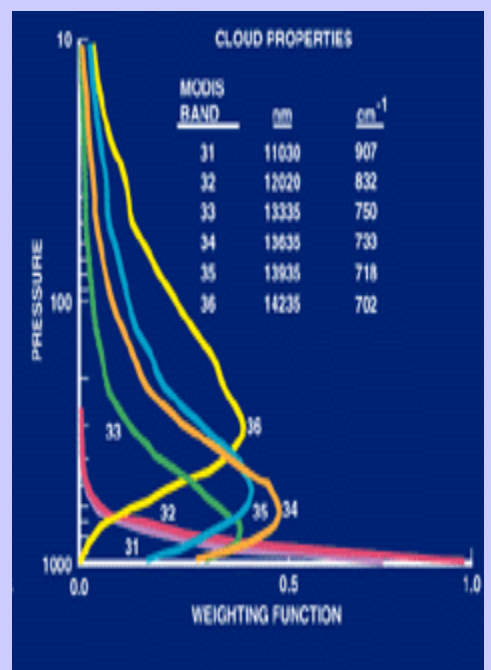
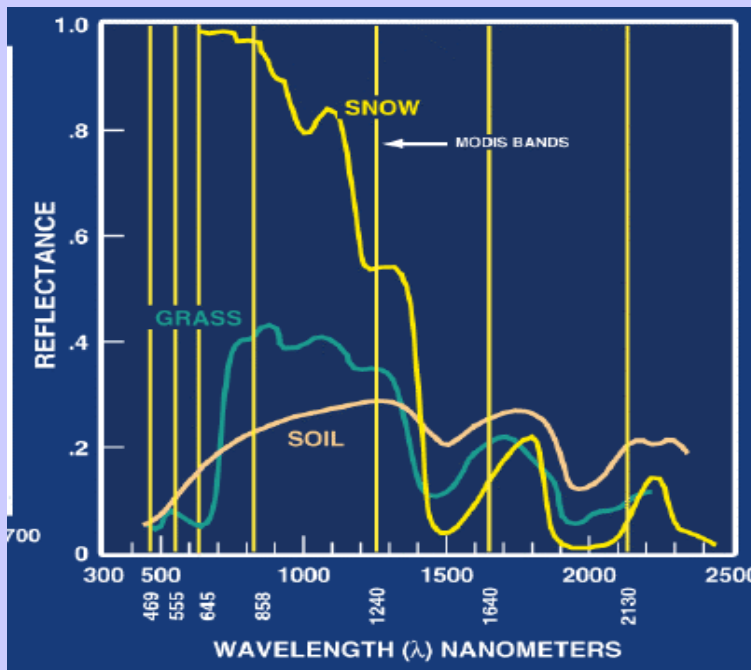
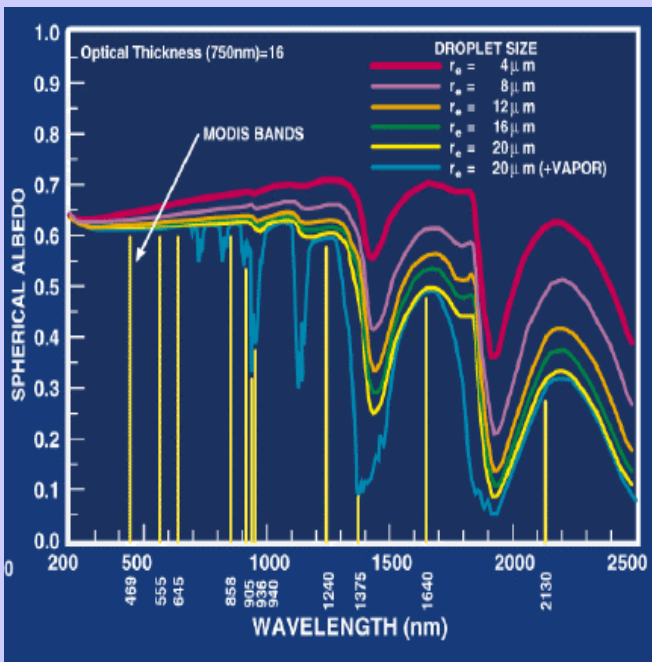
- Spectral radiances (LUT) to derive the aerosol size distribution

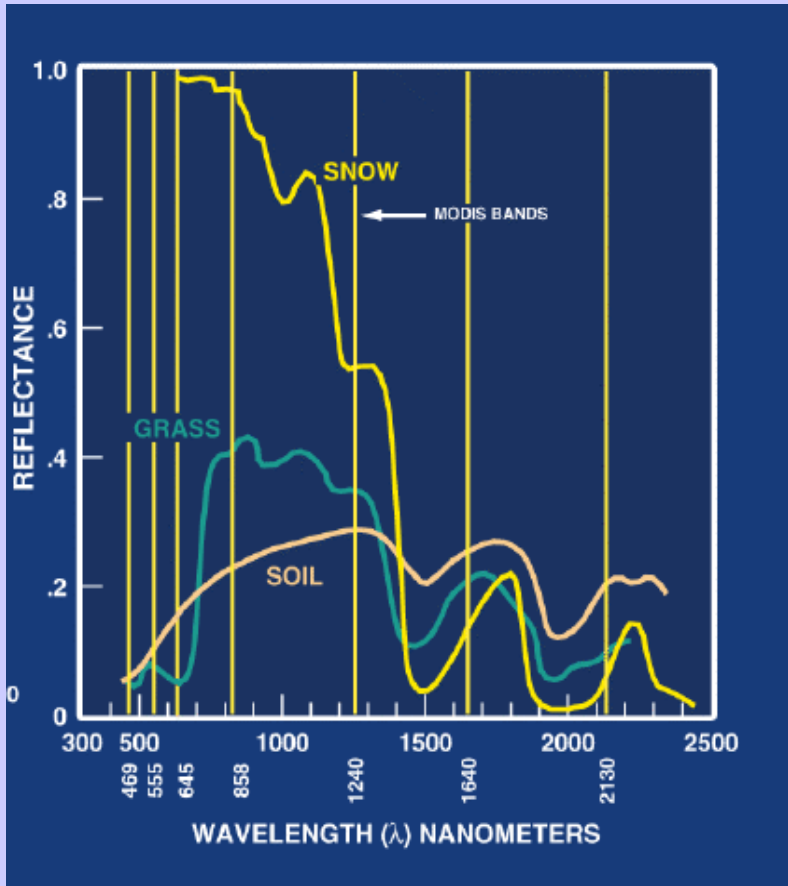
- Two modes (accumulation 0.10-0.25 μm ; coarse 1.0-2.5 μm); ratio is a free parameter

- Radiance at $865\mu\text{m}$ to derive τ

Ocean products :

- The total Spectral Optical thickness
- The effective radius
- The optical thickness of small & large modes/ratio between the 2 modes



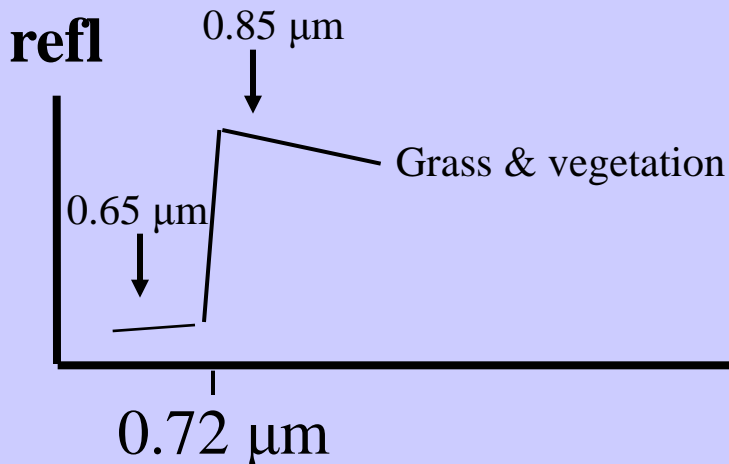


Investigating with Multi-spectral Combinations

Given the spectral response of a surface or atmospheric feature

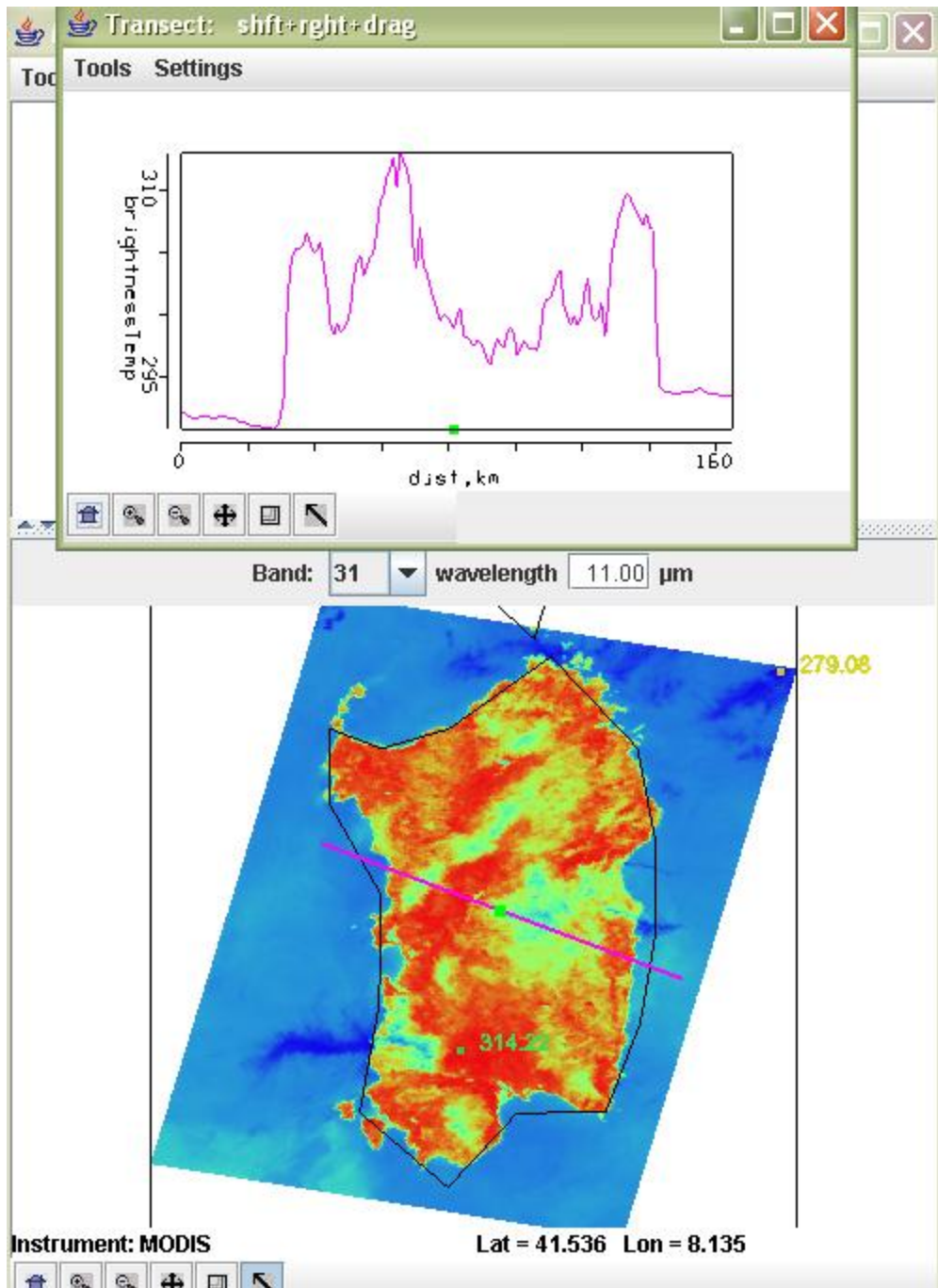
Select a part of the spectrum where the reflectance or absorption changes with wavelength

e.g. reflection from grass



If 0.65 μm and 0.85 μm channels see the same reflectance than surface viewed is not grass;

if 0.85 μm sees considerably higher reflectance than 0.65 μm then surface might be grass



NOTE: transect of BT11 through vegetated to non-vegetated areas in clear skies. – vegetated areas are warmer than the sea but cooler in BT than non-vegetated areas (displayed in RED)

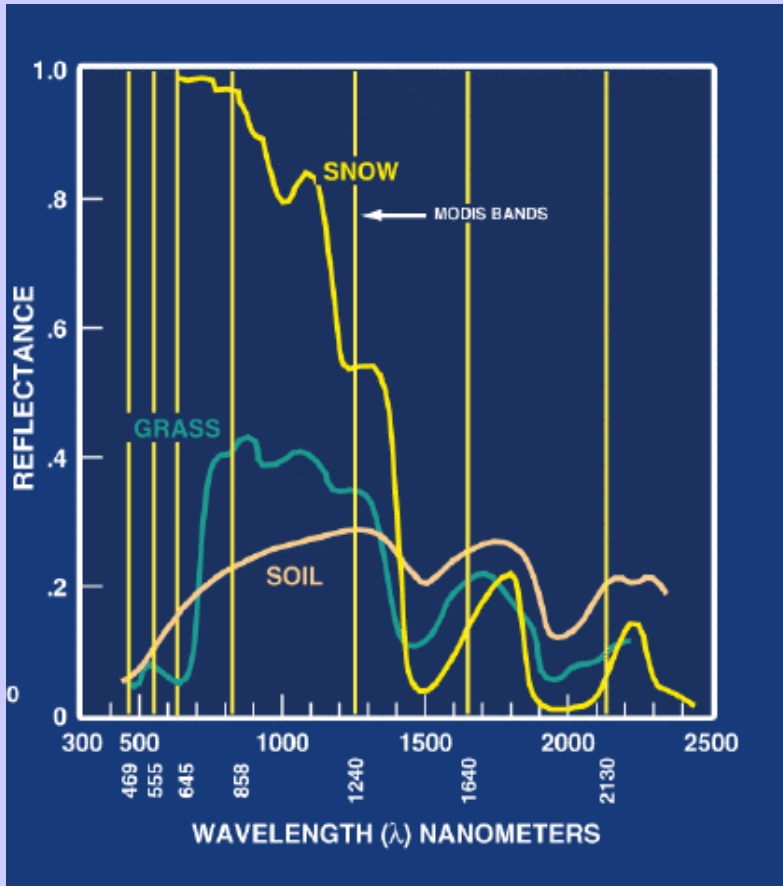
Investigating with Multi-spectral Combinations

Given the spectral response of a surface or atmospheric feature

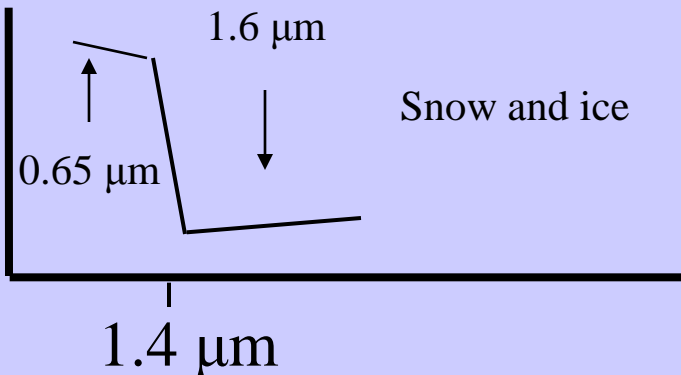
Select a part of the spectrum where the reflectance or absorption changes with wavelength

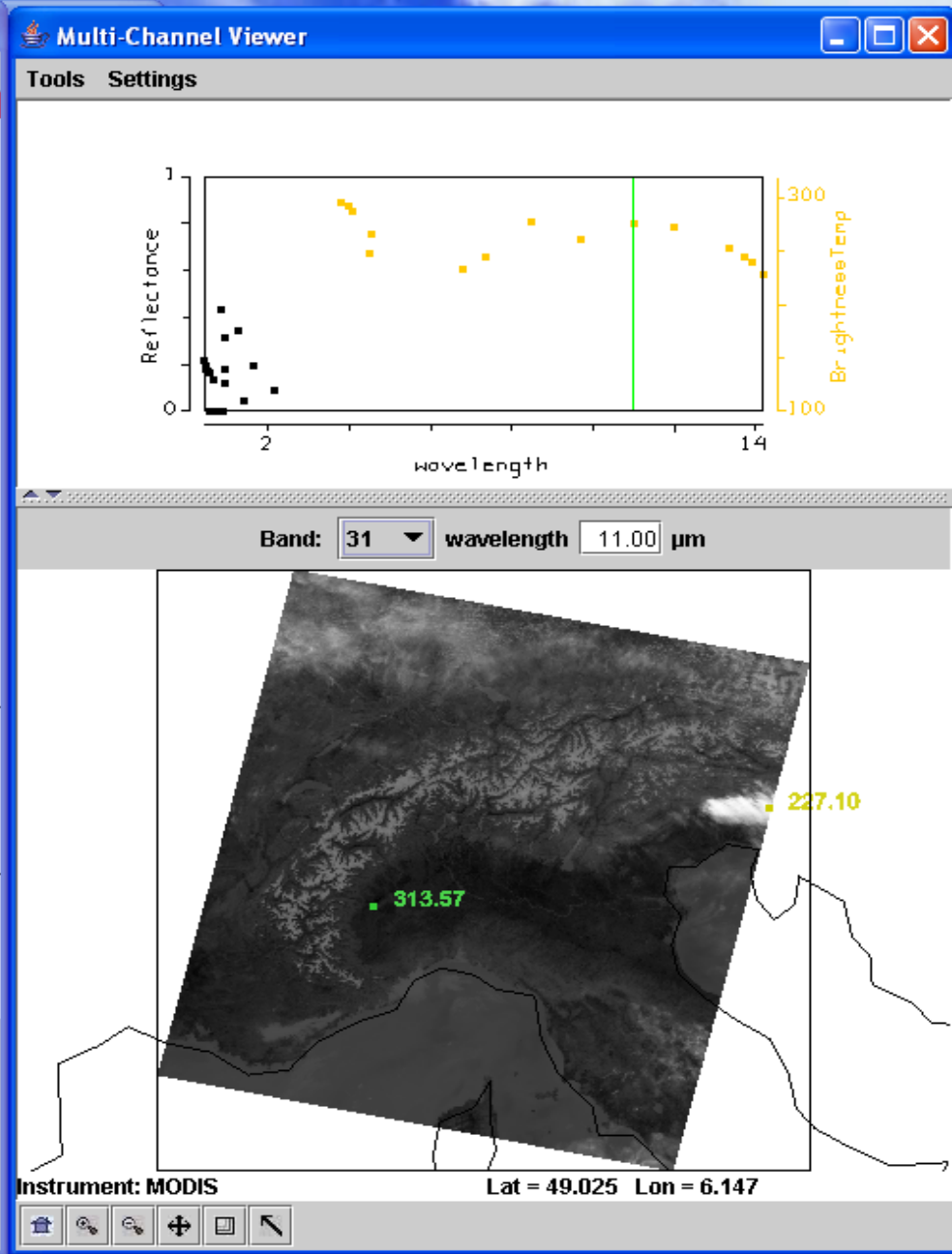
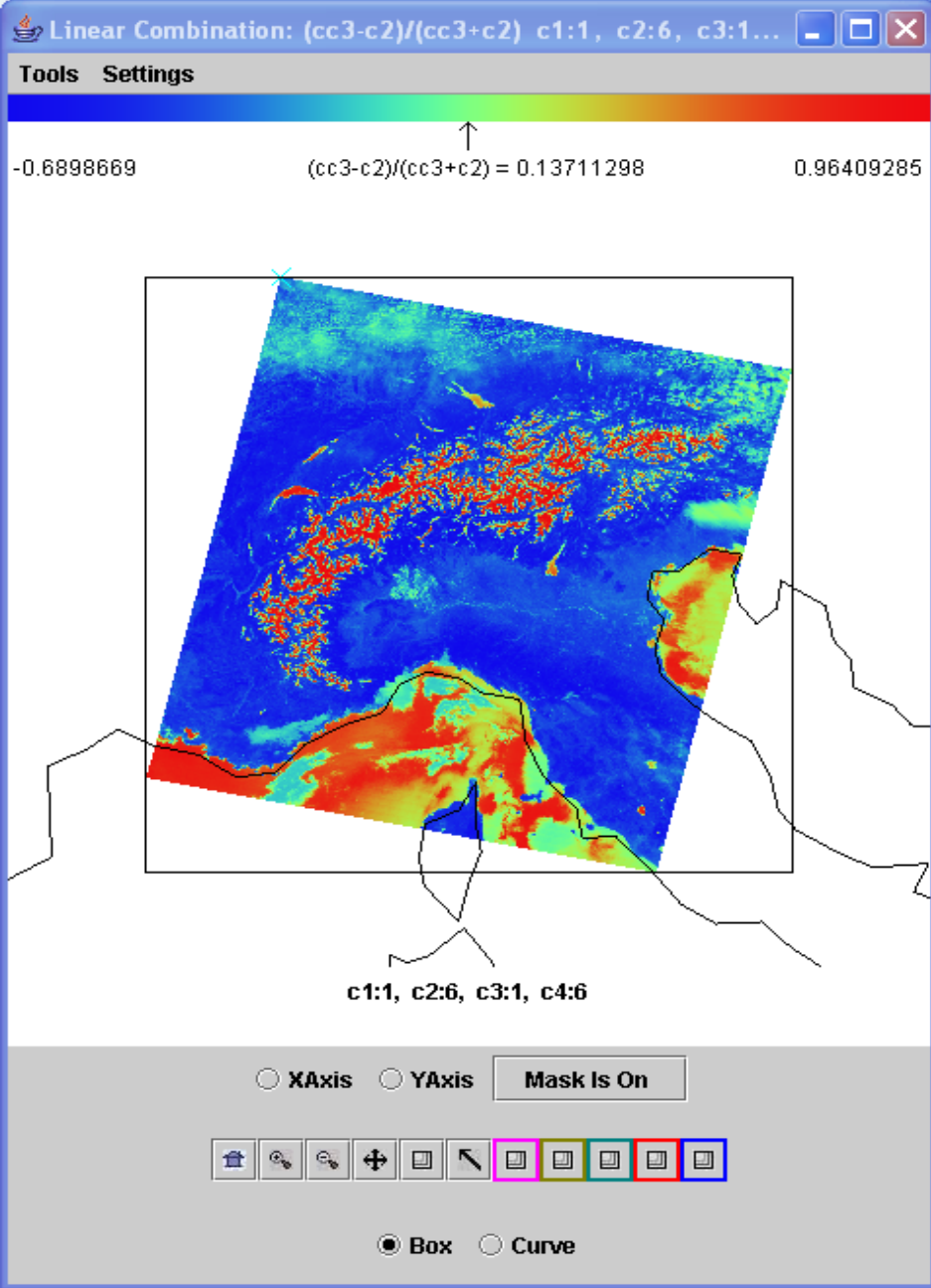
e.g. reflection from snow/ice

If $0.65 \mu\text{m}$ and $1.6 \mu\text{m}$ channels see the same reflectance than surface viewed is not snow;
if $1.6 \mu\text{m}$ sees considerably lower reflectance than $0.65 \mu\text{m}$ then surface might be snow



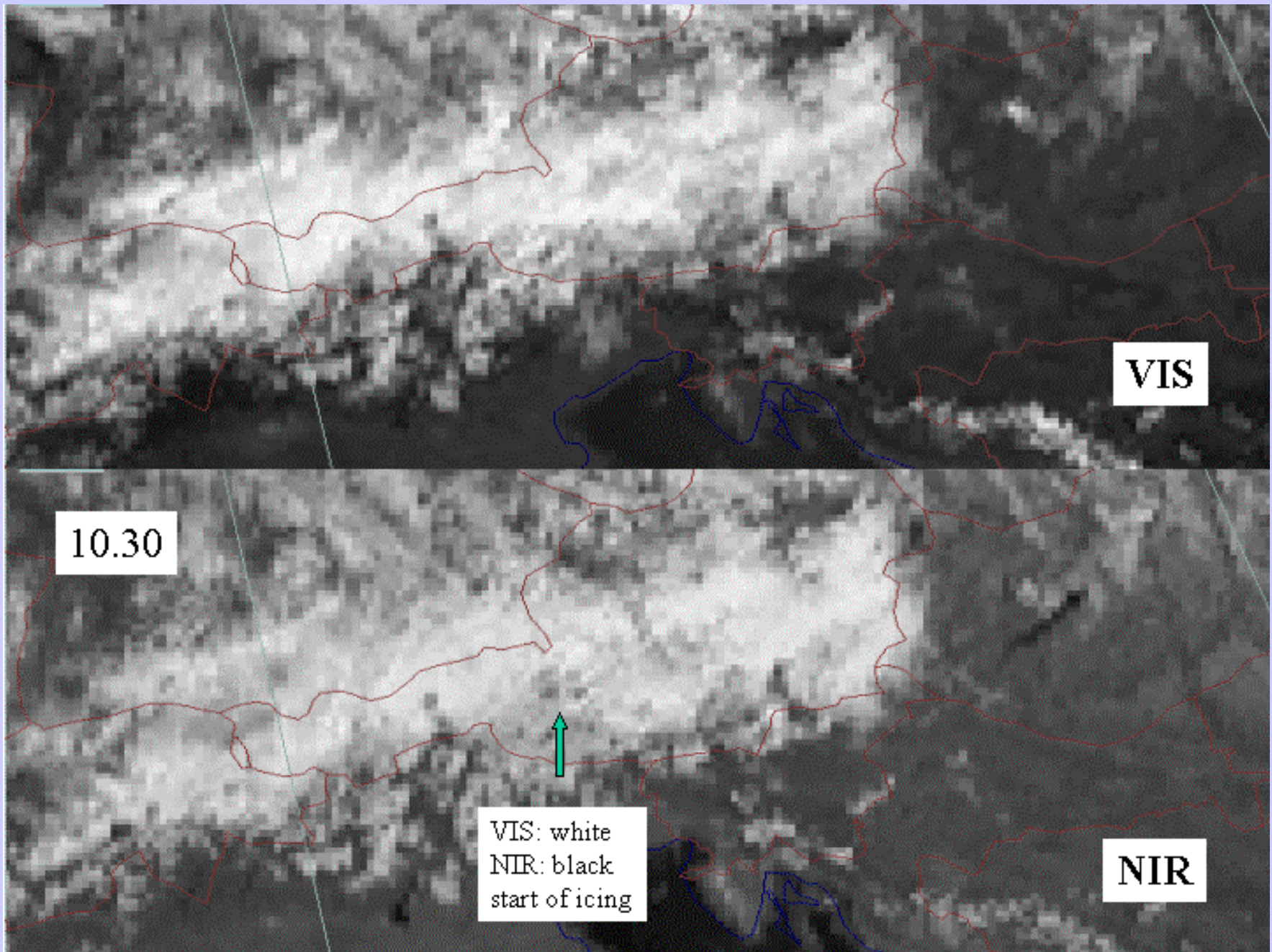
refl



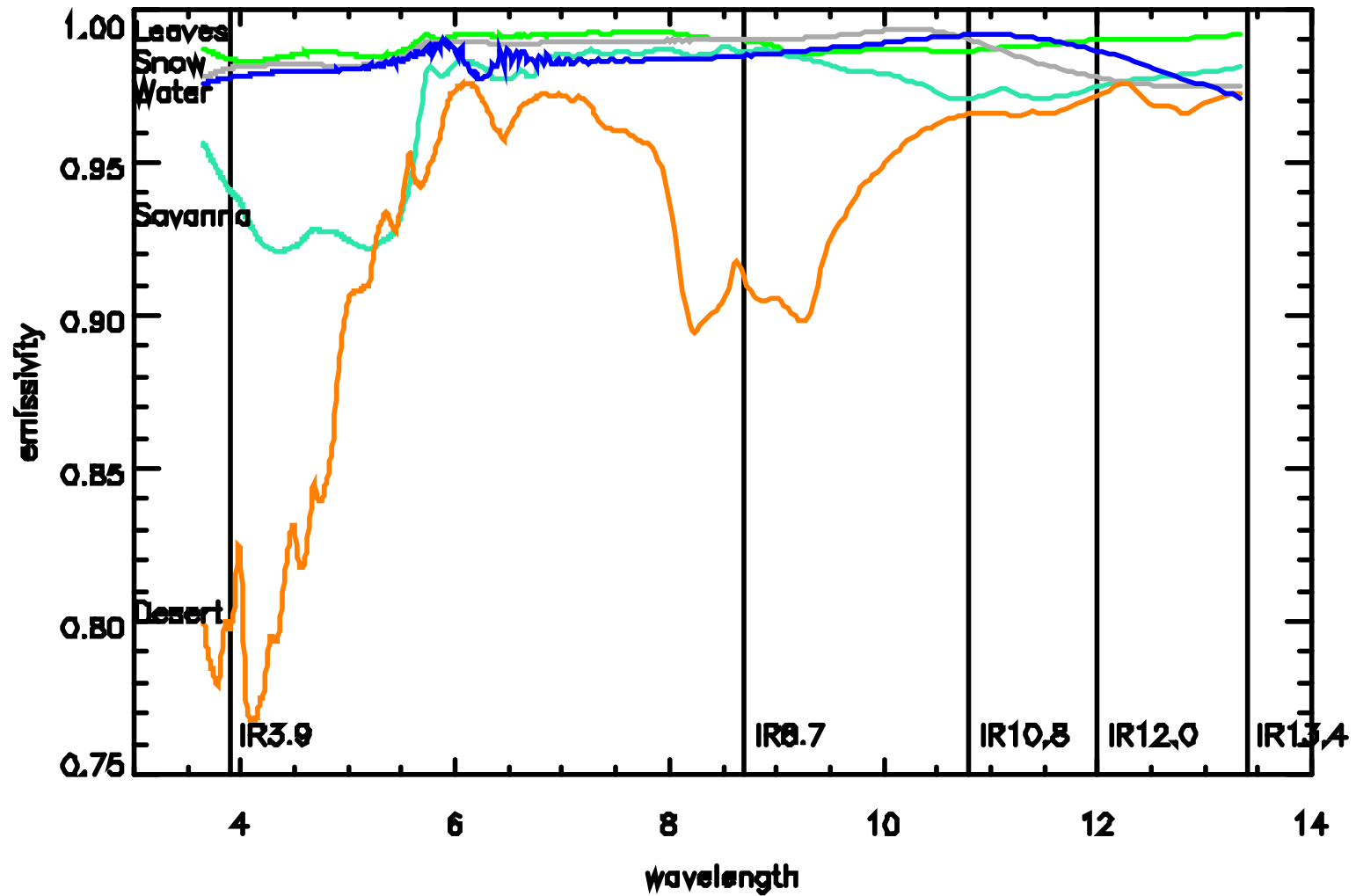


$NDSI = [r_{0.6} - r_{1.6}] / [r_{0.6} + r_{1.6}]$ is near one in snow in Alps

Meteosat-8 sees icing in clouds (Lutz et al)

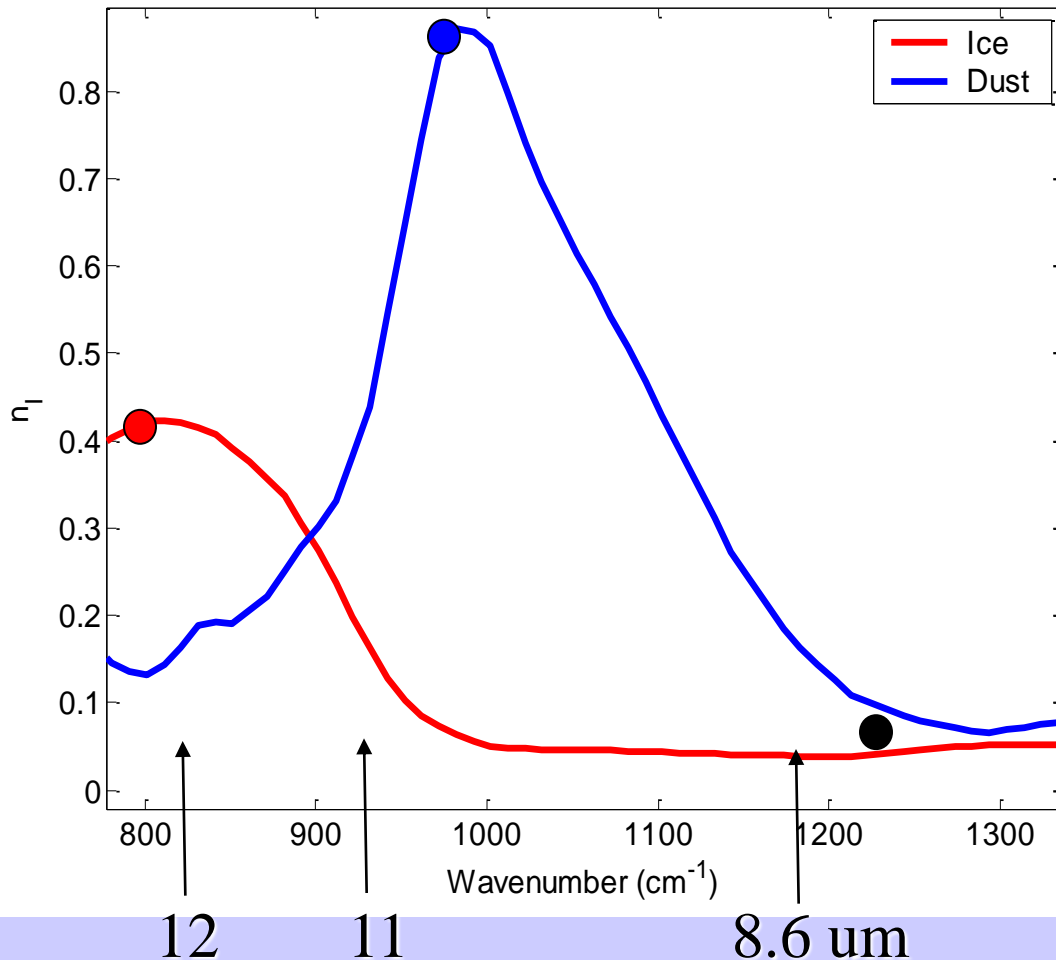


Surface Emissivity



Dust and Cirrus Signals

Imaginary Index of Refraction of Ice and Dust



- Both ice and silicate absorption small in 1200 cm⁻¹ window

- In the 800-1000 cm⁻¹ atmospheric window:

Silicate index increases

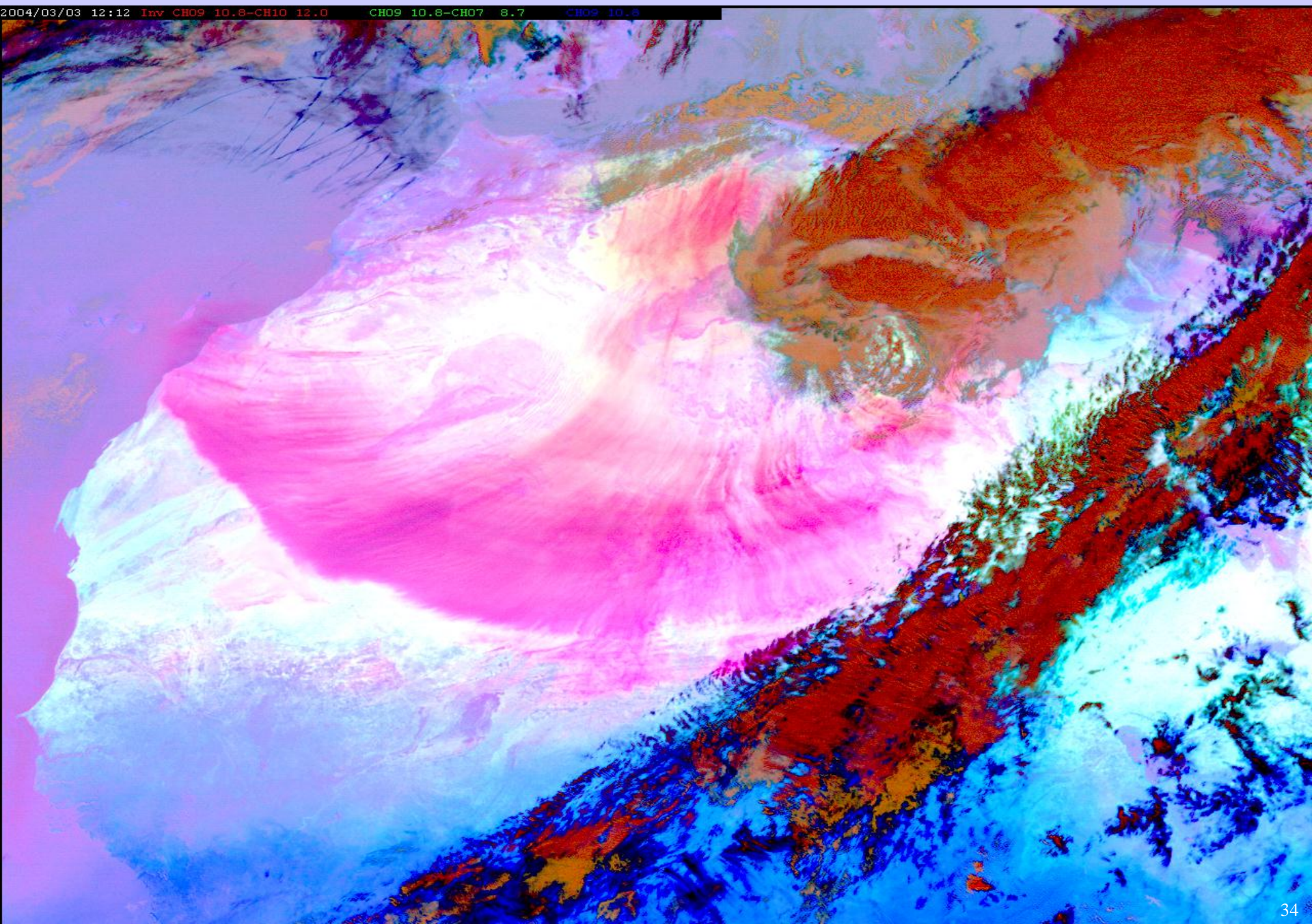
Ice index decreases

with wavenumber

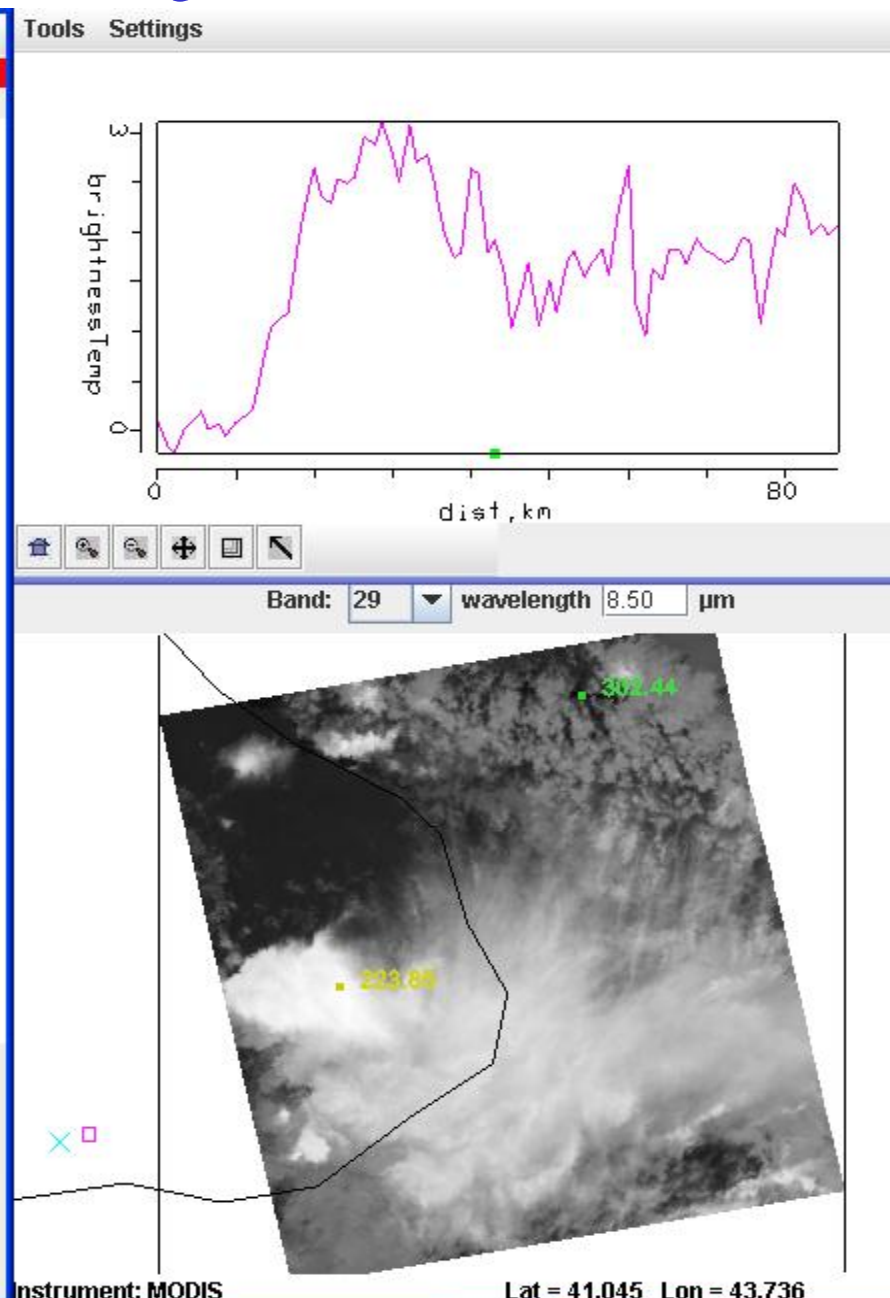
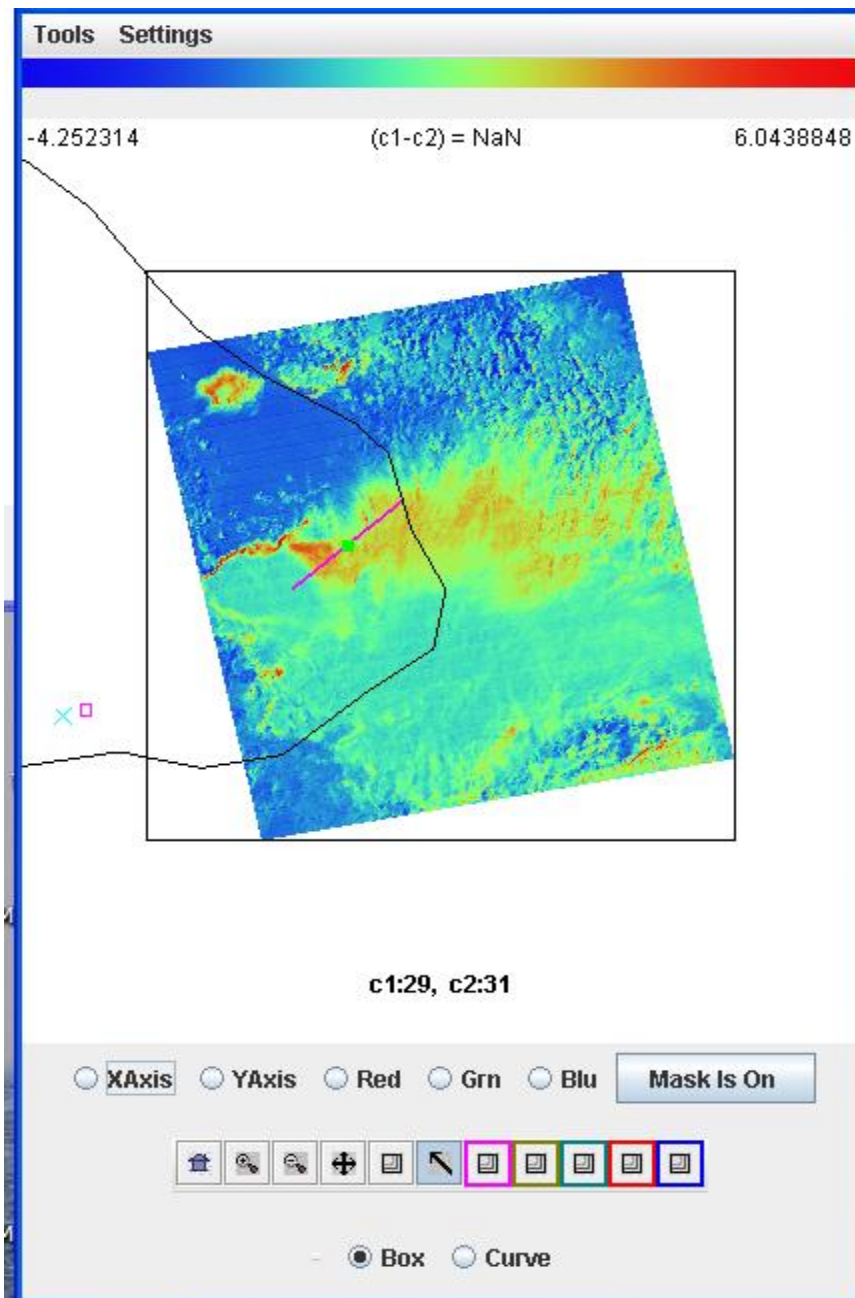
Volz, F.E. : Infrared optical constant of ammonium sulphate, Sahara Dust, volcanic pumice and flash, *Appl Optics* **12** 564-658 (1973)

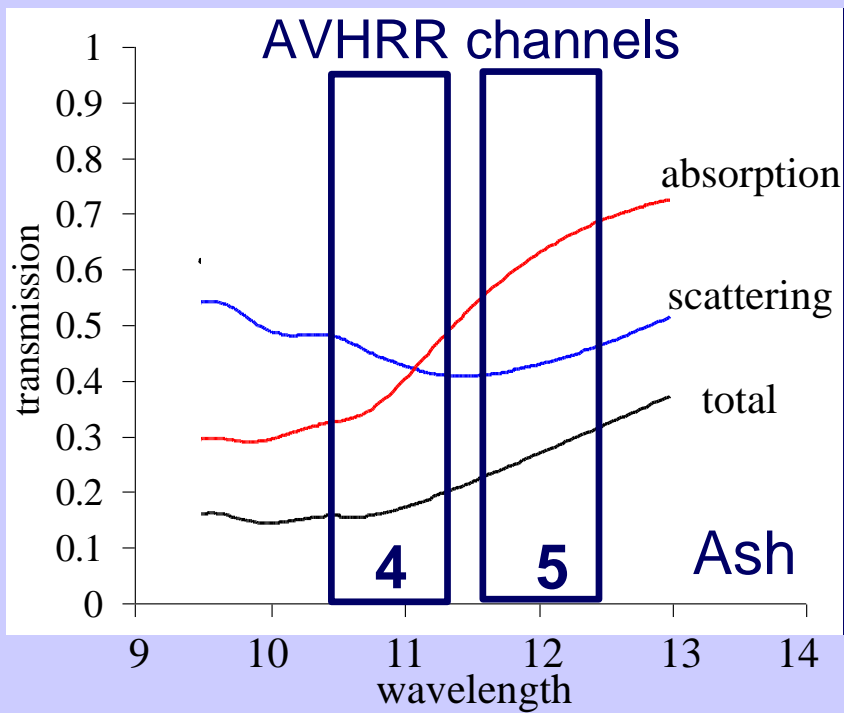
SEVIRI sees dust storm over Africa

2004/03/03 12:12 Inv CH09 10.8-CH10 12.0 CH09 10.8-CH07 8.7 CH09 10.8



[BT8.6-BT11] changes sign from thin (transmitting) to thick (emitting) ice cloud





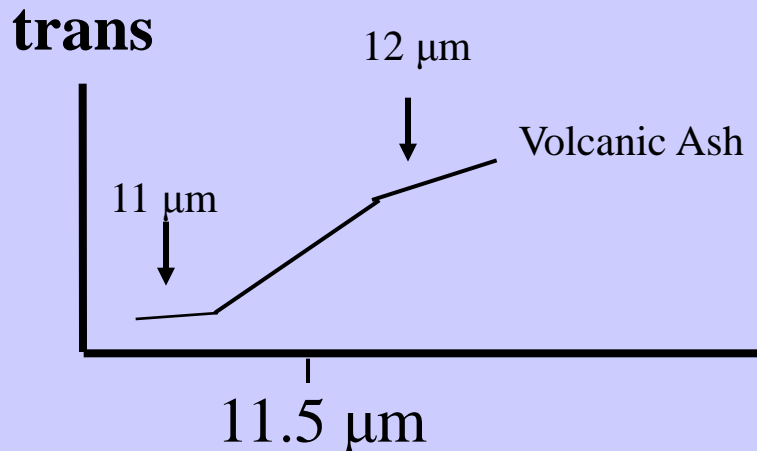
Investigating with Multi-spectral Combinations

Given the spectral response of a surface or atmospheric feature

Select a part of the spectrum where the reflectance or absorption changes with wavelength

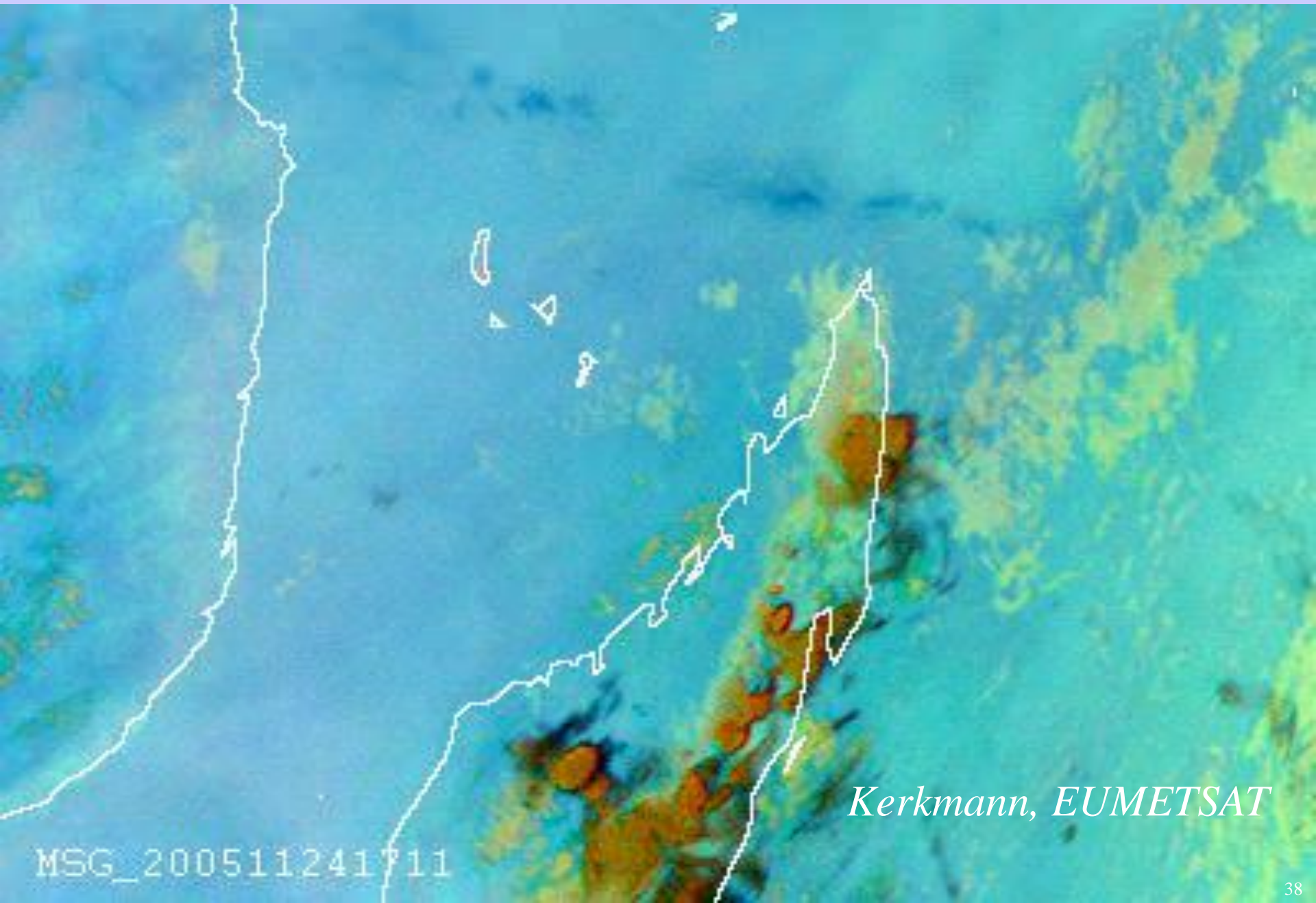
e.g. transmission through ash

If 11 μm sees the same or higher BT than 12 μm the atmosphere viewed does not contain volcanic ash;
 if 12 μm sees considerably higher BT than 11 μm then the atmosphere probably contains volcanic ash



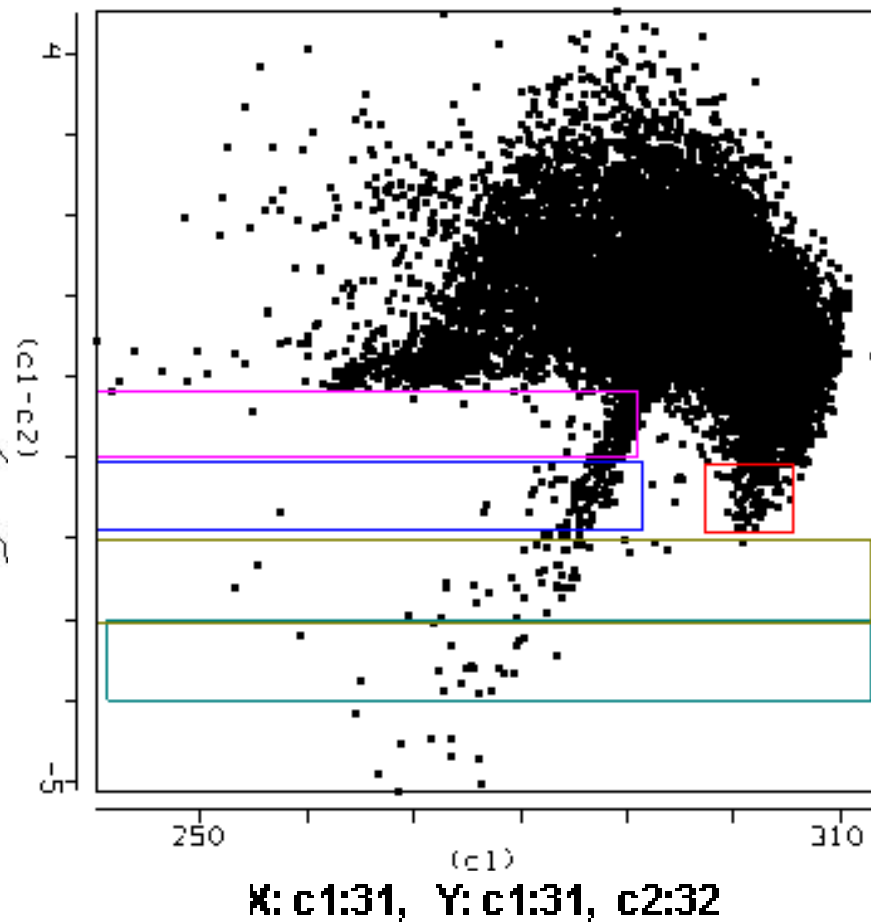
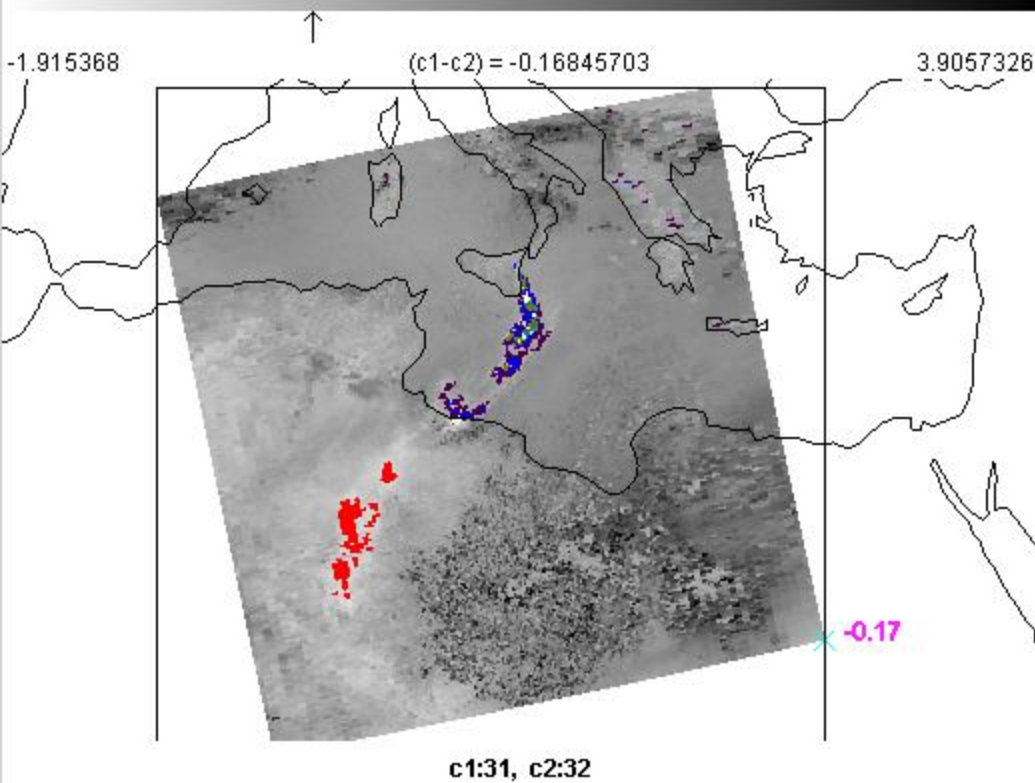
Frank Honey, CSIRO 1980s

SEVIRI sees volcanic ash & SO2 and downwind inhibition of convection



MSG_200511241711

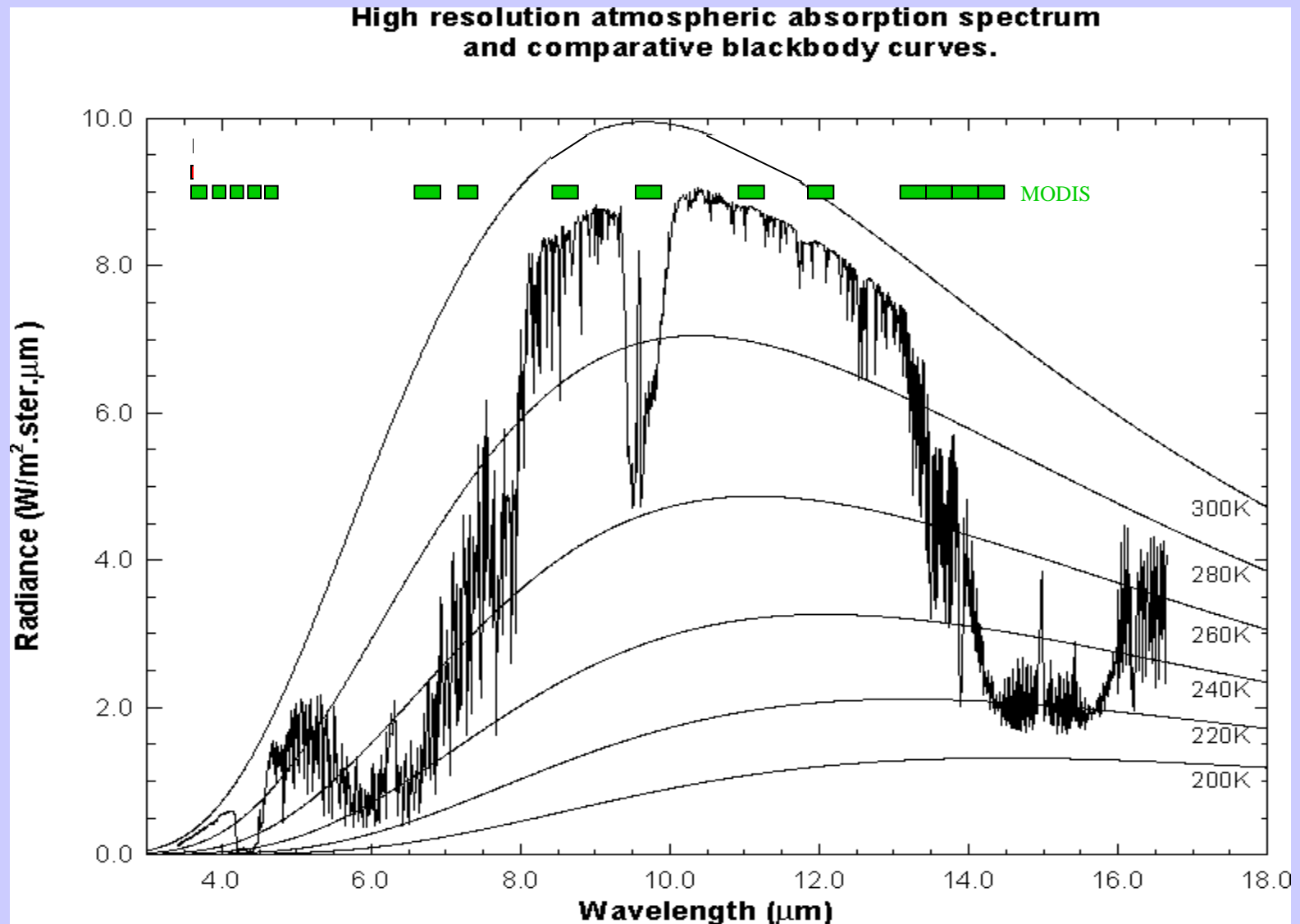
Kerkmann, EUMETSAT



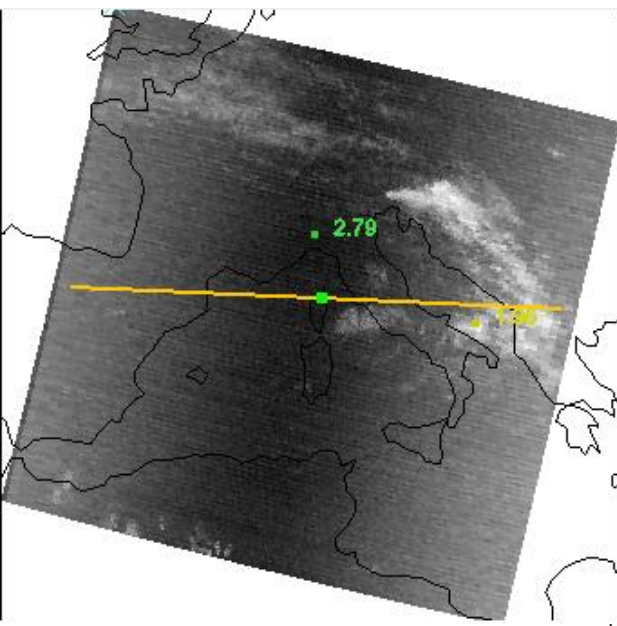
Volcanic Ash is characterised by low brightness temperatures (i.e. High in the atmosphere) and negative differences in band 31-32.

The emissivity of desert at 12 μm is higher than at 11 μm , and hence $\text{BT}(12 \mu\text{m}) > \text{BT}(11 \mu\text{m})$ thus negative values. The red pixels are very arid regions of the desert and are not ash clouds.

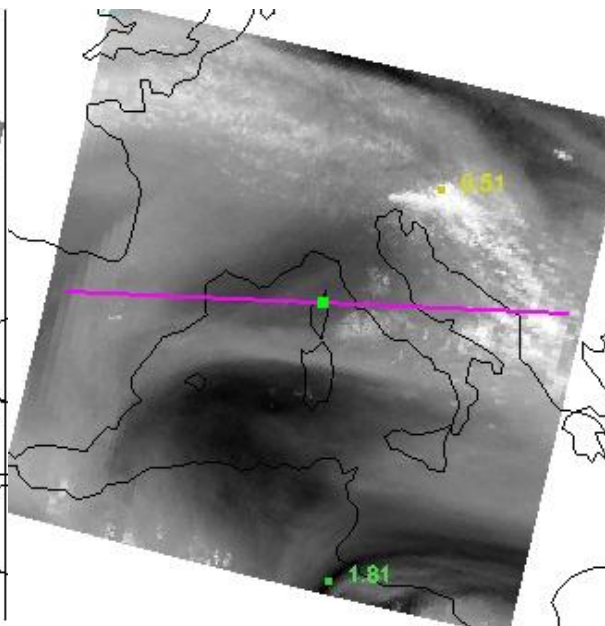
MODIS IR Spectral Bands



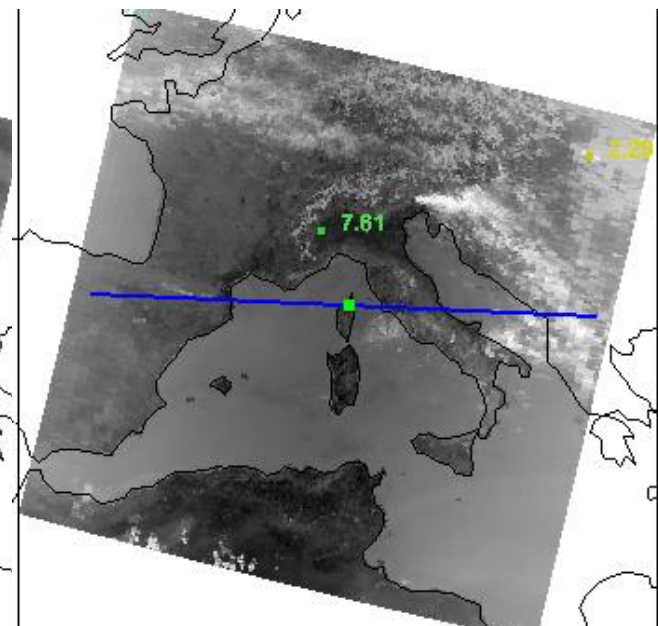
Absorption of the various atmospheric gases in the Infrared channels



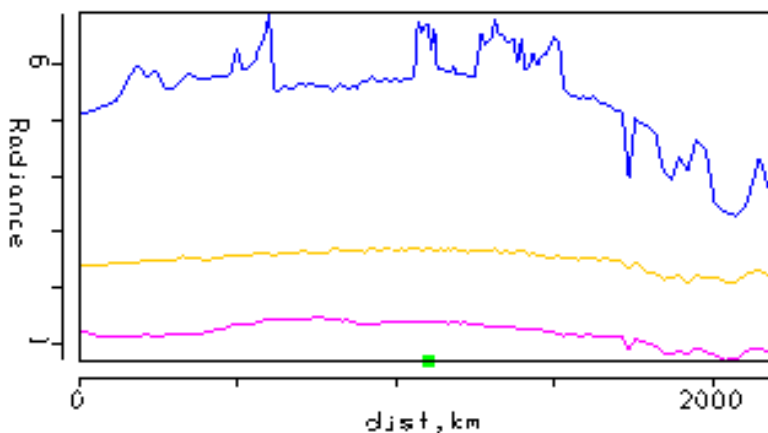
CO₂ absorption at 14.2 μm



H₂O absorption at 6.78 μm



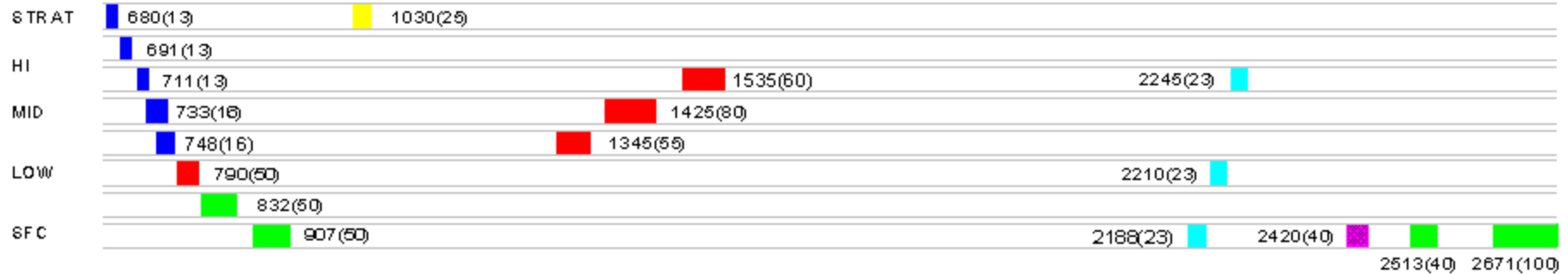
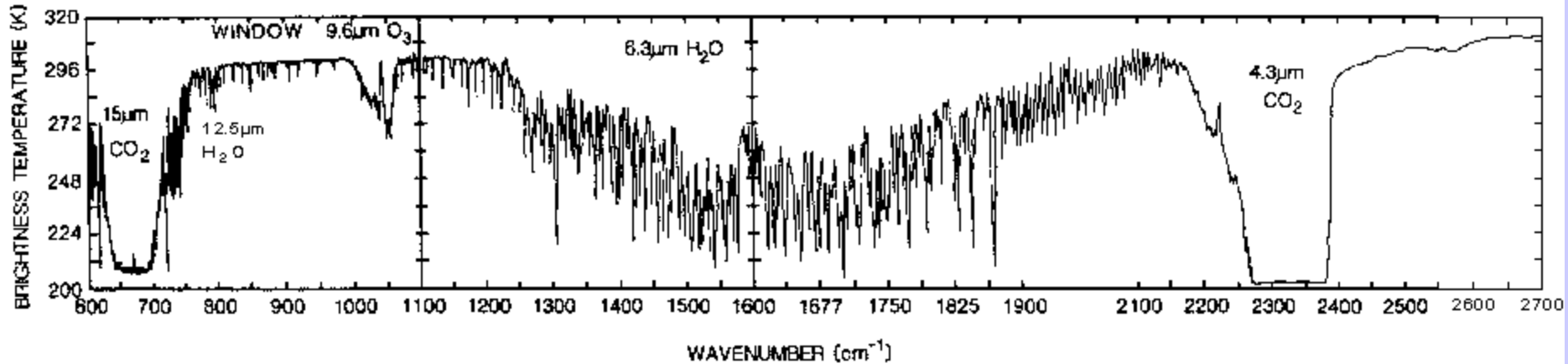
O₃ absorption at 9.70 μm



The surface features cannot be distinguished in the CO₂ and H₂O absorption band. The transect shows that the radiance for CO₂ is always higher than H₂O which states that the weighing function caused by CO₂ absorption is lower than that caused by the H₂O absorption. In other words you could look deeper into the atmosphere at 14.2 μm than at 6.78 μm. The transect also shows that absorption by O₃ is less than H₂O and CO₂ as you can “see” deeper into the atmosphere.

GOES Sounder Spectral Bands: 14.7 to 3.7 um and vis

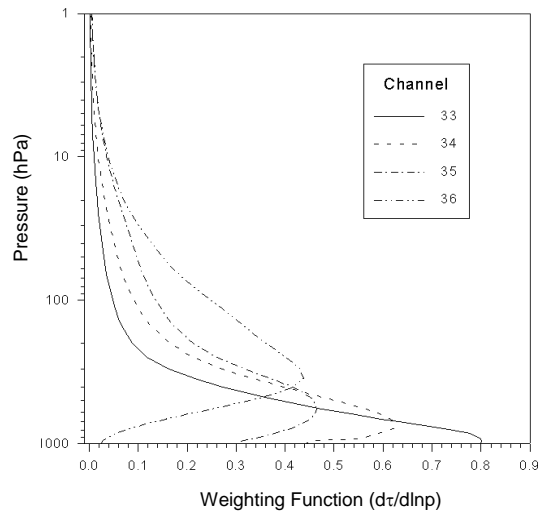
EARTH EMITTED SPECTRA



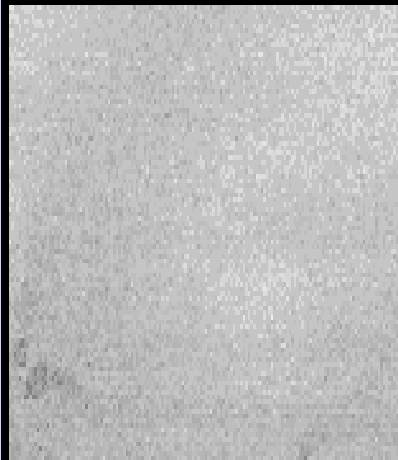
GOES-I SOUNDER SPECTRAL BANDS



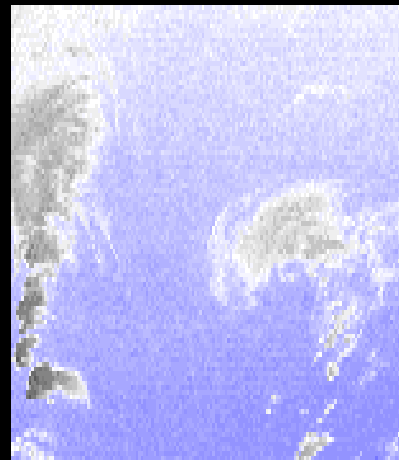
COOPERATIVE INSTITUTE FOR METEOROLOGICAL SATELLITE STUDIES



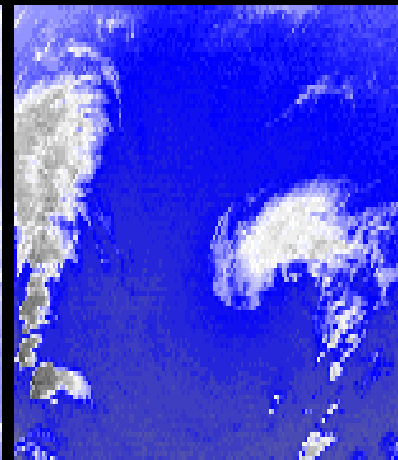
CO2 channels see different layers in the atmosphere



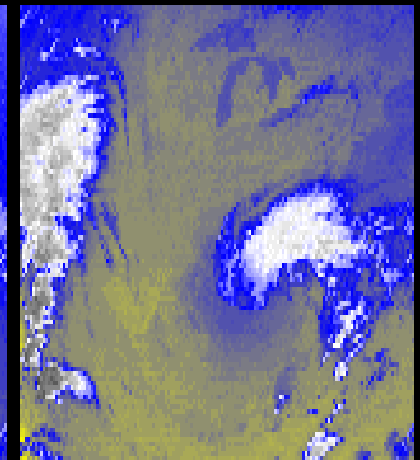
14.2 μm



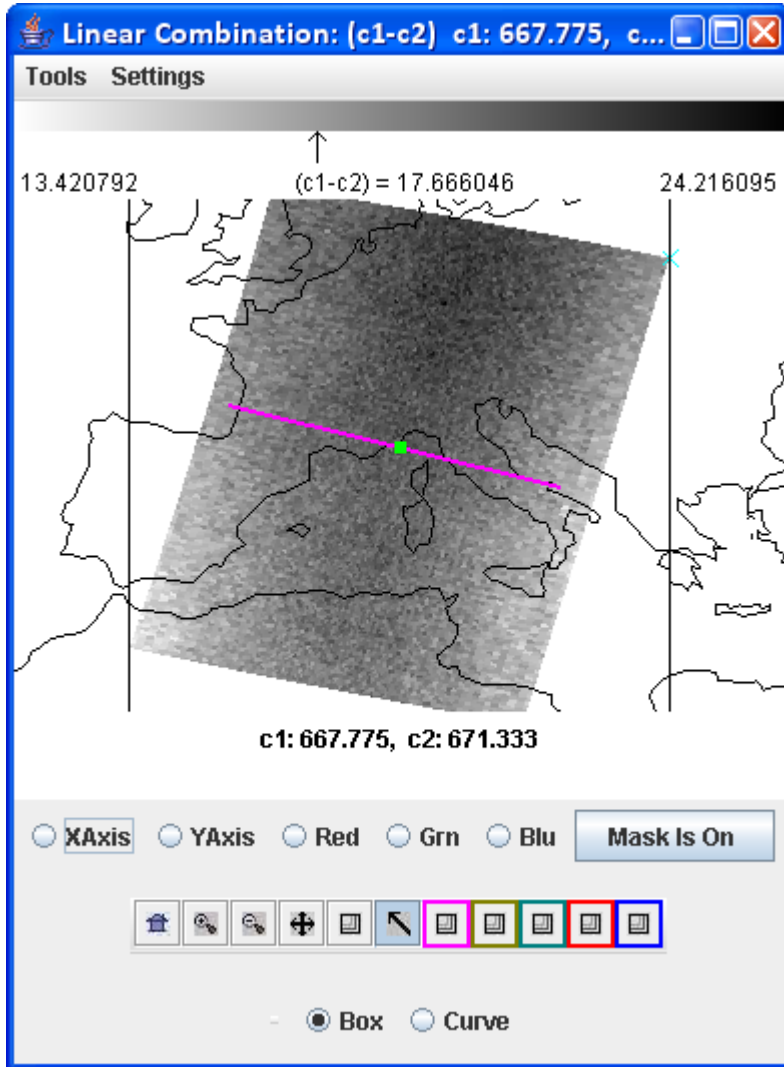
13.9 μm



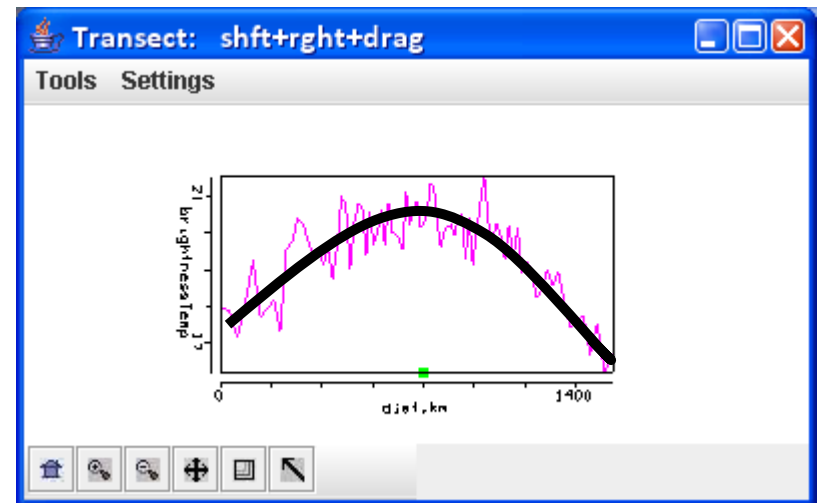
13.6 μm



13.3 μm



Perpedicular at nadir



Limb darkening

Radiative Transfer Equation

When reflection from the earth surface is also considered, the RTE for infrared radiation can be written

$$I_{\lambda} = \varepsilon_{\lambda}^{\text{sfc}} B_{\lambda}(T_s) \tau_{\lambda}(p_s) + \int_{p_s}^0 B_{\lambda}(T(p)) F_{\lambda}(p) [d\tau_{\lambda}(p) / dp] dp$$

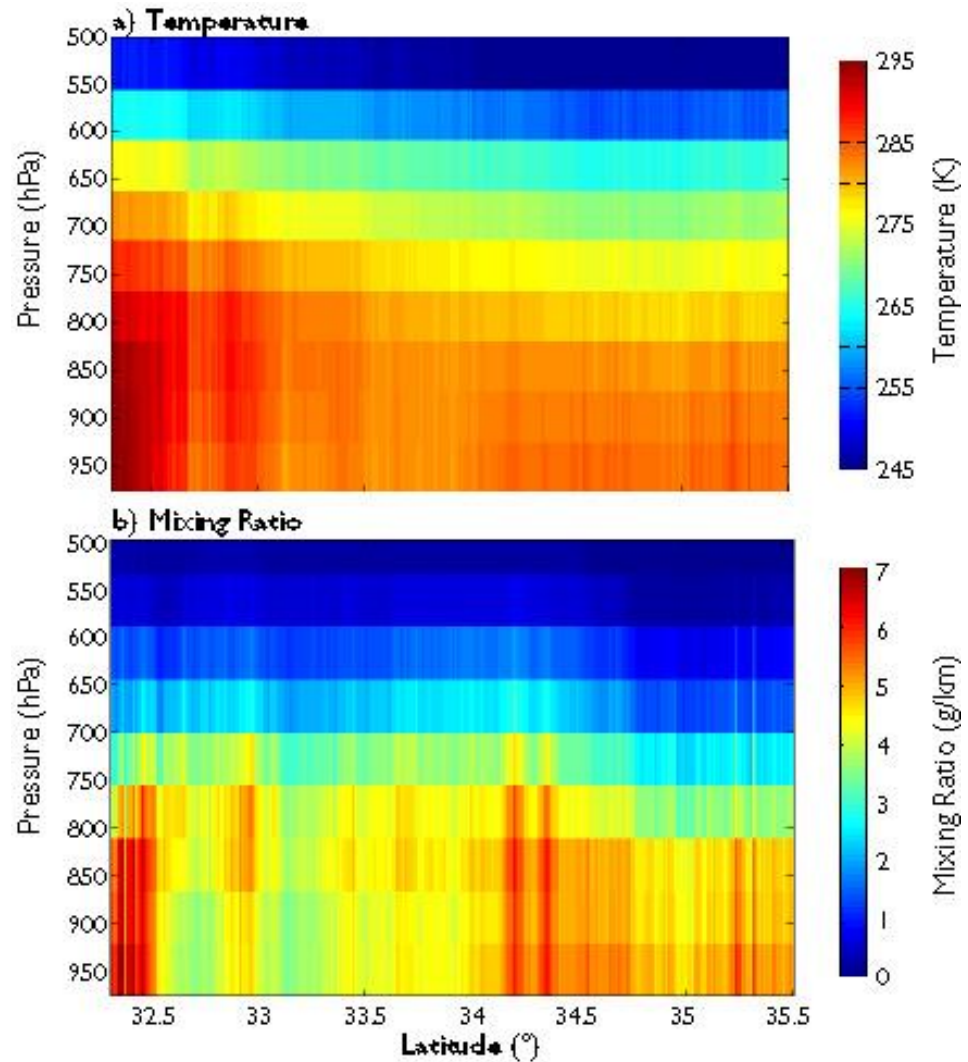
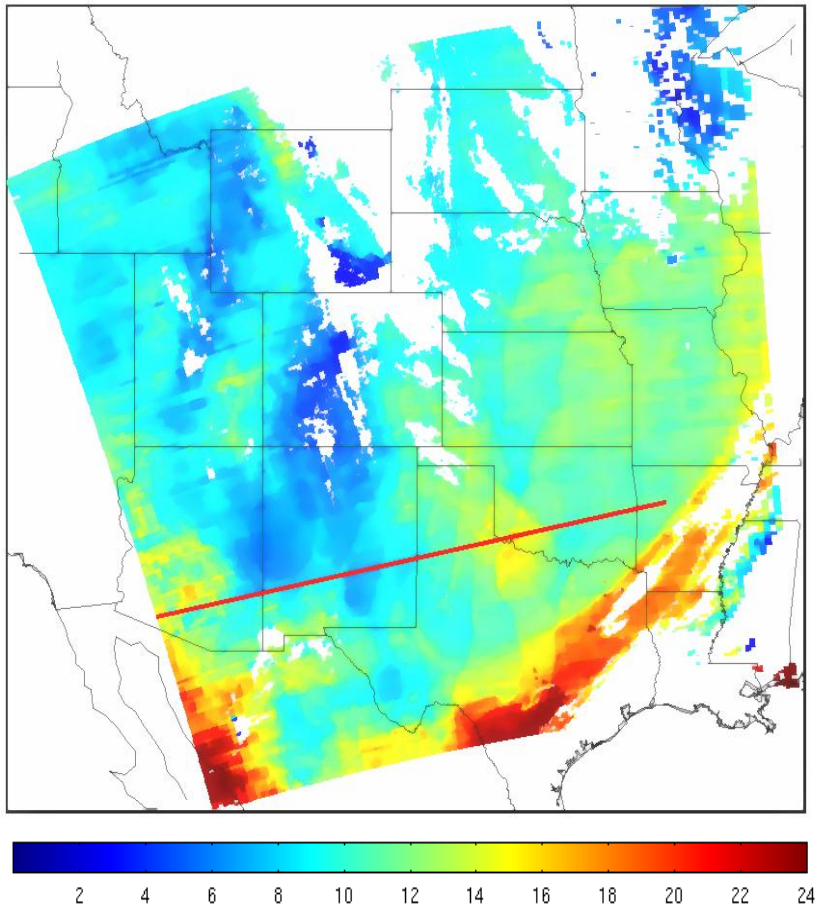
where

$$F_{\lambda}(p) = \{ 1 + (1 - \varepsilon_{\lambda}) [\tau_{\lambda}(p_s) / \tau_{\lambda}(p)]^2 \}$$

The first term is the spectral radiance emitted by the surface and attenuated by the atmosphere, often called the boundary term and the second term is the spectral radiance emitted to space by the atmosphere directly or by reflection from the earth surface.

The atmospheric contribution is the weighted sum of the Planck radiance contribution from each layer, where the weighting function is $[d\tau_{\lambda}(p) / dp]$. This weighting function is an indication of where in the atmosphere the majority of the radiation for a given spectral band comes from.

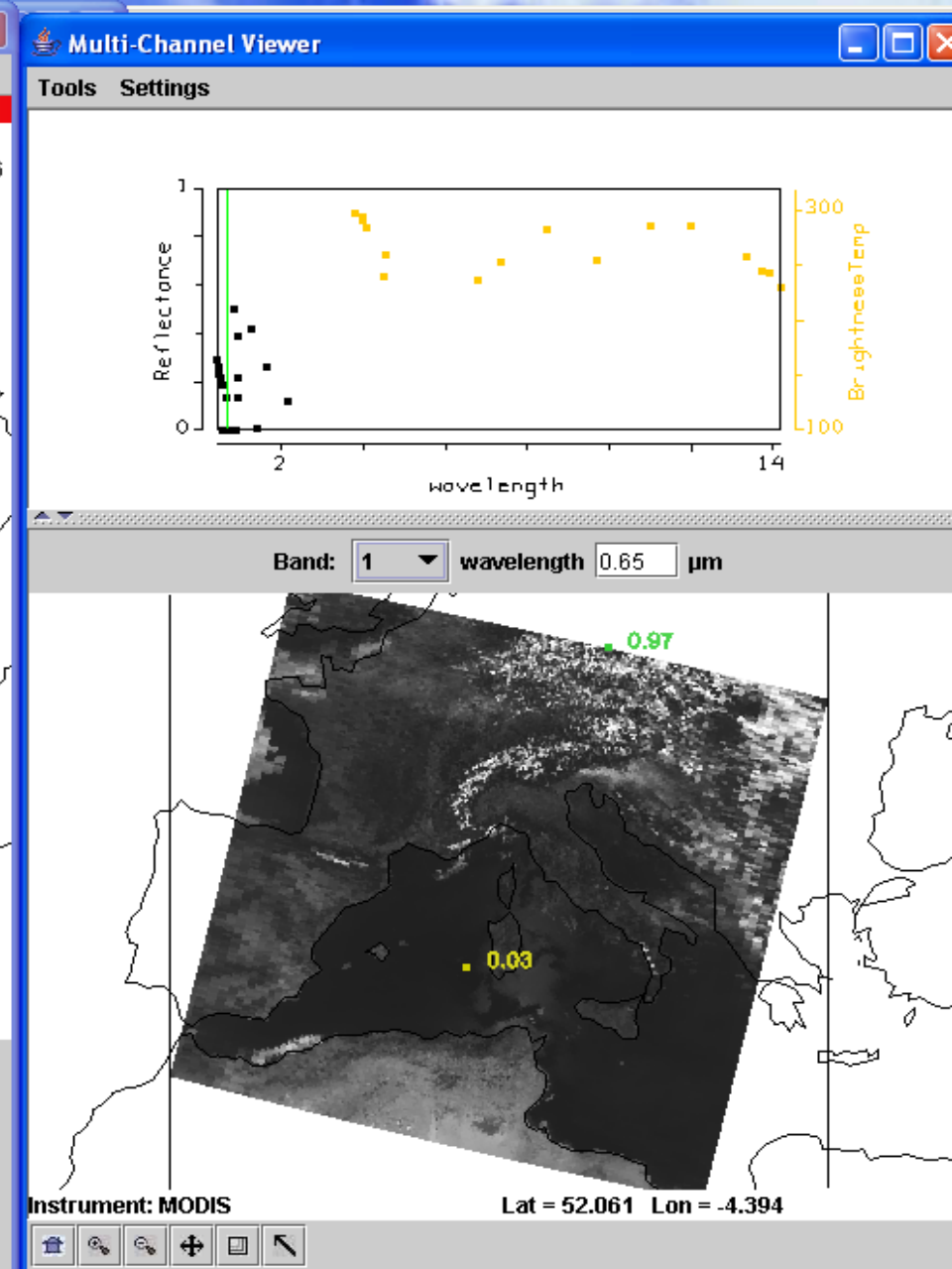
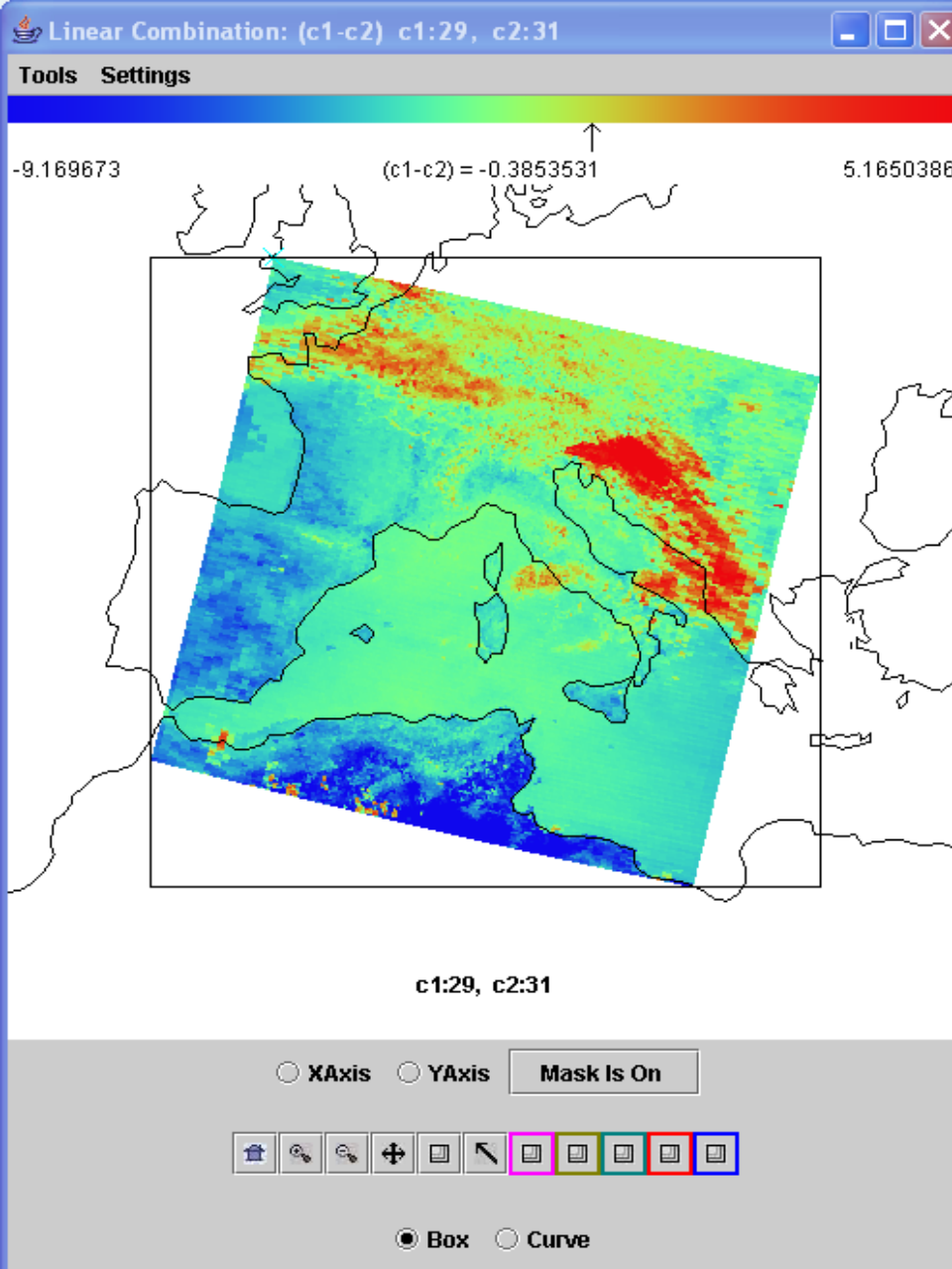
MODIS TPW



Clear sky layers of temperature and moisture on 2 June 2001

Cloud Mask Tests

- BT11 clouds over ocean
- BT13.9 high clouds
- BT6.7 high clouds
- BT3.9-BT11 broken or scattered clouds
- BT11-BT12 high clouds in tropics
- BT8.6-BT11 ice clouds
- BT6.7-BT11 or BT13.9-BT11 clouds in polar regions
- BT11+aPW(BT11-BT12) clouds over ocean
- r0.65 clouds over land
- r0.85 clouds over ocean
- r1.38 thin cirrus
- r1.6 clouds over snow, ice cloud
- r0.85/r0.65 or NDVI clouds over vegetation
- σ (BT11) clouds over ocean



Ice clouds are revealed with $BT_{8.6} - BT_{11} > 0$ & water clouds and fog show in $r_{0.65}$

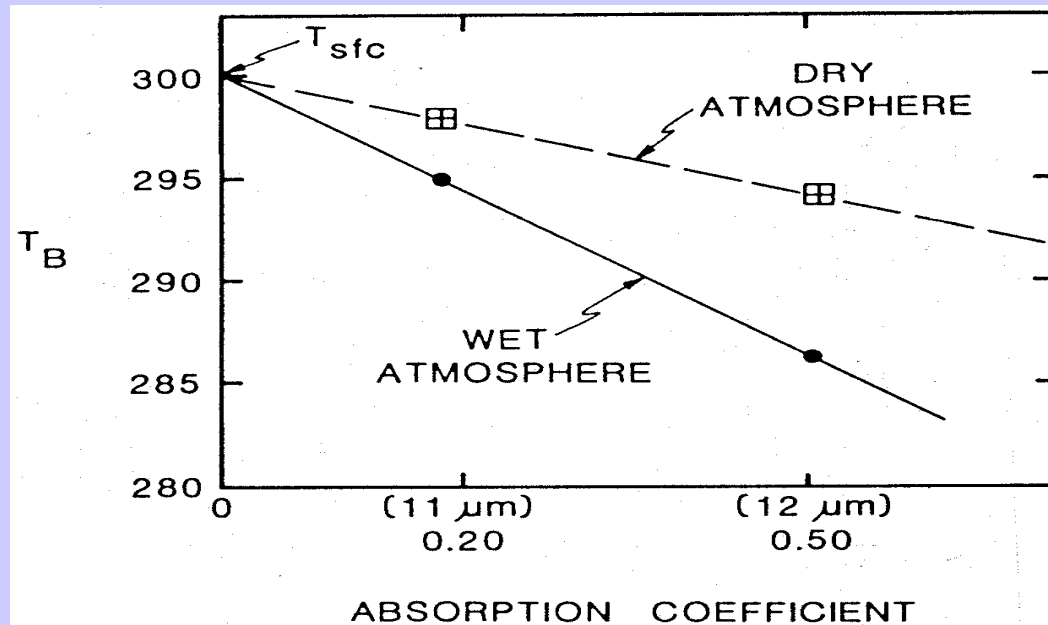
Moisture

Moisture attenuation in atmospheric windows varies linearly with optical depth.

$$\tau_\lambda = e^{-k_\lambda u} \approx 1 - k_\lambda u$$

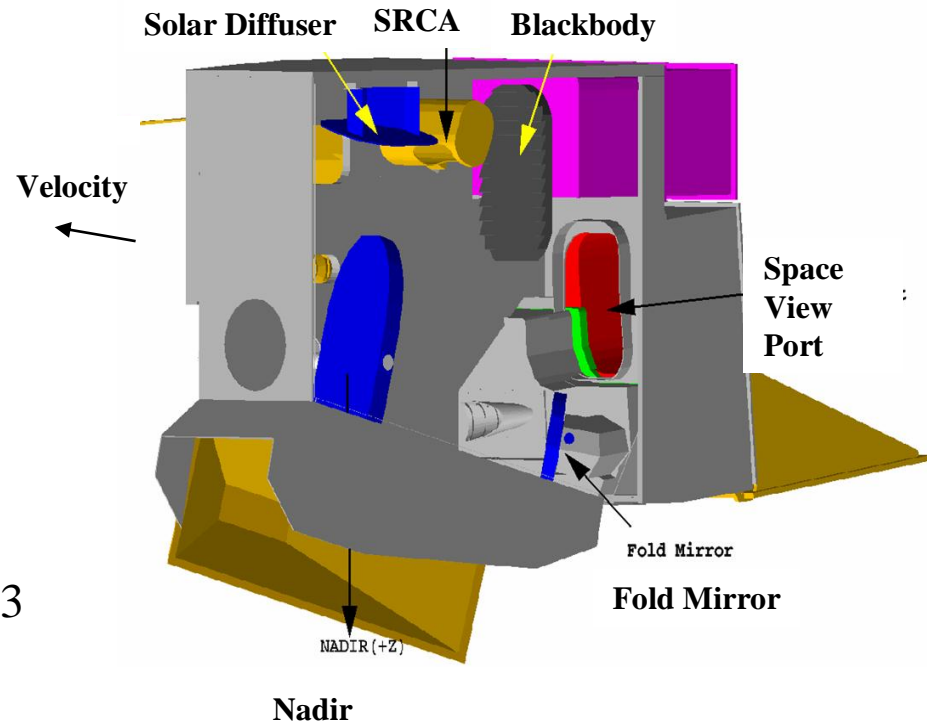
For same atmosphere, deviation of brightness temperature from surface temperature is a linear function of absorbing power. Thus moisture corrected SST can be inferred by using split window measurements and extrapolating to zero k_λ

Moisture content of atmosphere inferred from slope of linear relation.

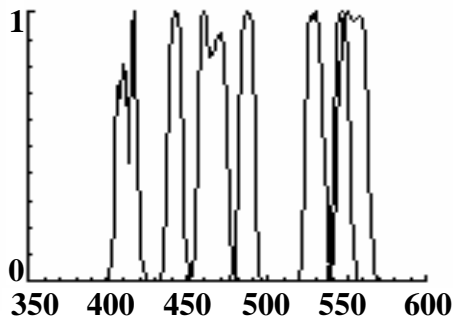


MODIS Instrument Overview

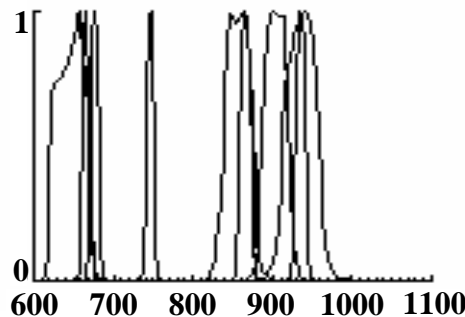
- 36 spectral bands (490 detectors) cover wavelength range from 0.4 to 14.5 μm
- Spatial resolution at nadir: 250m (2 bands), 500m (5 bands) and 1000m
- 4 FPAs: VIS, NIR, SMIR, LWIR
- On-Board Calibrators: SD/SDSM, SRCA, and BB (plus space view)
- 12 bit (0-4095) dynamic range
- 2-sided Paddle Wheel Scan Mirror scans 2330 km swath in 1.47 sec
- Day data rate = 10.6 Mbps; night data rate = 3.3 Mbps (100% duty cycle, 50% day and 50% night)



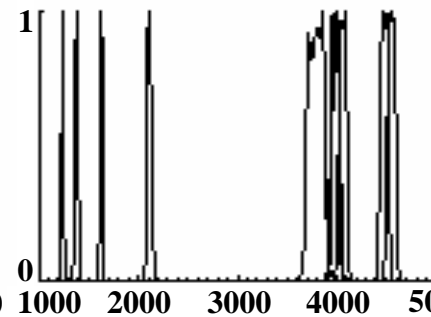
VIS



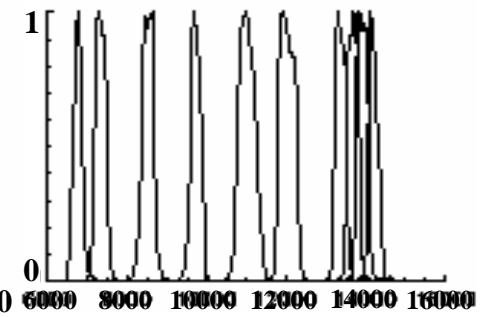
NIR



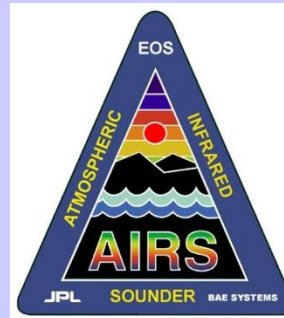
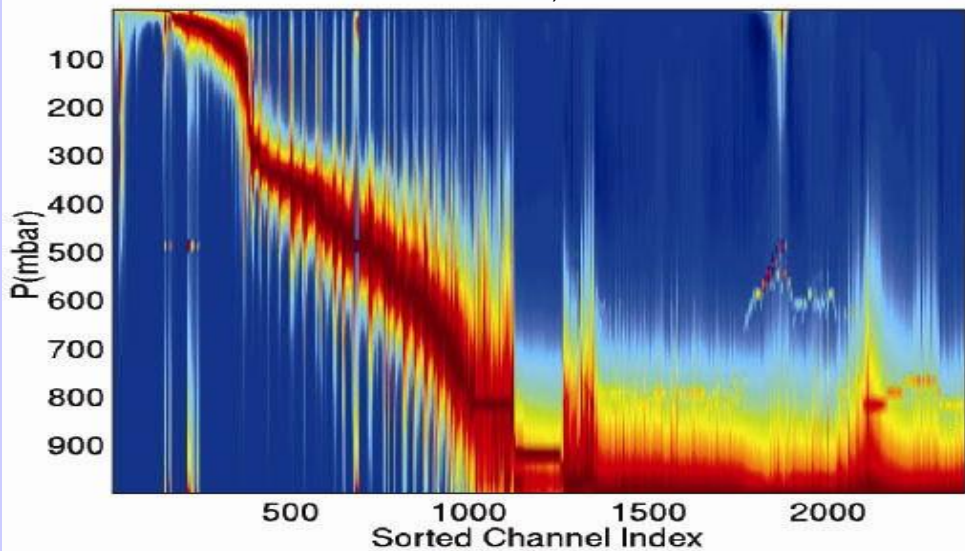
S/MWIR



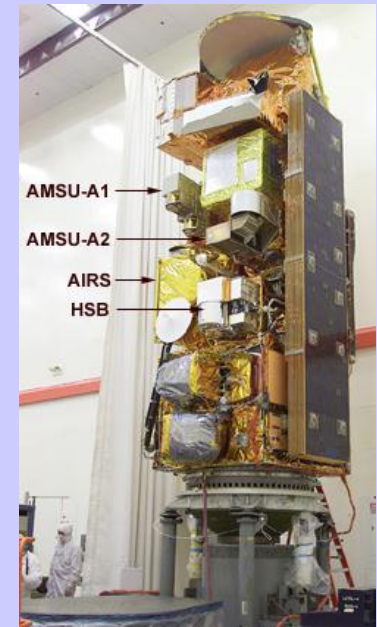
LWIR



temperature weighting functions sorted by pressure of their peak (blue = 0)



AIRS On Aqua

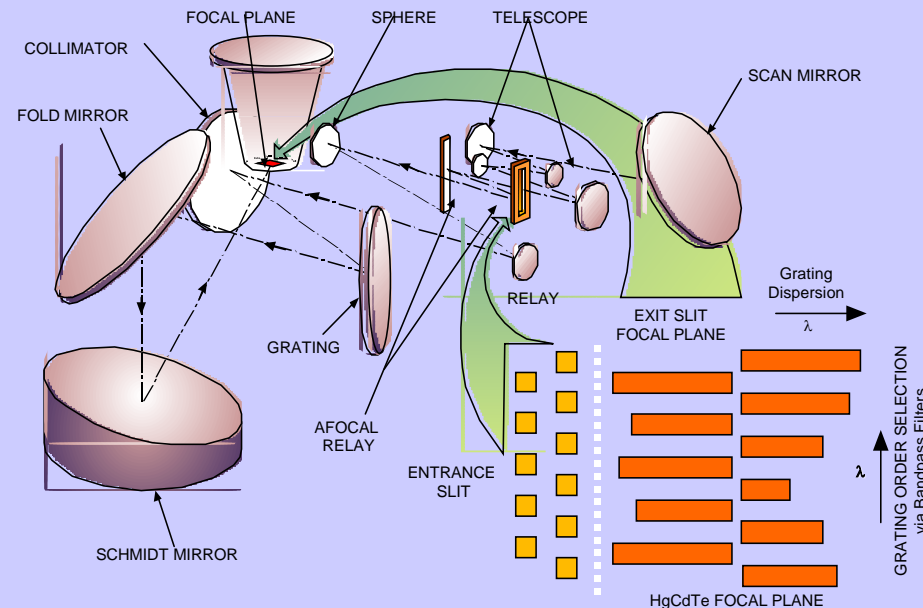


Instrument

- Hyperspectral radiometer with **resolution of 0.5 – 2 cm⁻¹**
- Extremely well calibrated pre-launch
- **Spectral range: 650 – 2700 cm⁻¹**
- Associated microwave instruments (AMSU, HSB)

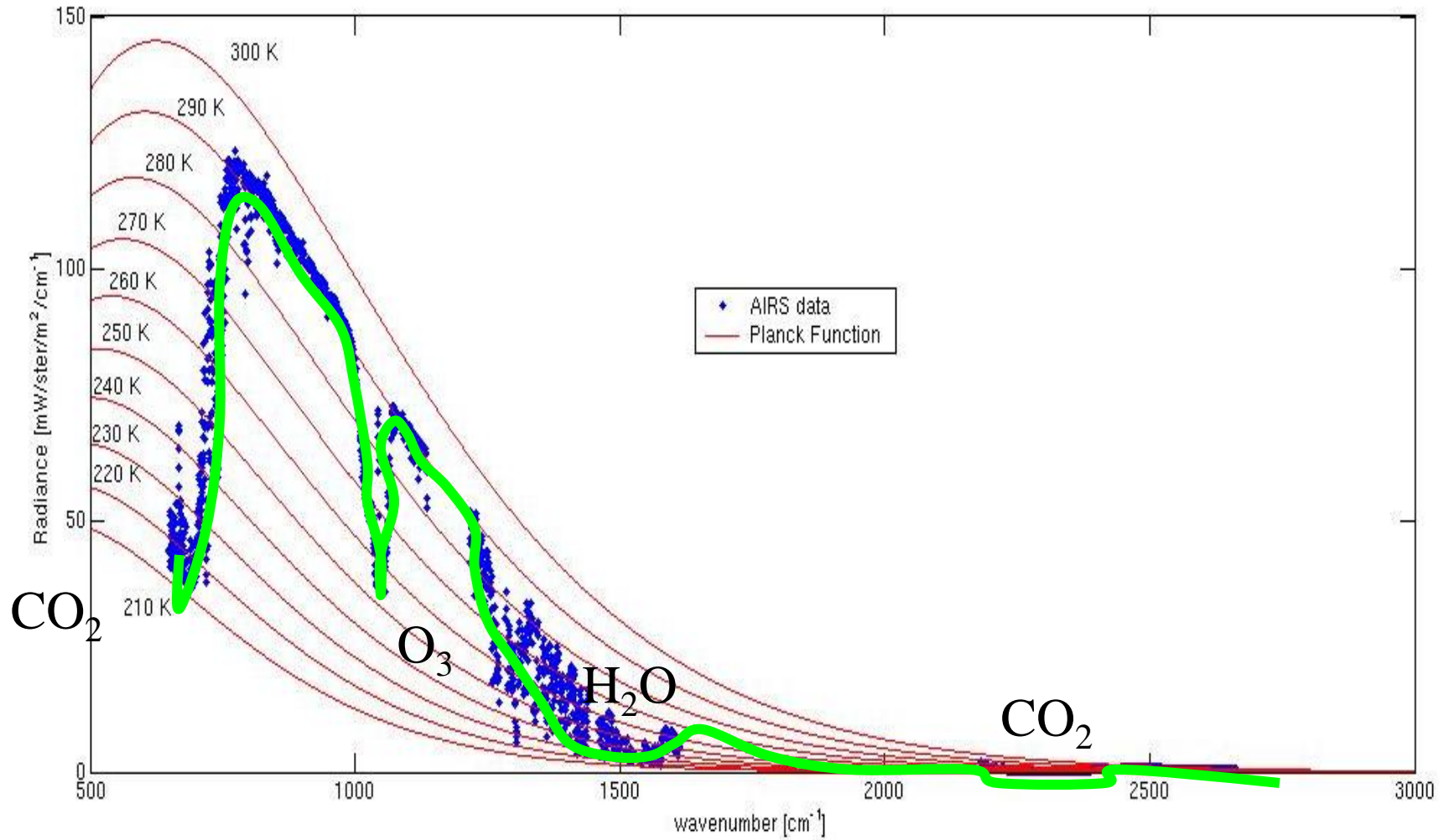
Design

- Grating Spectrometer passively cooled to 160K, stabilized to 30 mK
- **PV and PC HgCdTe focal plane cooled to 60K** with redundant active pulse tube cryogenic coolers
- **Focal plane has ~5000 detectors**, 2378 channels. PV detectors (all below 13 microns) are doubly redundant. Two channels per resolution element ($n/D_n = 1200$)
- 310 K Blackbody and space view provides radiometric calibration
- Paralyene coating on calibration mirror and upwelling radiation provides spectral calibration
- **NEDT (per resolution element) ranges from 0.05K to 0.5K**

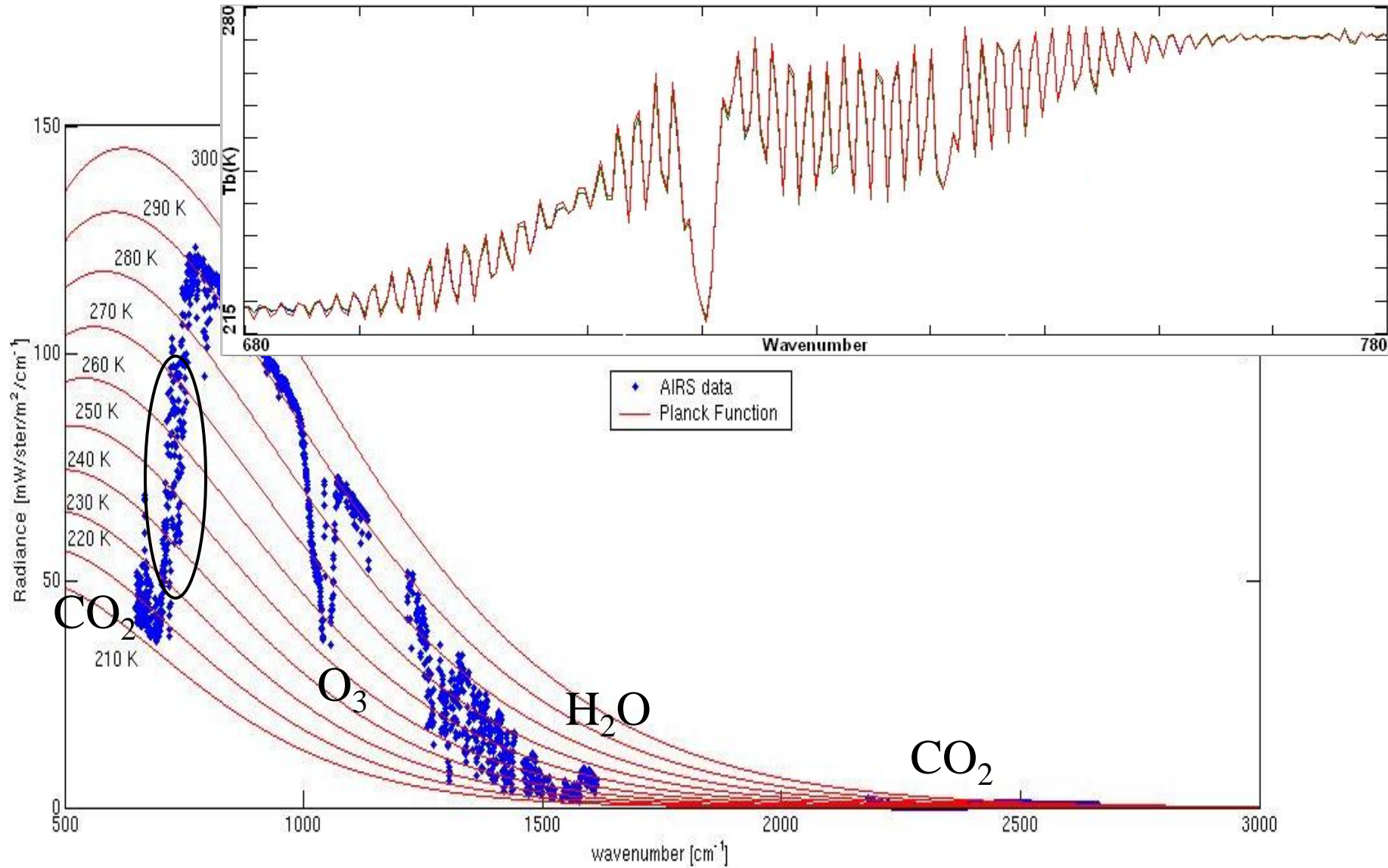


Spectral filters at each entrance slit and over each FPA array isolate color band (grating order) of interest

Vibrational Lines

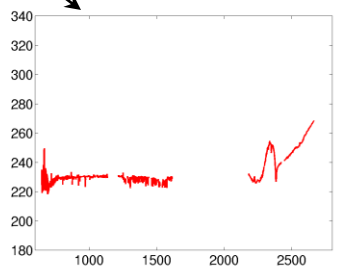
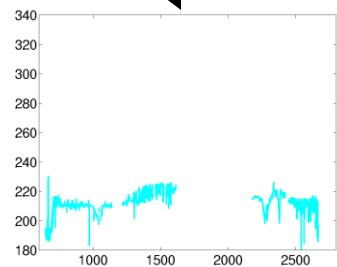
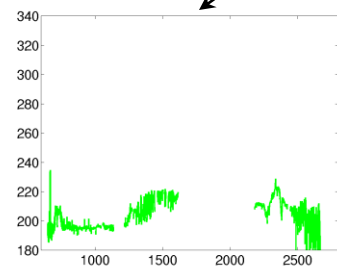
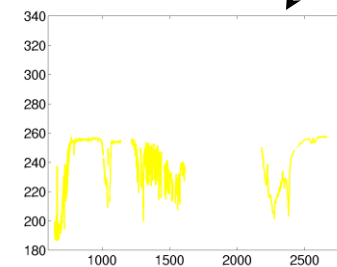
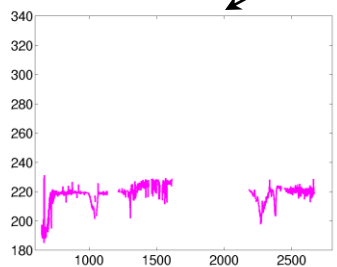
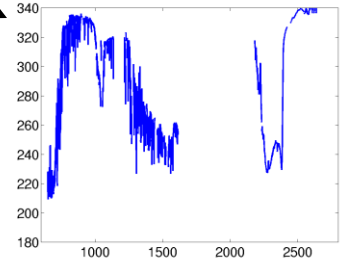
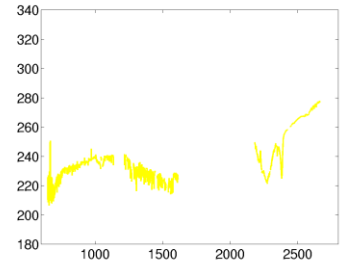
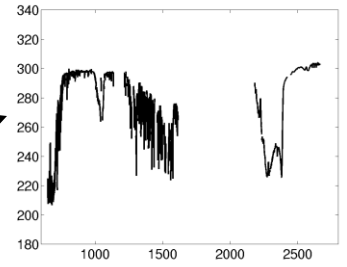
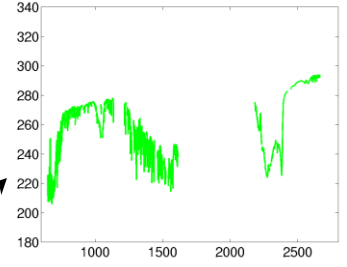
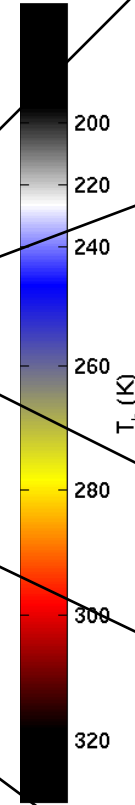
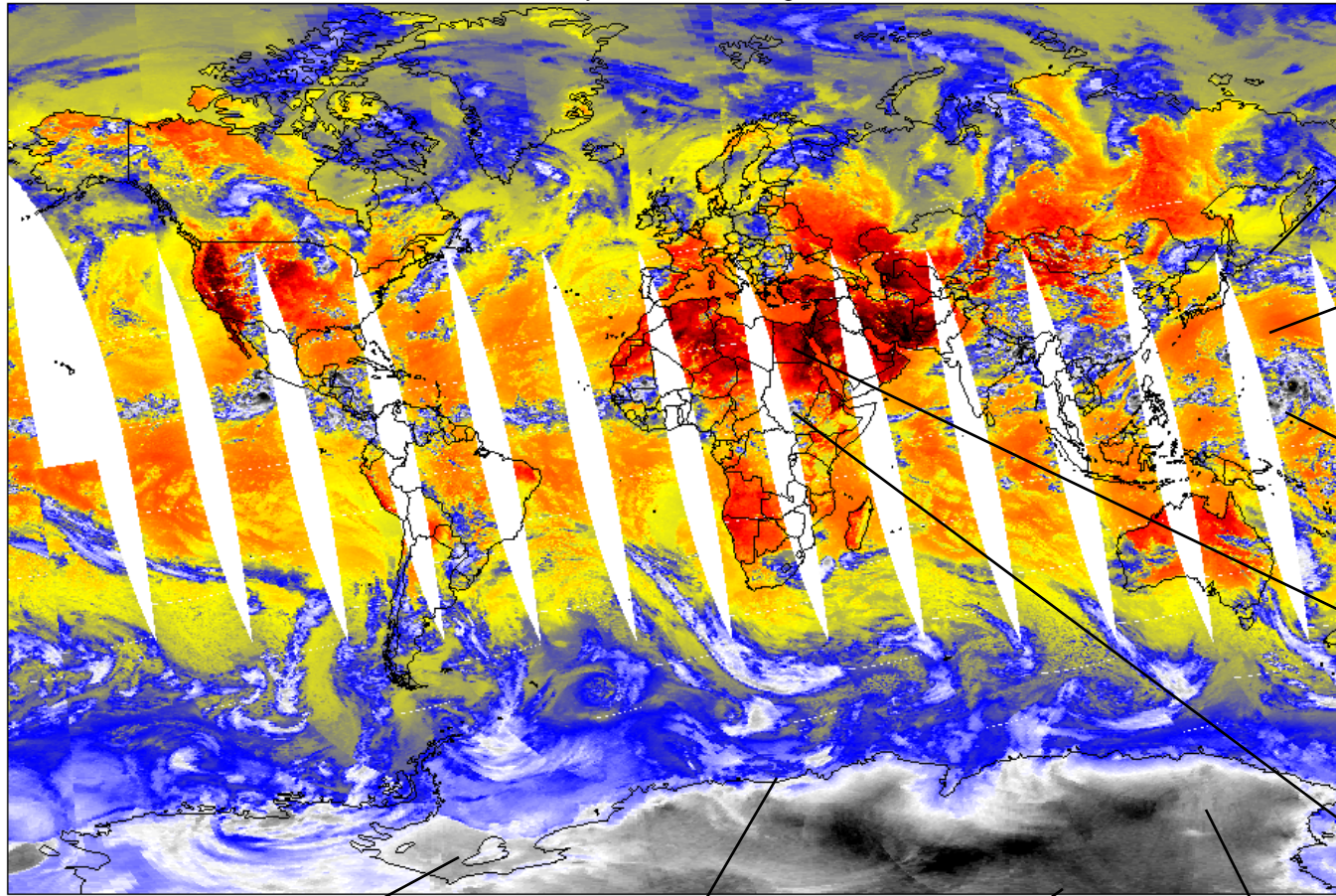


Rotational Lines



AIRS Spectra from around the Globe

20-July-2002 Ascending LW_Window



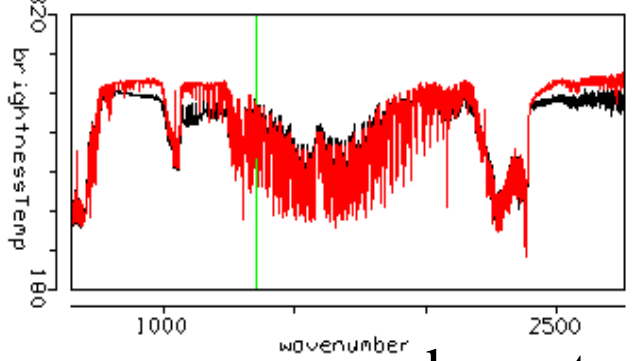
AIRS data from 28 Aug 2005

The image displays a Windows XP desktop environment with several open applications. The desktop background is a blue sky with clouds. In the top-left corner, there are icons for Mozilla Firefox, VZAccess Manager, Mozilla Thunderbird, and a shortcut to IEXPLORE. The taskbar at the bottom shows the Start button and several open applications: ET EGOS input to..., run HYDRA, Microsoft Power..., Hydra (Version: v1.6b2), Multi-Channel Vie..., and a system tray with a battery icon at 80% and the time 10:40 AM.

The **Hydra (Version: v1.6b2)** window is the primary focus on the left. It has a menu bar with 'File', 'Load', 'Tools', 'Settings', and 'Start'. Below the menu is a toolbar with icons for home, search, zoom, pan, and zoom reset. The main area shows a map of Europe with a rectangular region highlighted in black, containing a grayscale satellite image of a cloud field.

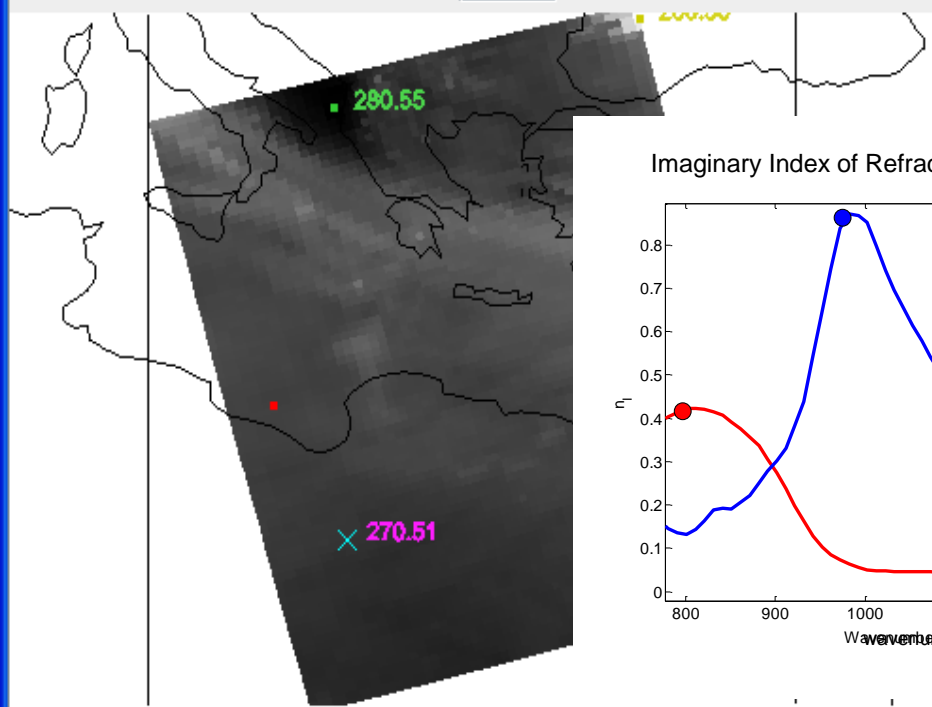
The **Multi-Channel Viewer** window is on the right. It has a menu bar with 'Tools' and 'Settings'. The title bar reads 'Clear Sky vs Opaque High Cloud Spectra'. The main plot area shows a line graph with 'brightnessTemp' on the y-axis (ranging from 180 to 220) and 'wavenumber' on the x-axis (ranging from 1000 to 2500). Two lines are plotted: a black line representing 'Clear Sky' and a red line representing 'Opaque High Cloud Spectra'. A vertical green line is drawn at approximately 2446.20 cm⁻¹. Below the plot, a text box shows 'wavenumber 2446.20 cm⁻¹'. Below this is a map of Europe with a rectangular region highlighted in black, containing a grayscale satellite image of a cloud field. Three data points are marked on the map: a cyan 'x' at 294.25, a yellow square at 236.65, and a green square at 327.09. At the bottom of the window, it says 'Instrument: AIRS' and has a toolbar with icons for home, search, zoom, pan, and zoom reset.

IASI detection of dust



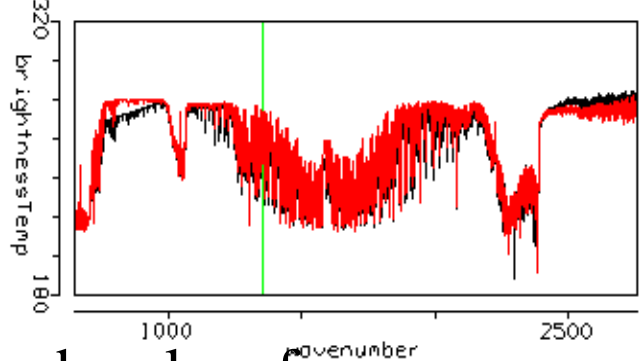
red spectrum is from nearby clear fov

wavenumber 1349.75 cm⁻¹

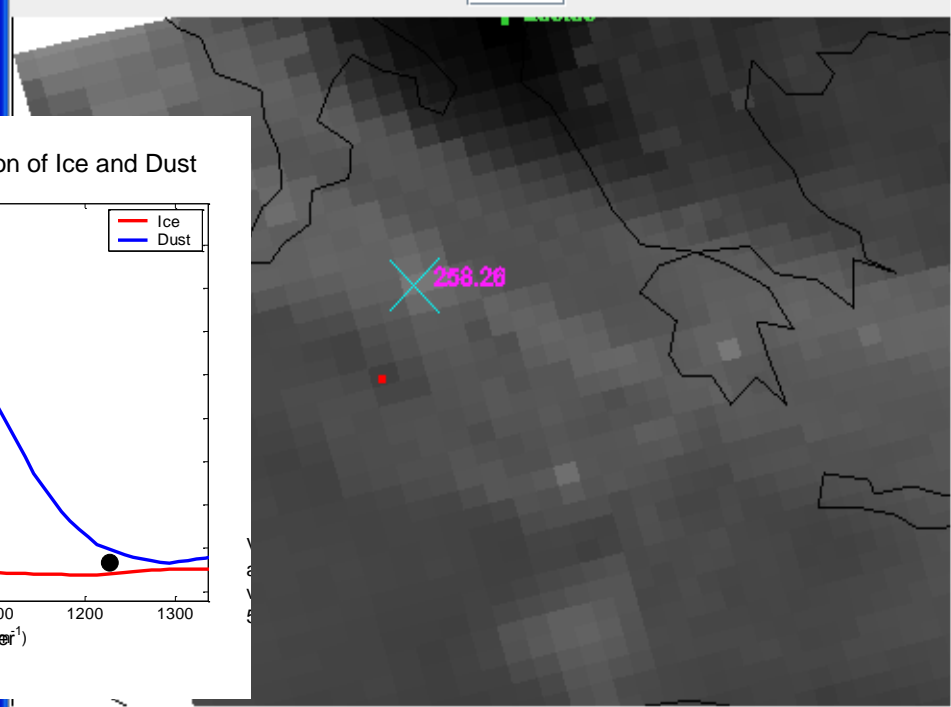


Lat = 27.557 Lon = 20.077

IASI detection of cirrus

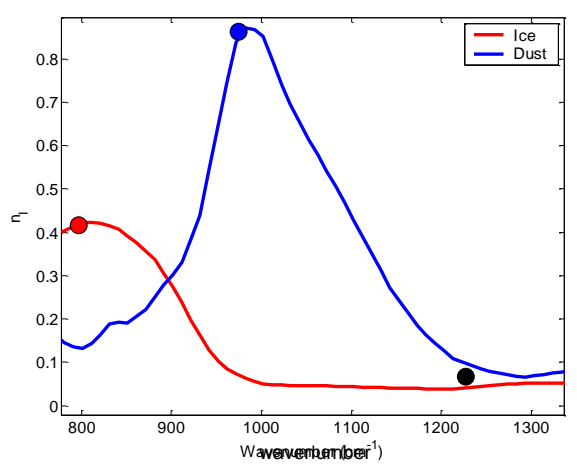


wavenumber 1349.75 cm⁻¹



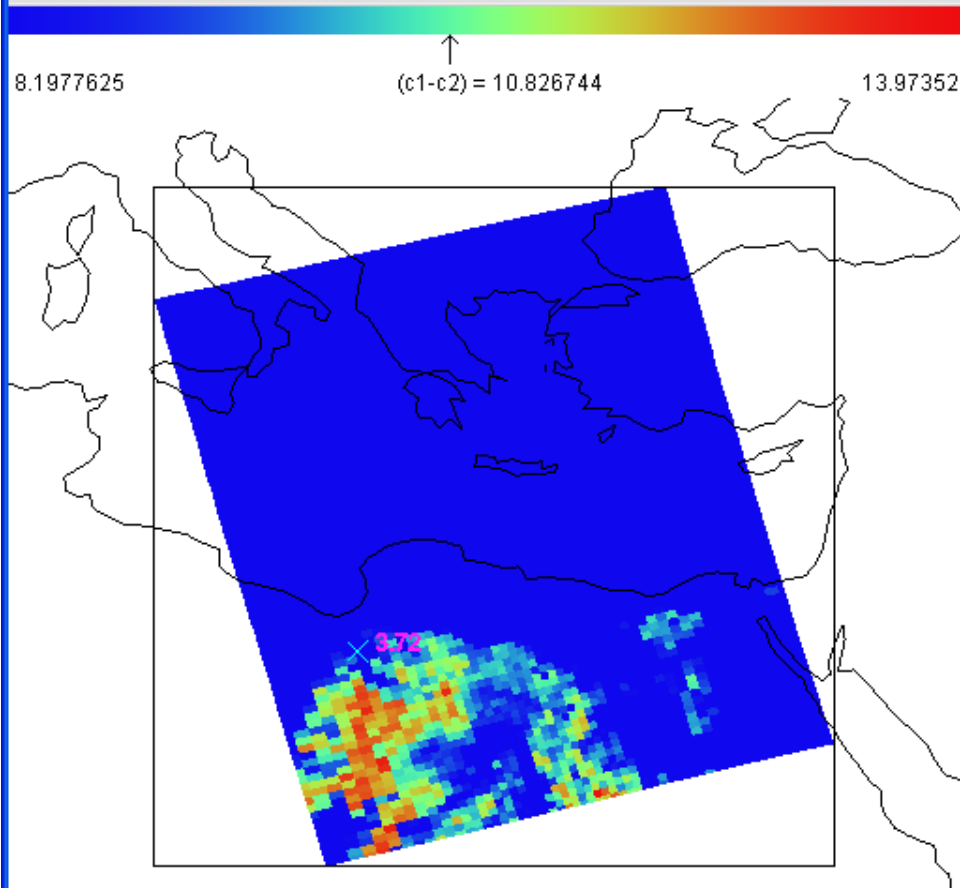
Lat = 36.595 Lon = 17.650

Imaginary Index of Refraction of Ice and Dust



Tools Settings

Tools Settings Import



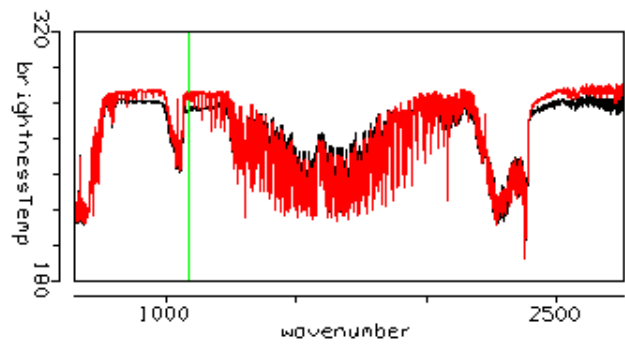
IASI detects barren regions

c1: 981.000, c2:1086.000

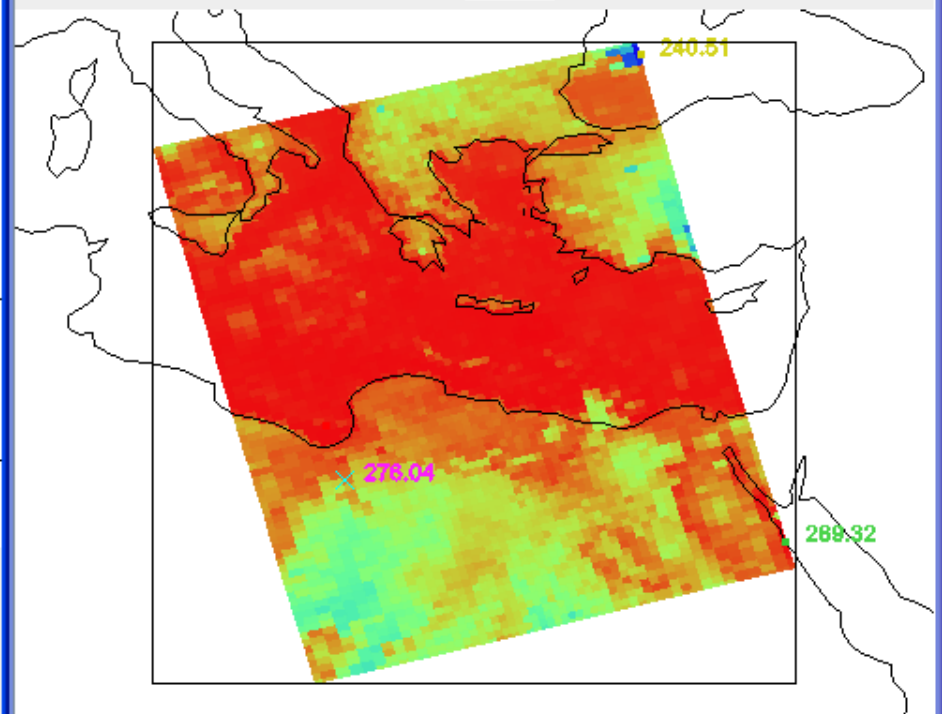
XAxis YAxis Red Grn Blu



Box Curve



wavenumber 1086.00 cm⁻¹



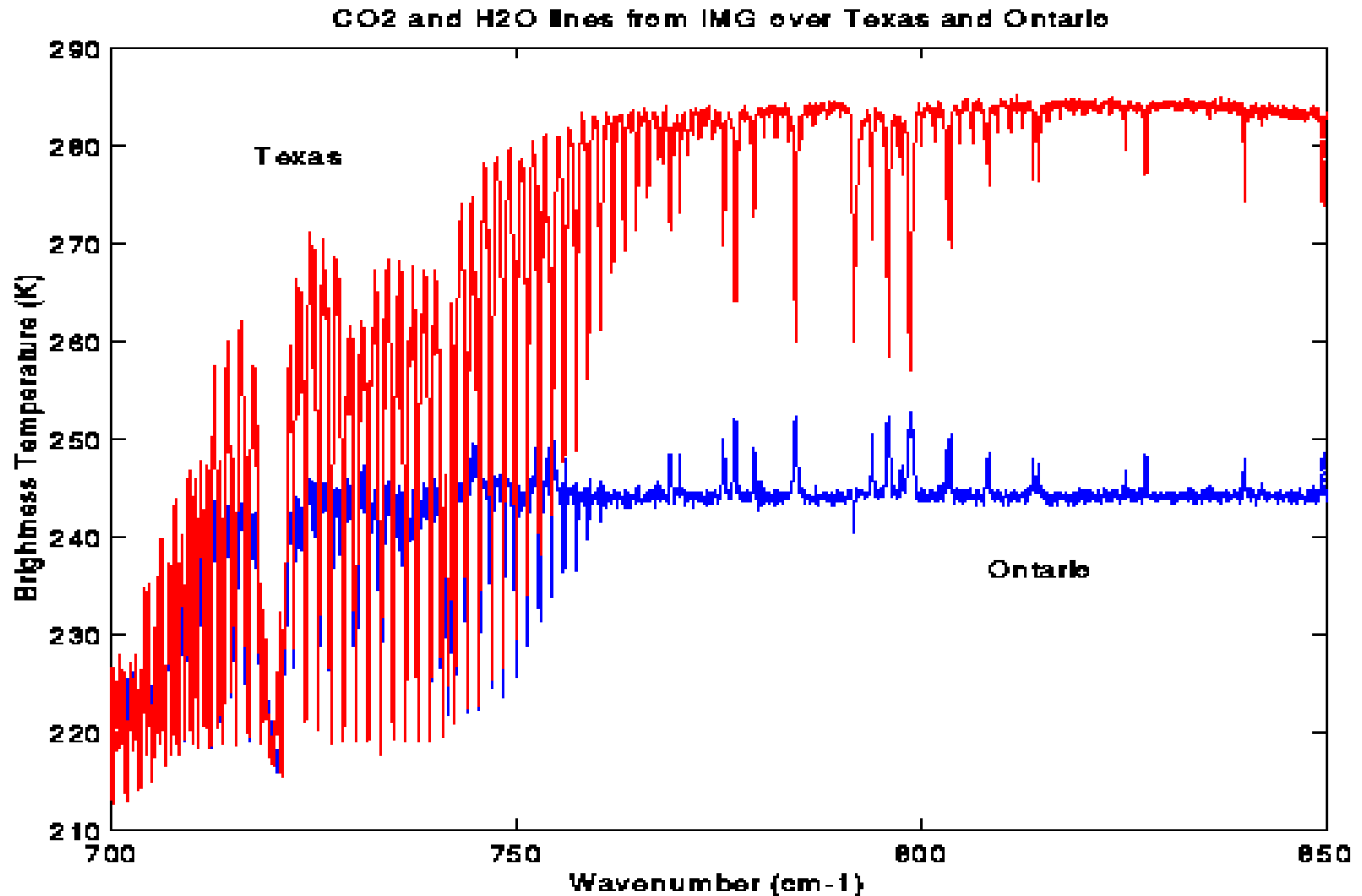
Instrument: ""

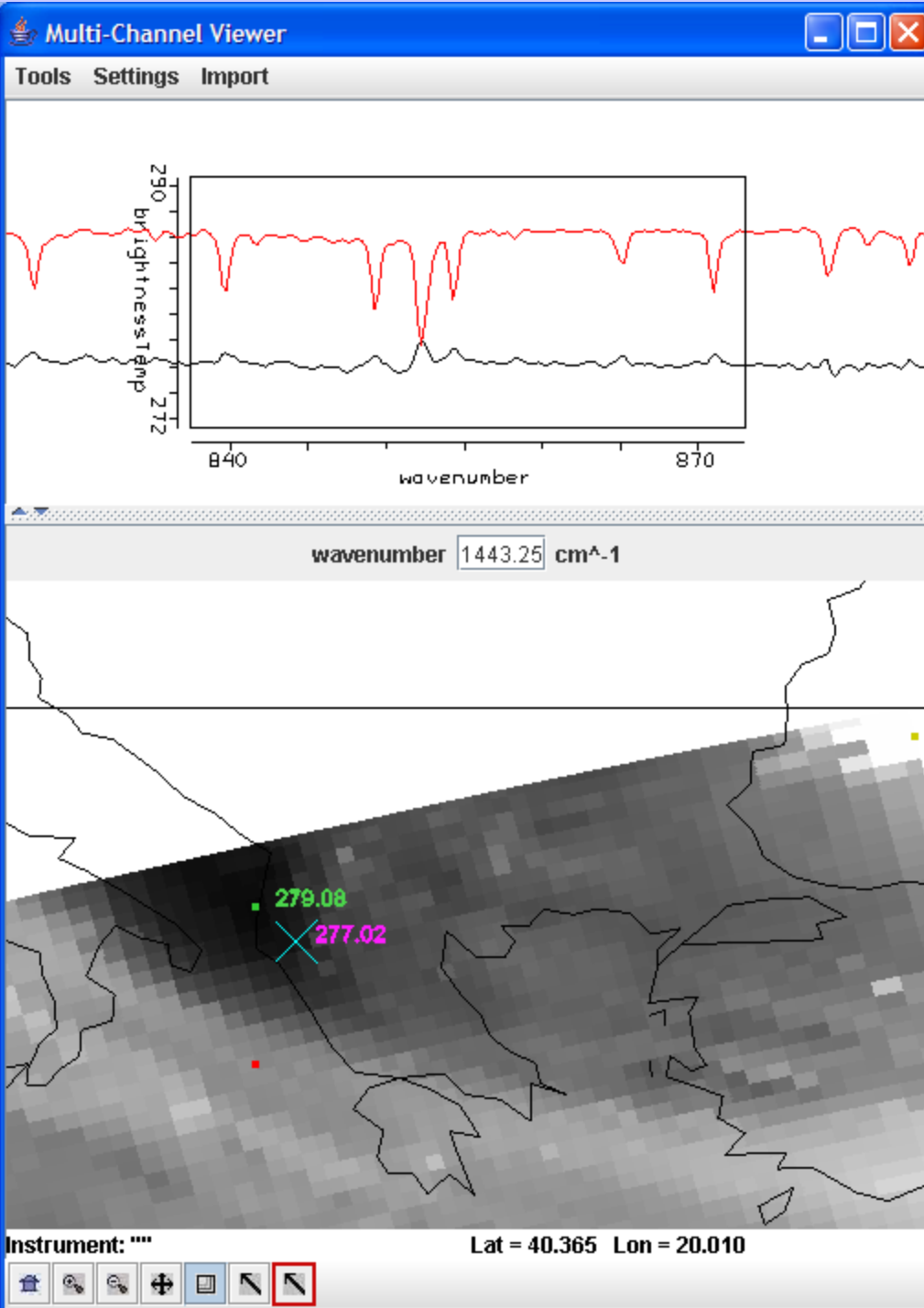
Lat = 31.015 Lon = 19.149



Sensitivity of High Spectral Resolution to Boundary Layer Inversions and Surface/atmospheric Temperature differences

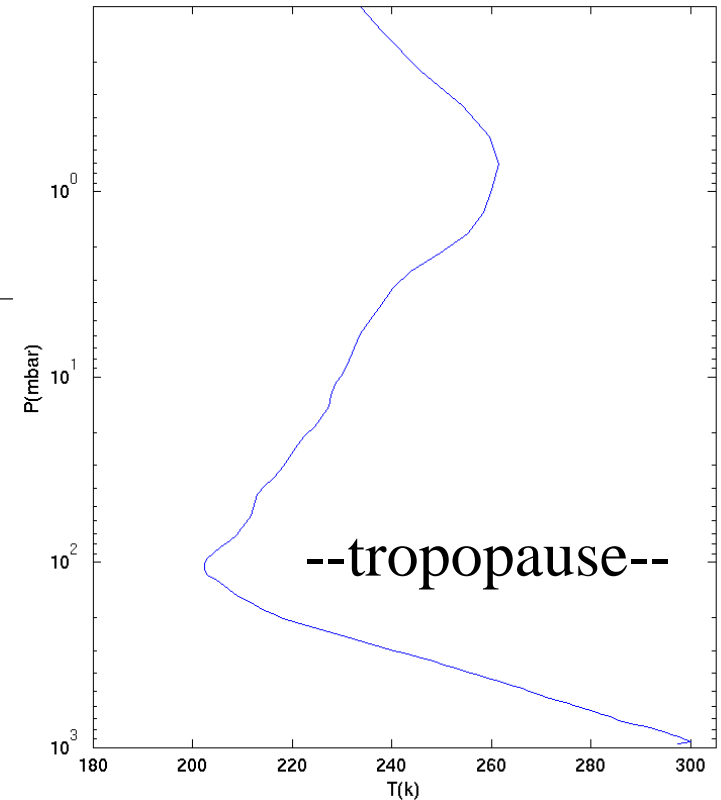
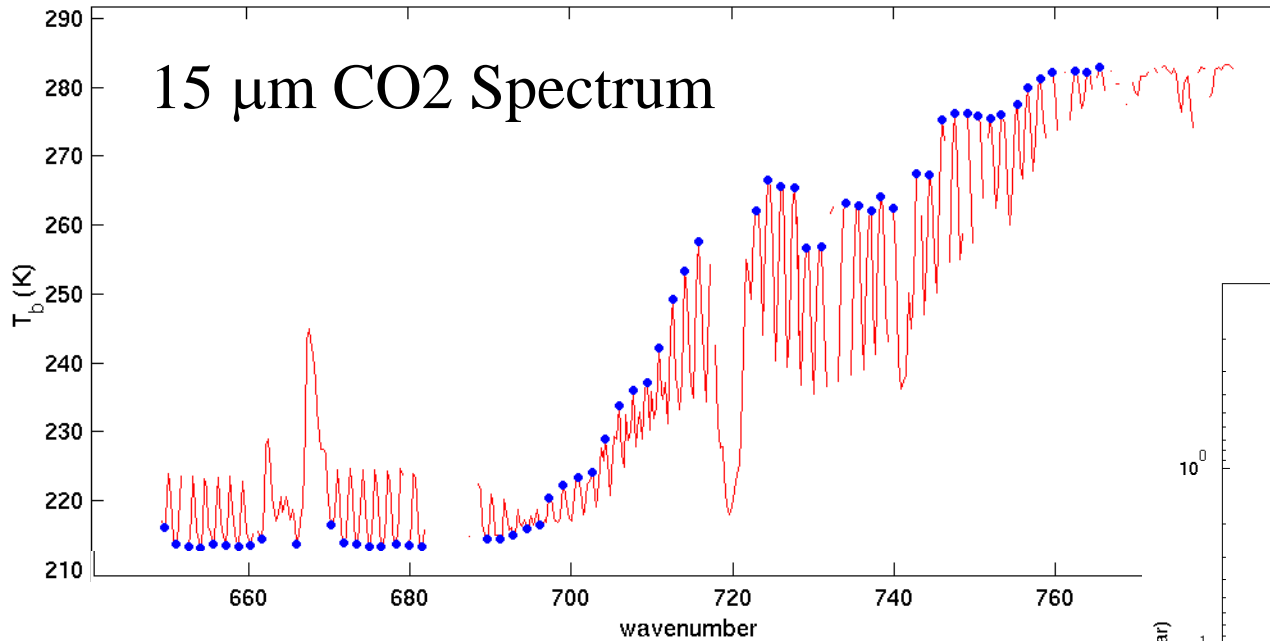
(from IMG Data, October, December 1996)





IASI sees
low level inversion
over land

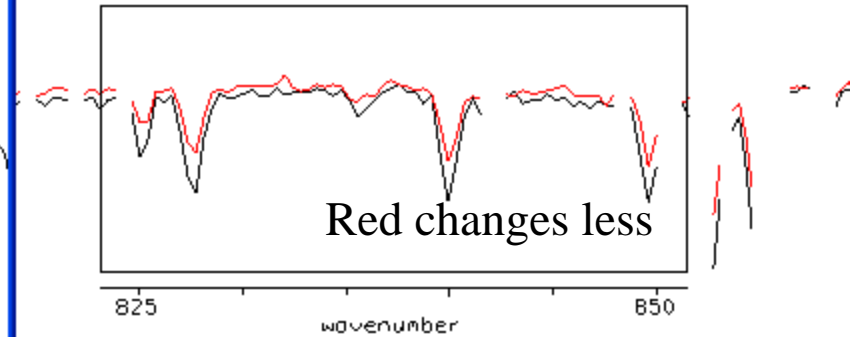
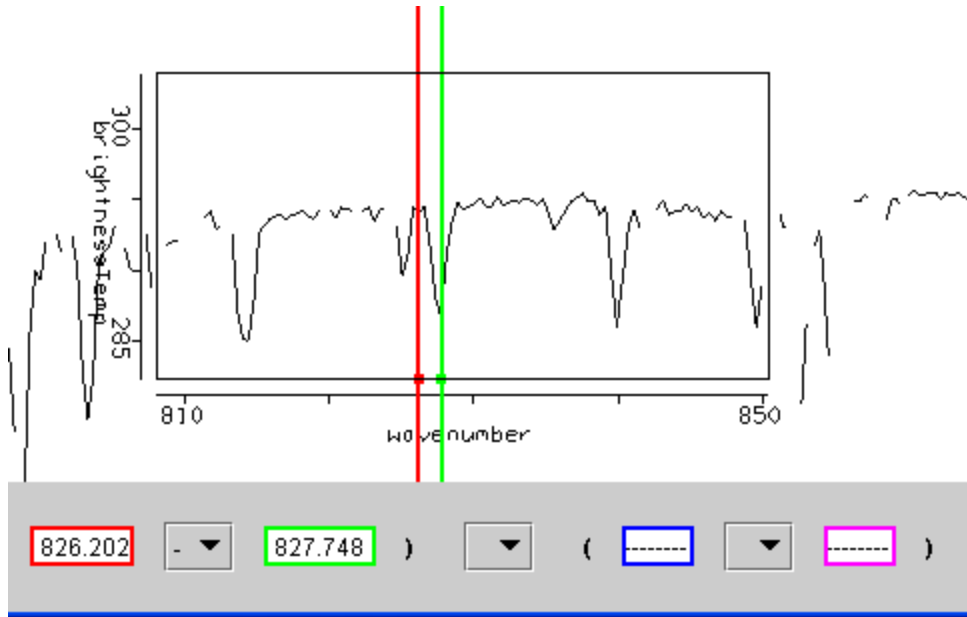
Twisted Ribbon formed by CO₂ spectrum: Tropopause inversion causes On-line & off-line patterns to cross



Blue between-line T_b
warmer for tropospheric channels,
colder for stratospheric channels

Signature not available at low resolution

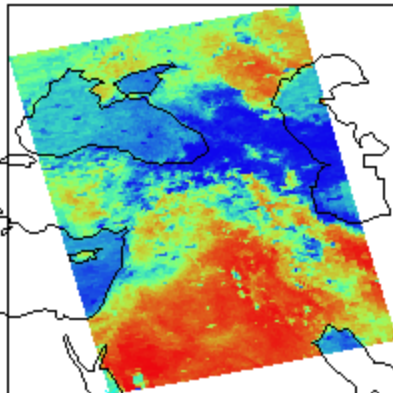
Offline-Online in LW IRW showing low level moisture



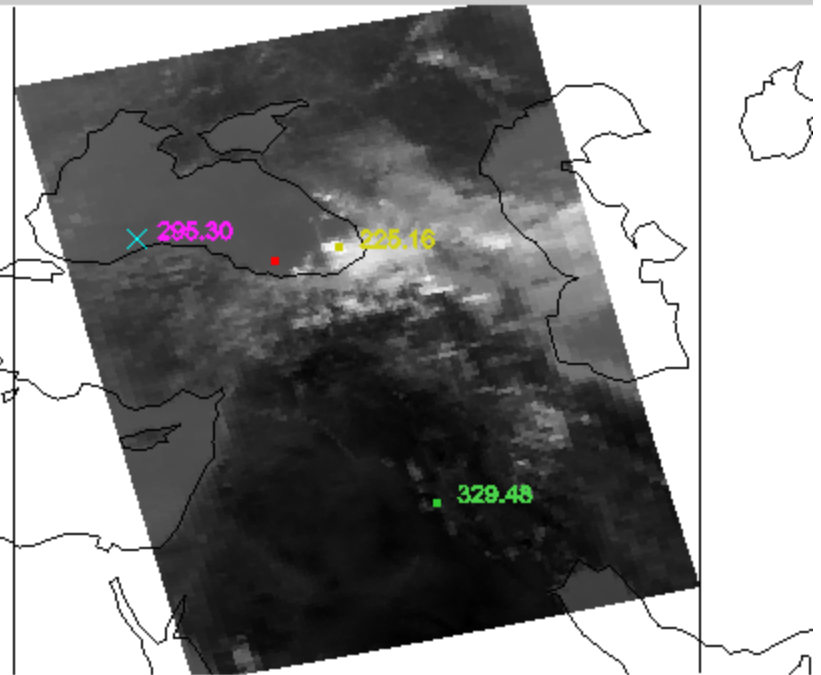
wavenumber 919.47 cm⁻¹

826.202 - 827.748

-0.37449604 (c1-c2) = 5.589554 21.83186

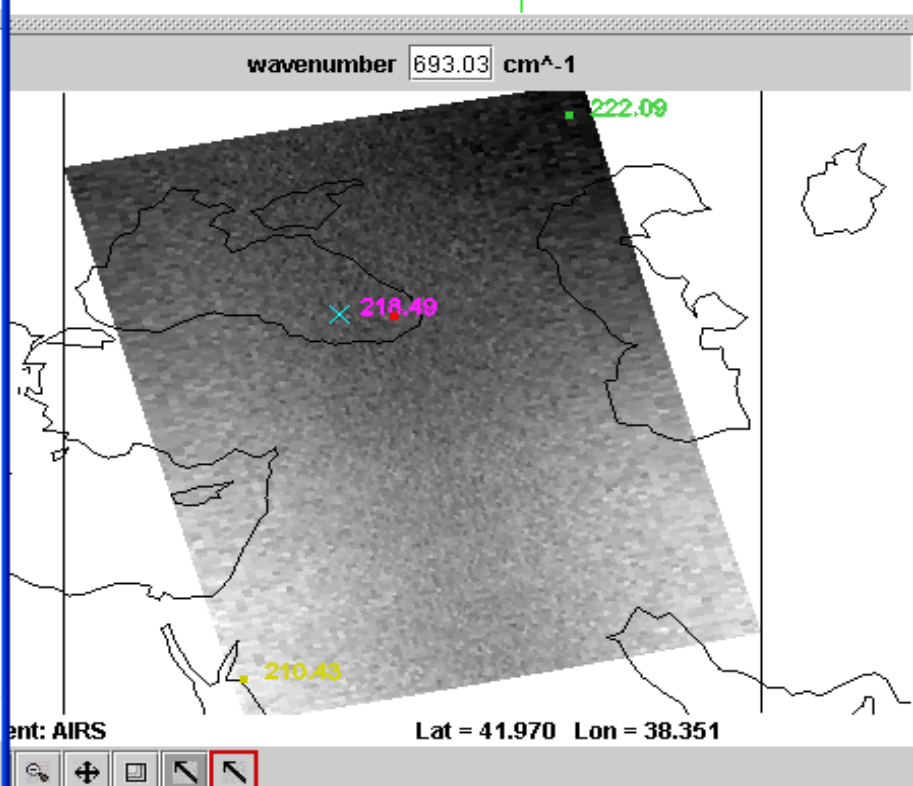
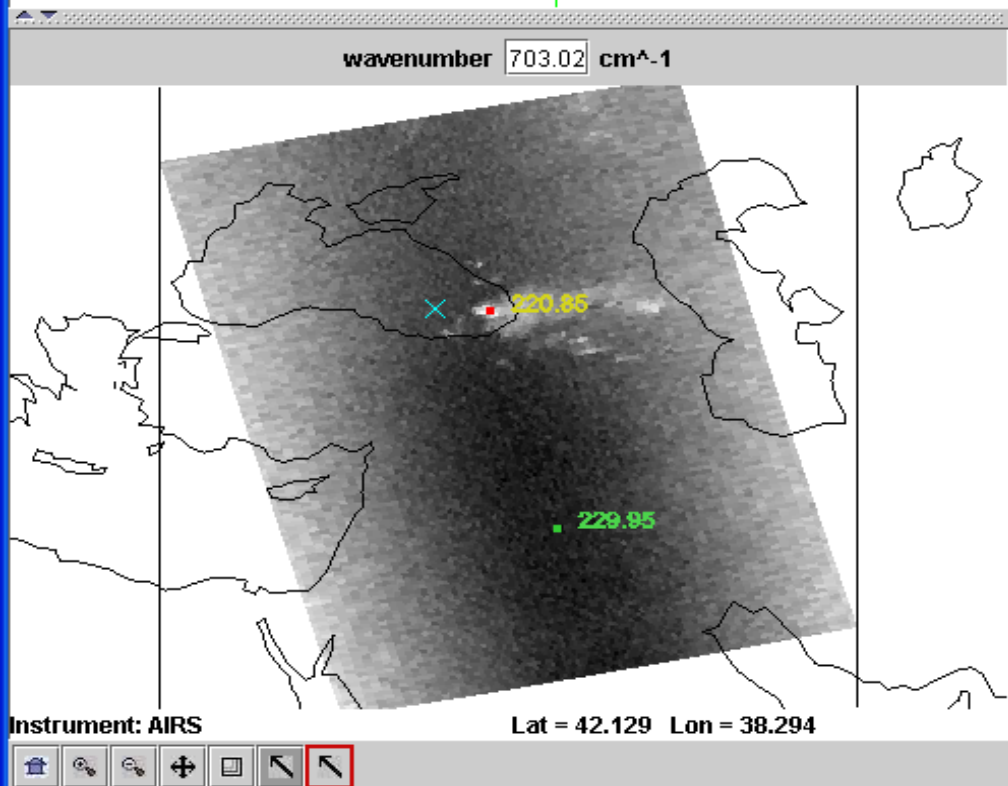
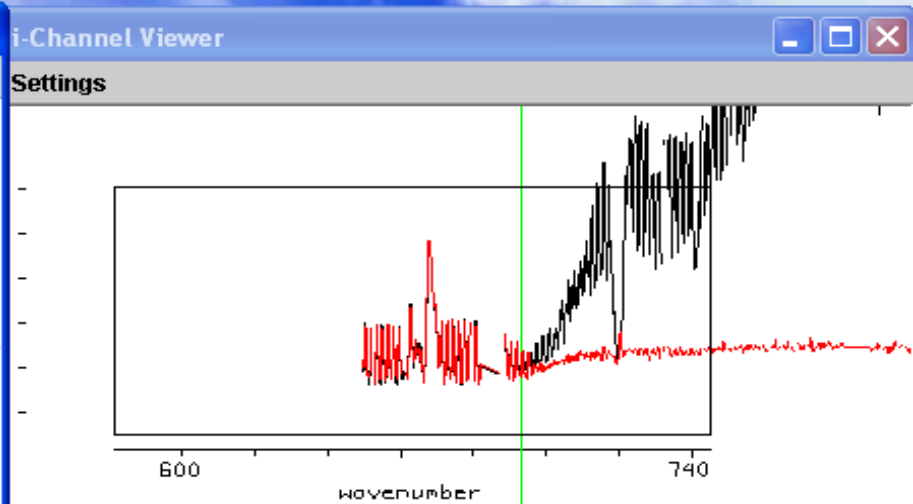
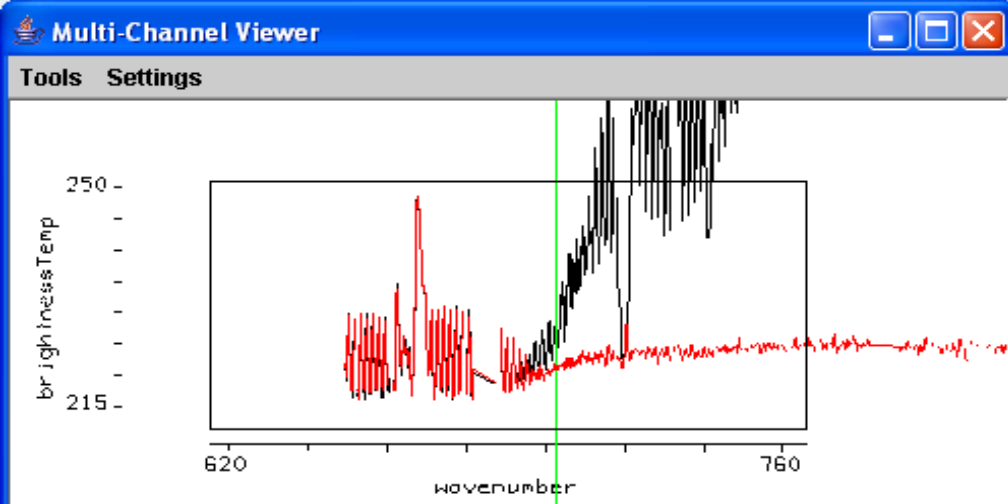


c1: 826.202, c2: 827.748

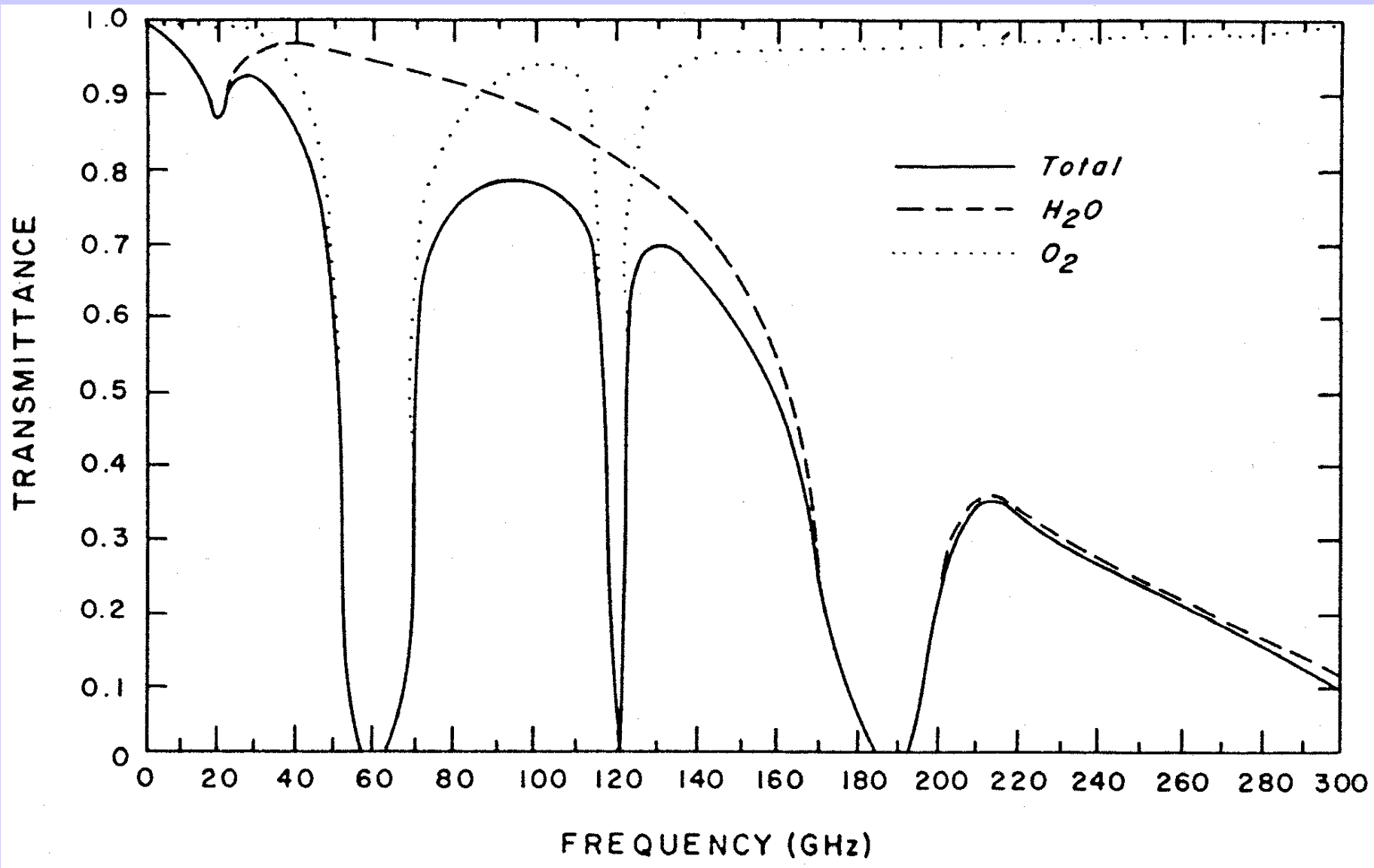


Instrument: AIRS





Cld and clr spectra in CO₂ absorption separate when weighting functions sink to cloud level



Radiation is governed by Planck's Law

$$B(\lambda, T) = \frac{c_1}{\lambda^5} \left[e^{-\frac{c_2}{\lambda T}} - 1 \right]^{-1}$$

In microwave region $c_2/\lambda T \ll 1$ so that

$$e^{-\frac{c_2}{\lambda T}} \approx 1 - \frac{c_2}{\lambda T} + \text{second order}$$

And classical Rayleigh Jeans radiation equation emerges

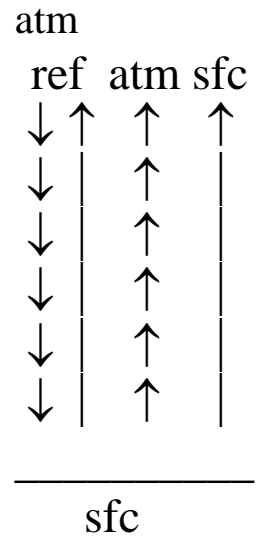
$$B_\lambda(T) \approx \left[\frac{c_1}{c_2} \right] \left[\frac{T}{\lambda^4} \right]$$

Radiance is linear function of brightness temperature.

Microwave Form of RTE

$$I_{\lambda}^{\text{sfc}} = \varepsilon_{\lambda} B_{\lambda}(T_s) \tau_{\lambda}(p_s) + (1-\varepsilon_{\lambda}) \tau_{\lambda}(p_s) \int_0^{p_s} B_{\lambda}(T(p)) \frac{\partial \tau'_{\lambda}(p)}{\partial \ln p} d \ln p$$

$$I_{\lambda} = \varepsilon_{\lambda} B_{\lambda}(T_s) \tau_{\lambda}(p_s) + (1-\varepsilon_{\lambda}) \tau_{\lambda}(p_s) \int_0^{p_s} B_{\lambda}(T(p)) \frac{\partial \tau'_{\lambda}(p)}{\partial \ln p} d \ln p + \int_{p_s}^0 B_{\lambda}(T(p)) \frac{\partial \tau_{\lambda}(p)}{\partial \ln p} d \ln p$$



In the microwave region $c_2/\lambda T \ll 1$, so the Planck radiance is linearly proportional to the temperature

$$B_{\lambda}(T) \approx [c_1 / c_2] [T / \lambda^4]$$

So

$$T_{b\lambda} = \varepsilon_{\lambda} T_s(p_s) \tau_{\lambda}(p_s) + \int_{p_s}^0 T(p) F_{\lambda}(p) \frac{\partial \tau_{\lambda}(p)}{\partial \ln p} d \ln p$$

where

$$F_{\lambda}(p) = \left\{ 1 + (1 - \varepsilon_{\lambda}) \left[\frac{\tau_{\lambda}(p_s)}{\tau_{\lambda}(p)} \right]^2 \right\} .$$

Wavelength Wavenumber Unnormalized Normalized

Wave Min

0.10

Wave Max

10000.00

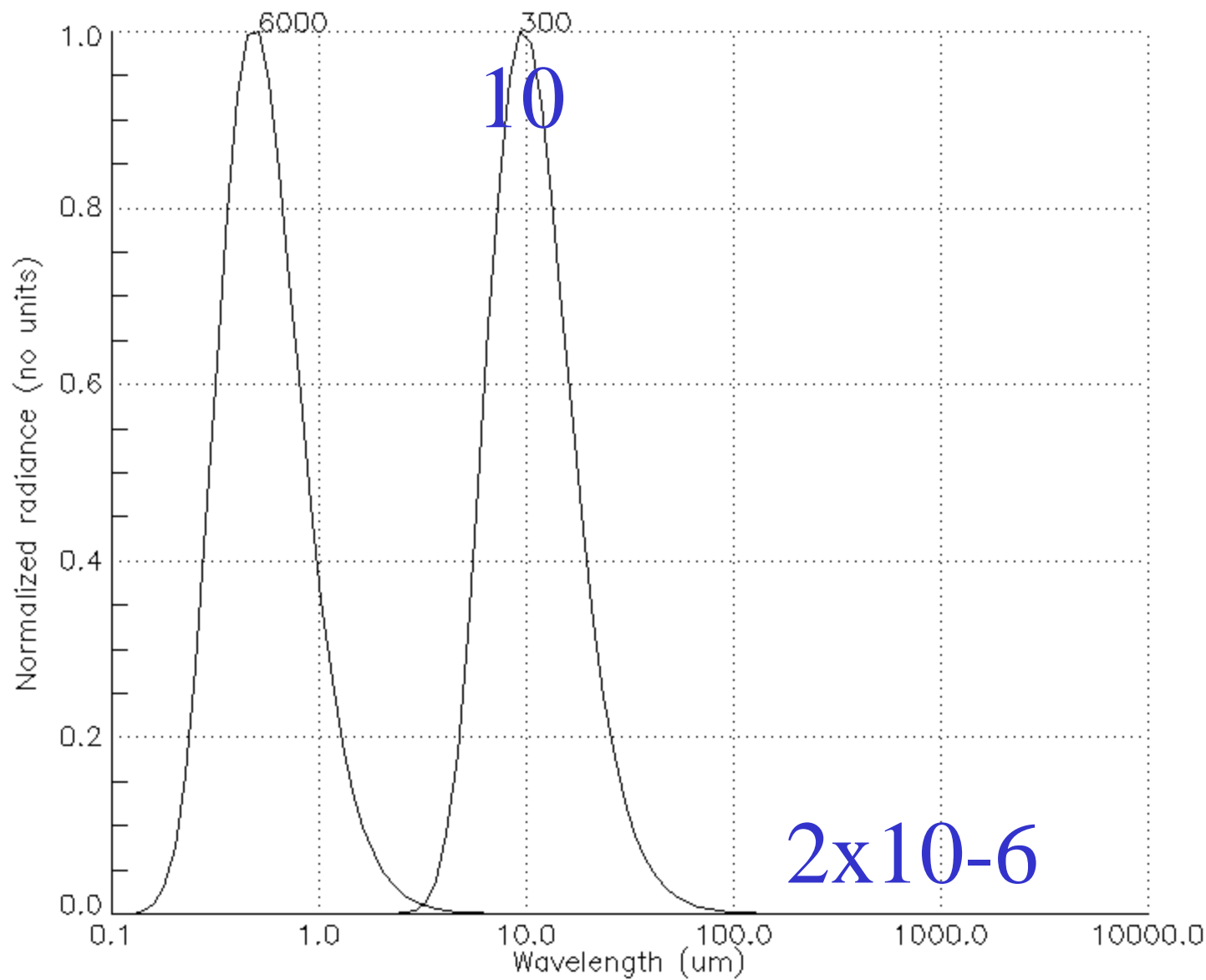
Temp (K)

300.00

New Plot

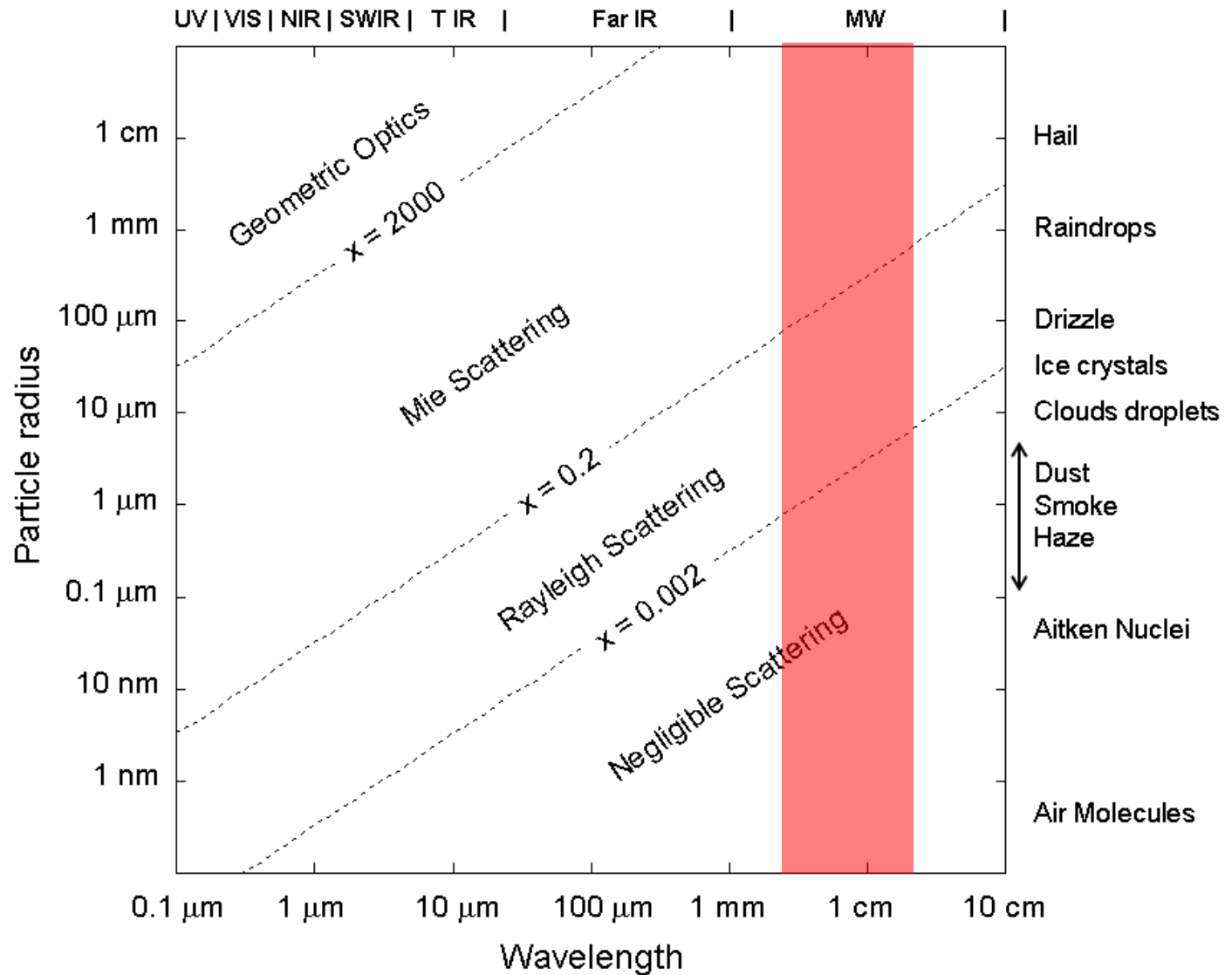
Add Plot

Save JPEG



Scattering of MW radiation

□ Scattering regimes



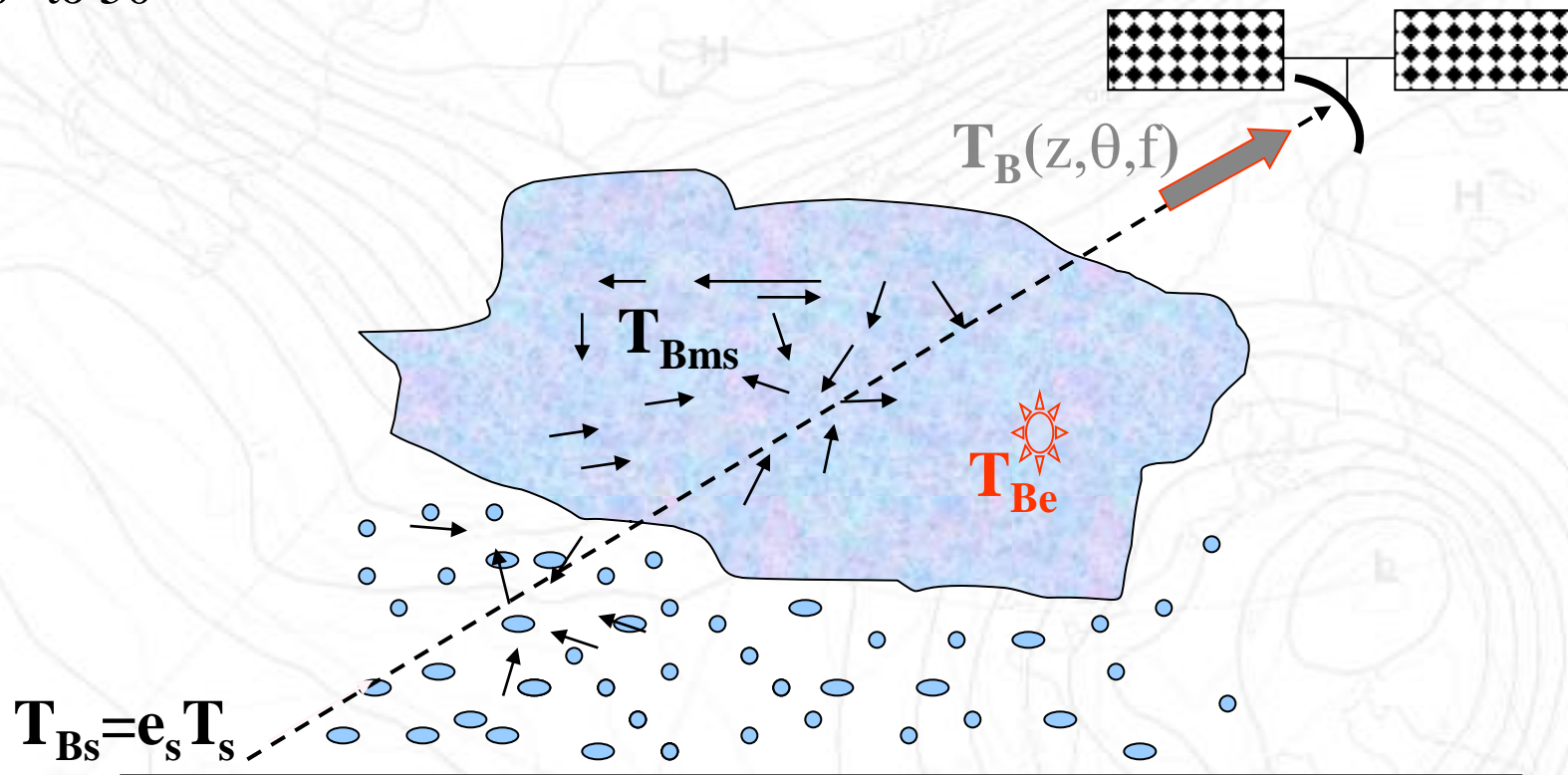
FORWARD PROBLEM

Physical basis

T_B : brightness temperature

$f=10-160$ GHz

$\theta=0^\circ$ to 50°



e_s : surface emissivity
 T_s : surface temperature

T_{Be} : emission T_B
 T_{Bms} : multiple scattering T_B

FORWARD PROBLEM

Radiative transfer equation

- T_B in a plane-parallel medium: non-scattering case

$$\frac{dT_B(\tau, \Omega)}{d\tau} = -\underbrace{T_B(\tau, \Omega)}_{\text{Extinction}} + \underbrace{T(\tau)}_{\text{Emission}}$$

⇒ **Ordinary differential equation: linearization of F**

⇒ **Inverse problem as a *Fredholm integral equation* (e.g., temperature retrieval)**

- T_B in a plane-parallel medium: scattering case

$$\frac{dT_B(\tau, \Omega)}{d\tau} = -\underbrace{T_B(\tau, \Omega)}_{\text{Extinction}} + \underbrace{\frac{w}{4\pi} \int_{4\pi} p(\Omega, \Omega') T_B(\tau, \Omega) d\Omega'}_{\text{Multiple scattering}} + \underbrace{(1-w)T(\tau)}_{\text{Emission}}$$

⇒ **Integro-differential equation: strongly non-linear F (e.g., rainfall retrieval)**



Precipitation in MW — Theory/Basis

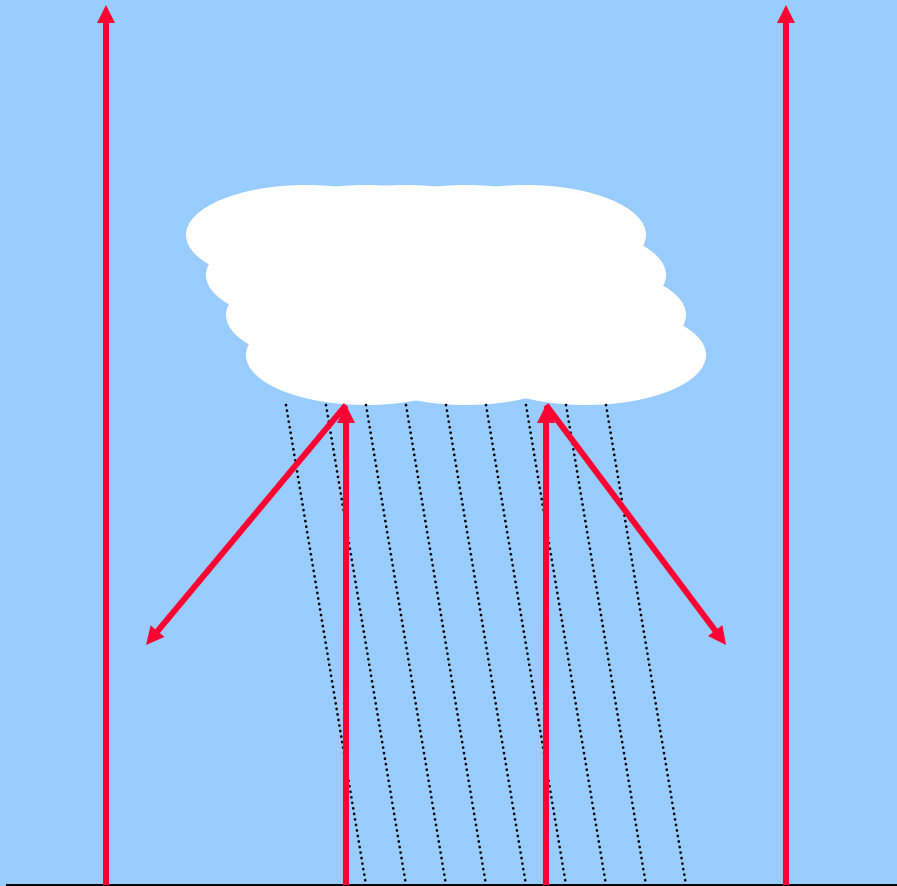
- **Scattering signal**
 - ice in clouds scatters terrestrial radiation (cold areas over warm bckg)
 - Rainfall rates are related to the magnitude of the resulting brightness temperature depression.
 - **Strength**: can be applied to high-frequency channels: works over both land and ocean
 - **Weakness**: poor at detecting precipitation clouds with little or no ice (e.g. warm orographic clouds in the tropics)

- **Emission signal**
 - water in clouds emits radiation, (warm areas over cold bckg, e.g. ocean)
 - Rainfall rates are related to the magnitude of the resulting brightness temperature difference
 - **Strength**: sensitive to clouds with little or no ice
 - **Weakness**: must know terrestrial radiances without cloud beforehand; generally applicable over oceans but not land



Lower T_b
above cloud

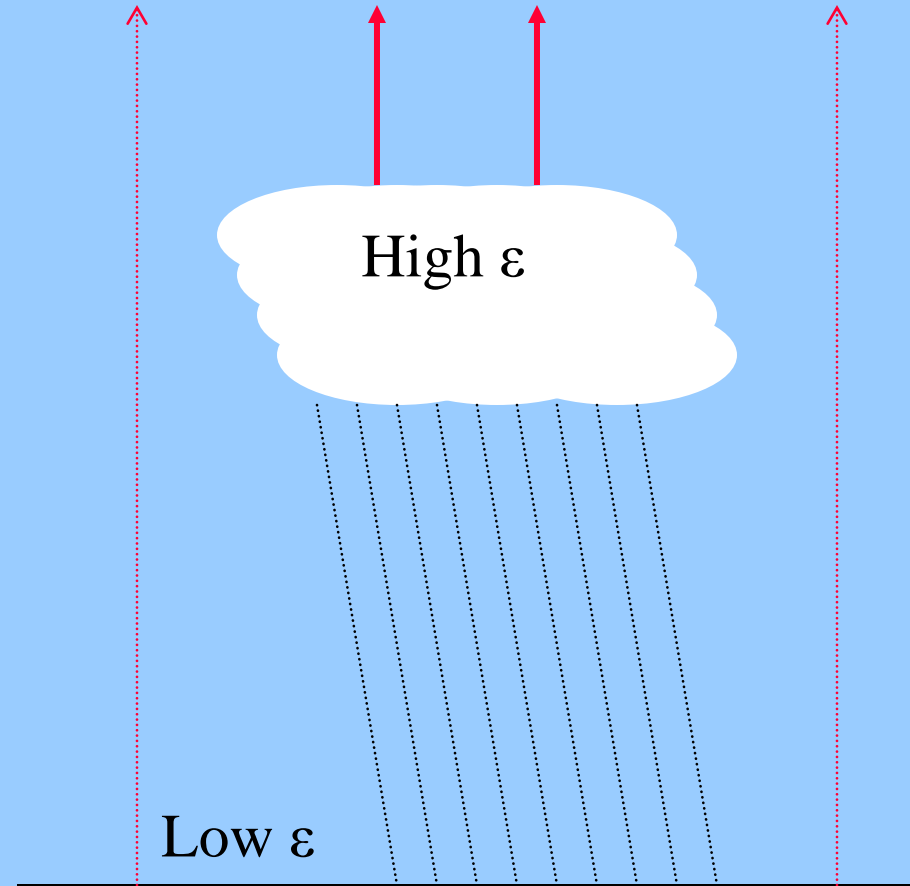
Higher T_b above
clear air



Scattering

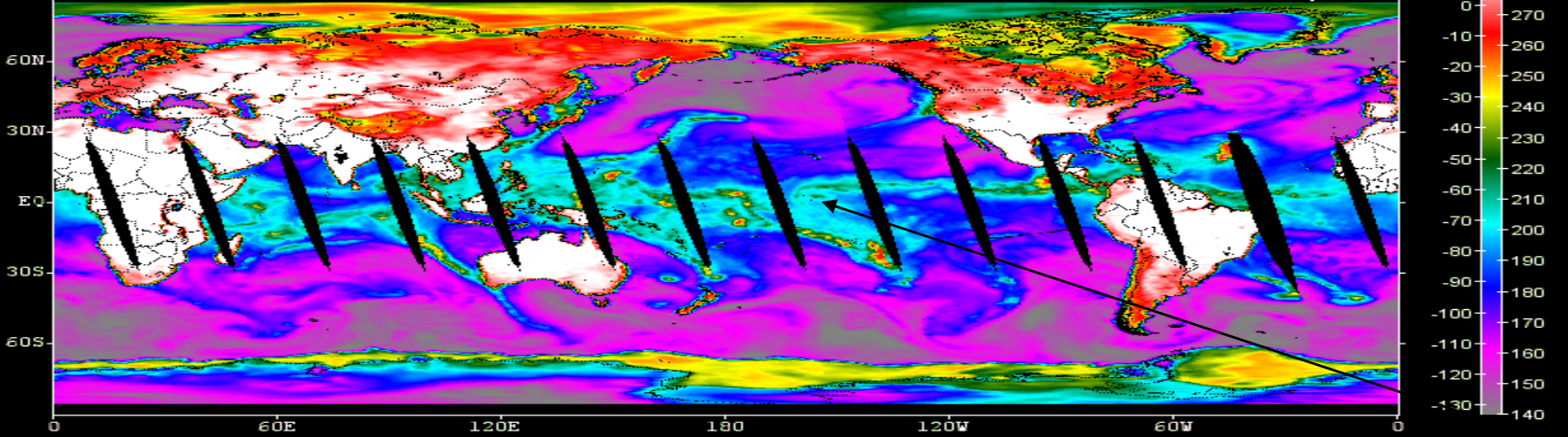
Higher T_b
above cloud

Lower T_b above
clear air

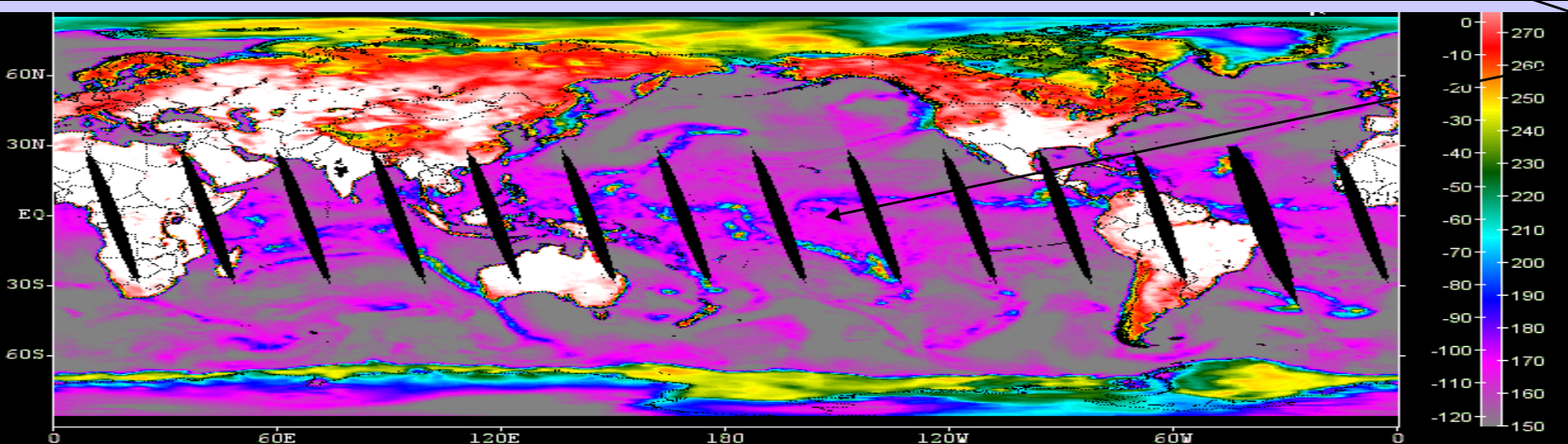


Emission (over ocean)

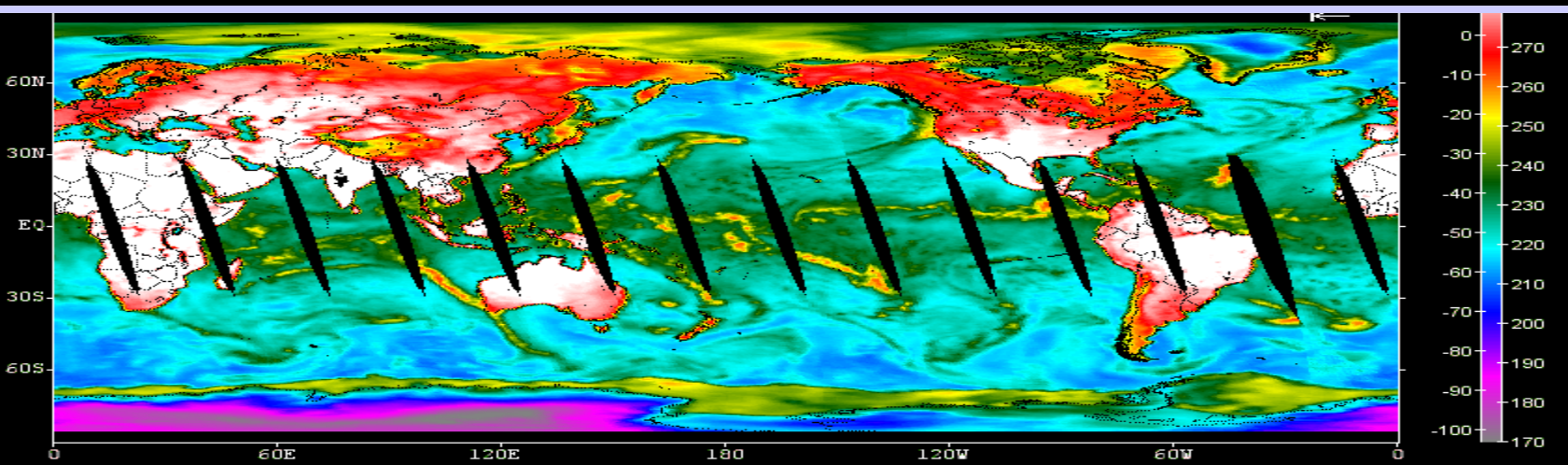




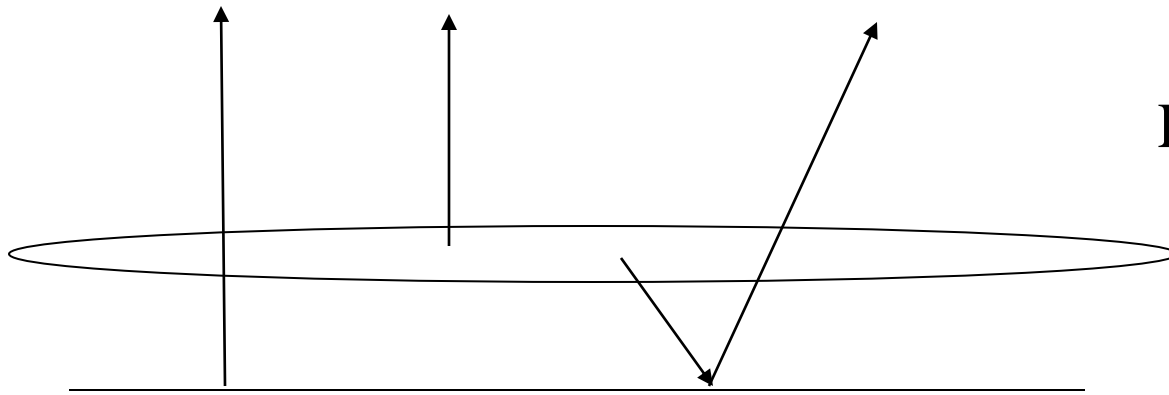
AMSU
23.8
dirty
window



atm Q
 warms
 BT
31.4
window



50.3
GHz



Low mist over ocean

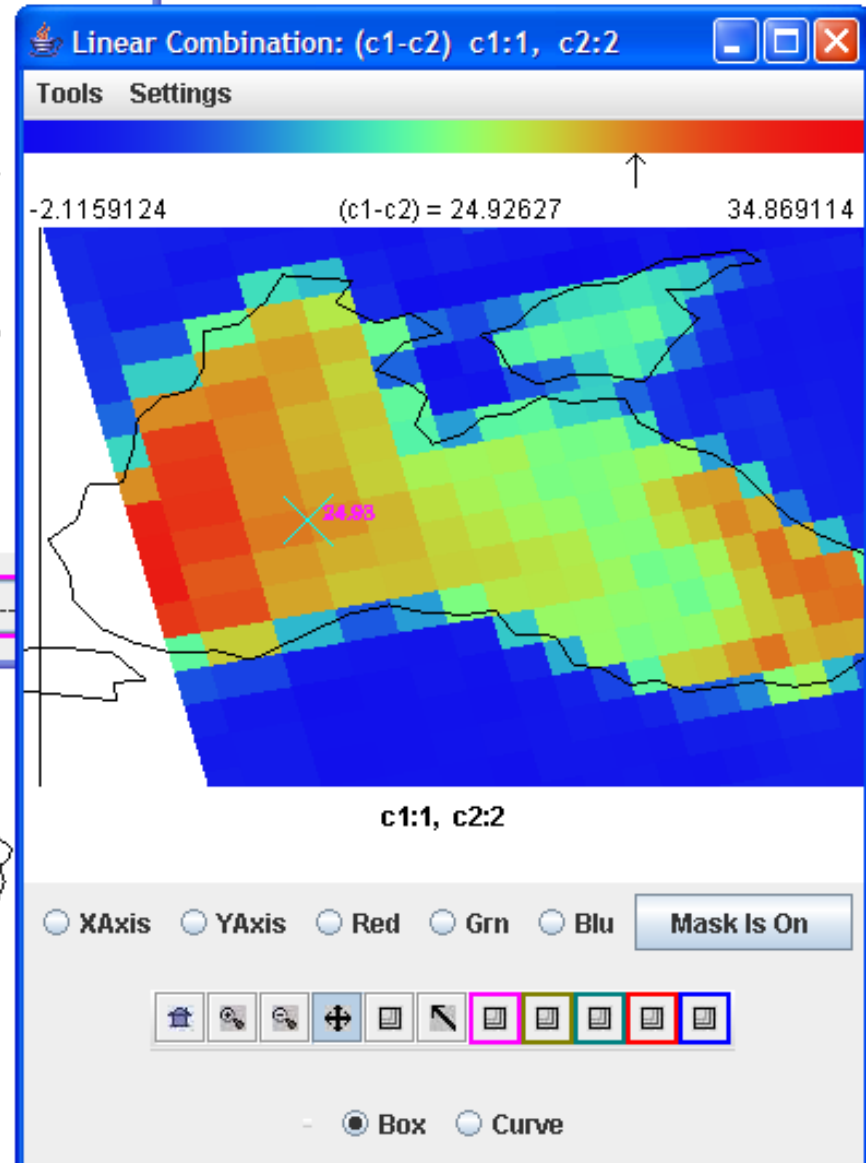
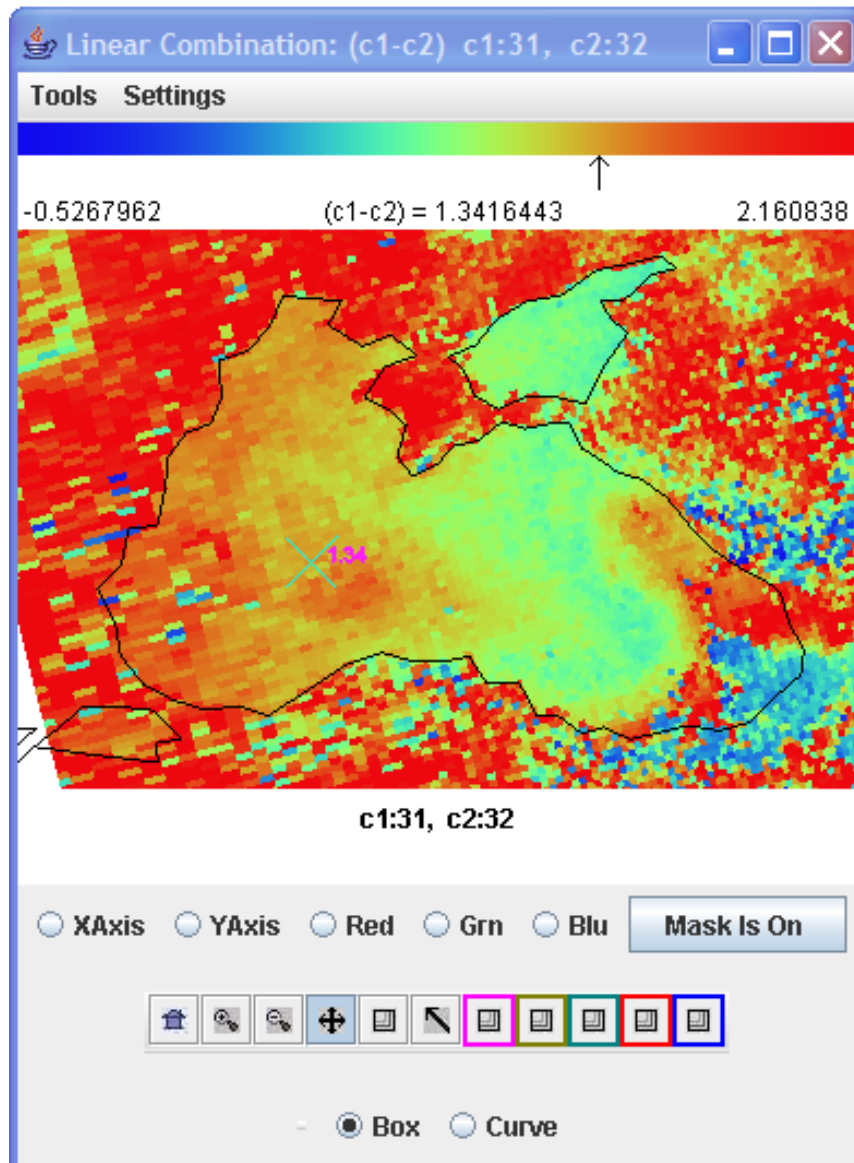
$$T_b = \epsilon_s T_s (1 - \sigma_m) + \sigma_m T_m + \sigma_m (1 - \epsilon_s) (1 - \sigma_m) T_m$$

So

$$\Delta T_b = - \epsilon_s \sigma_m T_s + \sigma_m T_m + \sigma_m (1 - \epsilon_s) (1 - \sigma_m) T_m$$

For $\epsilon_s \sim 0.5$ and $T_s \sim T_m$ this is always positive for $0 < \sigma_m < 1$

MW split window has larger signal for low level moisture than IR split window



Accuracy of Satellite Derived Met Parameters

T(p) within 1.5 C of raobs for 1 km layers

SST within 0.5 C of buoys

Q(p) within 15-20% of raobs for 2 km layers

TPW with 3 mm of ground based MW

TO3 within 30 Dobsons of ozone profilers

LI adjusted 3 C lower (for better agreement with raobs)

gradients in space and time more reliable than absolute

AMVs within 7 m/s (upper trop) and 5 m/s (lower trop)

CTPs within 50 hPa of lidar determination

Geopotential heights within 20 to 30 m

for 500 to 300 hPa

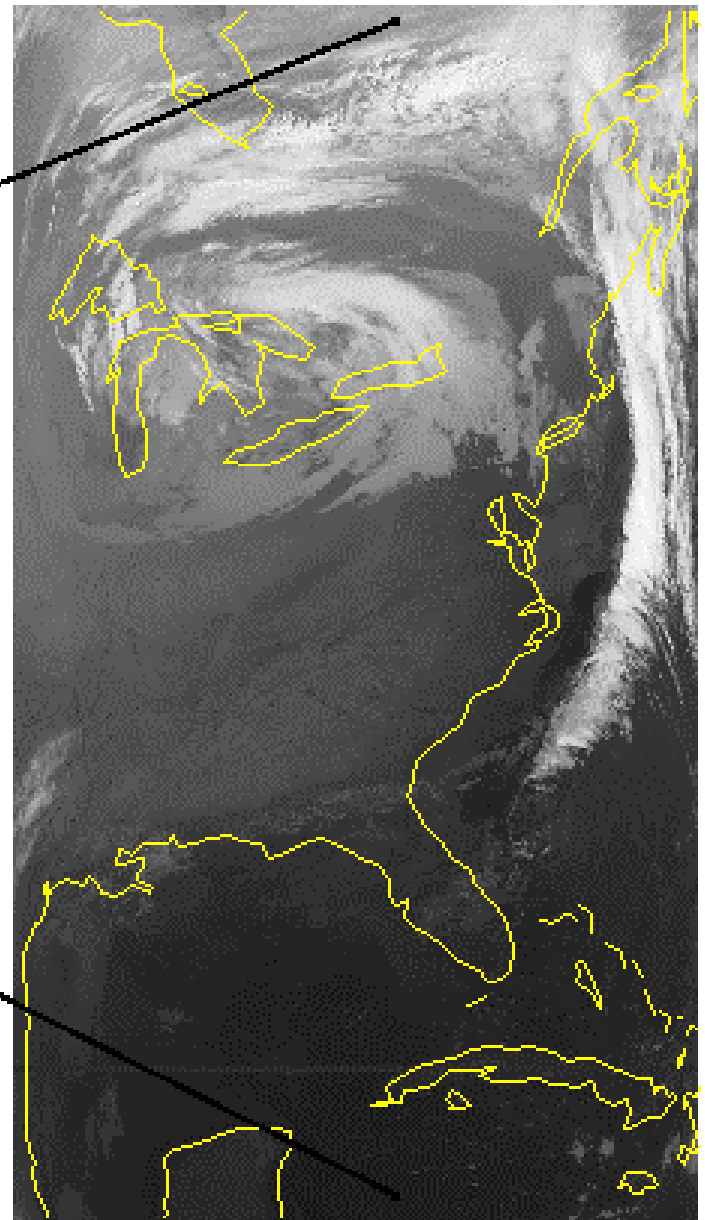
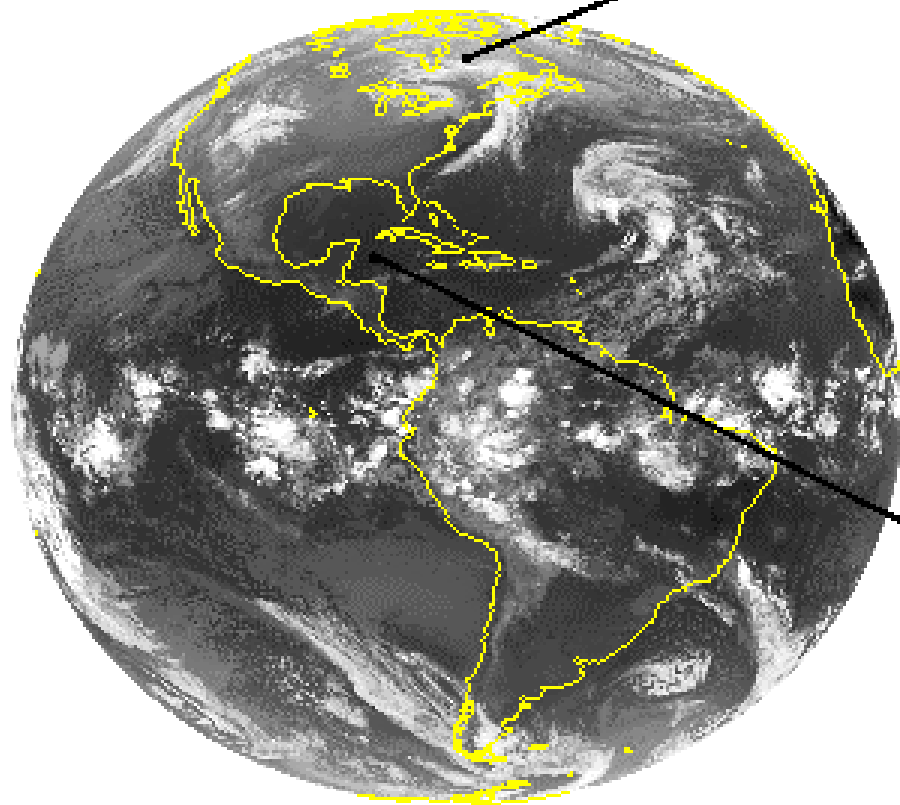
For TC, Psfc within 6 hPa and Vmax within 10 kts

(from MW ΔT_{250})

Trajectory forecast 72 hour error reduction about 10%



GEO vs LEO



Comparison of geostationary (geo) and low earth orbiting (leo) satellite capabilities

Geo

observes process itself
(motion and targets of opportunity)

repeat coverage in minutes
($\Delta t \leq 30$ minutes)

full earth disk only

best viewing of tropics

same viewing angle

differing solar illumination

visible, IR imager
(1, 4 km resolution)

one visible band

IR only sounder
(8 km resolution)

filter radiometer

diffraction more than leo

Leo

observes effects of process

repeat coverage twice daily
($\Delta t = 12$ hours)

global coverage

best viewing of poles

varying viewing angle

same solar illumination

visible, IR imager
(1, 1 km resolution)

multispectral in visible
(veggie index)

IR and microwave sounder
(17, 50 km resolution)

filter radiometer,
interferometer, and
grating spectrometer

diffraction less than geo

HYperspectral viewer for Development of Research Applications - HYDRA

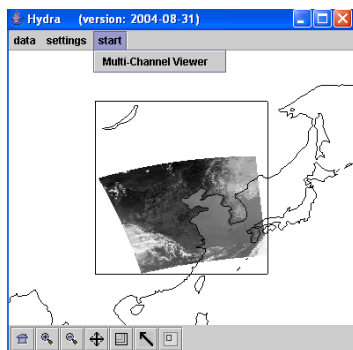
MSG,
GOES



MODIS,
AIRS, IASI,
AMSU,
CALIPSO

Freely available software
For researchers and educators
Computer platform independent
Extendable to more sensors and applications
Based in VisAD
(Visualization for Algorithm Development)
Uses Jython (Java implementation of Python)
runs on most machines
512MB main memory & 32MB graphics card suggested
on-going development effort

Rink et al, BAMS 2007



Developed at CIMSS by
Tom Rink
Tom Whittaker
Kevin Baggett

With guidance from
Paolo Antonelli
Liam Gumley
Paul Menzel
Allen Huang



<http://www.ssec.wisc.edu/hydra/>

For hydra

<http://www.ssec.wisc.edu/hydra/>

For MODIS data and quick browse images

<http://rapidfire.sci.gsfc.nasa.gov/realtime>

For MODIS data orders

<http://ladsweb.nascom.nasa.gov/>

For DB MODIS from SSEC (2007 onwards)

<http://ge.ssec.wisc.edu/modis-today/>

For AIRS data orders

<http://daac.gsfc.nasa.gov/>

One week is not enough

You have made a good start – continue using HYDRA, inspecting data, and asking questions – you will master remote sensing applications and help monitor the environment for weather and climate signals